DEVELOPMENT OF AN APPROACH FOR BUILDING EXTRACTION USING SATELLITE IMAGES

Ph.D. THESIS

by

SUSHEELA

DEPARTMENT OF CIVIL ENGINEERING
INDIAN INSTITUTE OF TECHNOLOGY ROORKEE
ROORKEE – 247667 (INDIA)
JULY, 2015

DEVELOPMENT OF AN APPROACH FOR BUILDING EXTRACTION USING SATELLITE IMAGES

A THESIS

Submitted in partial fulfilment of the requirements for the award of the degree

of

DOCTOR OF PHILOSOPHY

in

CIVIL ENGINEERING

by

SUSHEELA

DEPARTMENT OF CIVIL ENGINEERING
INDIAN INSTITUTE OF TECHNOLOGY ROORKEE
ROORKEE – 247667 (INDIA)
JULY, 2015

INDIAN INSTITUTE OF TECHNOLOGY ROORKEE
ROORKEE

CANDIDATE'S DECLARATION

I hereby certify that the work which is being presented in the thesis entitled "**DEVELOPMENT OF AN APPROACH FOR BUILDING EXTRACTION USING SATELLITE IMAGES**" in partial fulfilment of the requirements for the award of the degree of Doctor of Philosophy and submitted in the Department of Civil Engineering of the Indian Institute of Technology Roorkee is an authentic record of my own work carried out during a period from Dec., 2009 to July, 2015 under the supervision of Prof. P. K. Garg, Vice Chancellor, Uttarakhand Technical University, Dehradun, India and Dr. Mahesh Kumar Jat, Associate Professor, Civil Engineering Department, Malaviya National Institute of Technology Jaipur, Jaipur, India.

The matter presented in the thesis has not been submitted by me for the award of any other degree of this or any other Institute.

(SUSHEELA)

This is to certify that the above statement made by the candidate is correct to the best of our knowledge.

(Mahesh Kumar Jat)
Supervisor

(P. K. Garg)
Supervisor

Date:

ABSTRACT

The importance of increasing role of remote sensing and GIS technology in development of infrastructure has always posed varied challenges to the research community. Time and again, solutions have been provided by researchers for various matrices of physical built environment in different geographies. Amongst the several outcomes of the review of researches, one drawback in Indian context was that only limited studies had been carried out for fully automatic building extraction methods. It was also realized that established researches related to fully automatic building extraction methods were not tested for various types of buildings, but locally applied on construction materials. The identified gaps instigated to frame the objectivity of this research to develop a fully automated building extraction method confirming its applicability to Indian types of settlements. Based on the objectivity and target areas of these researches, each solution had its own strength and weaknesses and always left a scope for future research.

In the present research, four building extraction methods were developed for which the required broad parameters were espoused from earlier researches. In first method, a threshold value was calculated for identification of buildings based on areas. The second method involved shadows and corner information for the extraction of buildings. The third extraction method was based on the texture to find the highest mean cluster value, to identify the cluster containing buildings. The fourth method involved the combination of threshold method and texture method. For verification of this method, the shadow mask was applied to detect true buildings and remove false positives. All the four developed methods accept raw images and as such no pre-processing was required before using the image in the developed program. However, in all the methods, post processing has been done to fill the small holes present in the extracted building areas, to smoothen the edges and to remove very small artifacts extracted as buildings.

To test the developed methods for varied types and grouping of building in Indian settlement, the city of Jaipur in the state of Rajasthan, India, was chosen as the study area. Testing the proposed approach for complex variations in built environment and settlement formed the basis for choice of study area.

The accuracy assessment of the results of developed methods was done three folds. Firstly, it was done on the basis of visual interpretation. Secondly, by comparing the ground truth produced by manually delineating the building boundaries in ArcGIS environment and the

buildings extracted by developed methods. And thirdly, by comparing the OAP obtained from the supervised classification with the ones attained from the extracted buildings. The best texture combination was selected on the basis of 'time taken' and the '% error rate' of area extracted.

Analyzing the output results, it was observed that the method based on threshold value successfully extracted all types of buildings, but the shapes of the buildings were not retained. Also, the buildings close to each other were grouped together and extracted as one building. This method also resulted in some 'False Positives' and 'False Negatives', depending on the spectral reflectance values. The method based on shadow and corner information was not able to extract the buildings having complex shapes, and also the buildings without shadow associated with them. The method based on texture successfully extracted all types of buildings but resulted in high % error rate of area. As the number of texture methods increased in the combination, the % error decreased but the time taken for completing the extraction process also increased. However, using combination of Laws, Wavelet and GLCM, texture methods produced comparatively less % error and took less time to complete the extraction process. The method based on threshold, texture and shadow extracted all types of buildings successfully. All texture combinations used in this method gave higher accuracy than the accuracy obtained from supervised classification. Also, the % error rate of the area extracted was very less for all texture combinations.

On comparison of four developed methods, it was found that the method based on threshold, texture and shadow produced best results for all types of building irrespective of their shapes, sizes and Orientation. This method also gave best results for slum buildings over other methods and extracted most of the slum buildings.

The output of the research can be summarized that a fully automatic building extraction method has been developed for the complex settlement tested for an Indian case. The strength of this method is that no skills of remote sensing, Geographical Information System (GIS) or software development are required for its application, thus confirming it to be cost effective, time efficient and user friendly. Since, it is an initial attempt to develop a fully automatic building extraction method in Indian context, future researches are advised to test its application in various geographies and suggest the improvements to improve accuracy of extraction of ground features.

ACKNOWLEDGEMENTS

"Gurur Brahma Gurur Vishnu, Gurur Devo Maheshvarah, Guru Shakshat Param Brahma, Tasmai Sri Gurave Namah" means "Know the Guru (teacher) to be Brahma Himself. He is Vishnu. He is Also Shiva. Know him to be the Supreme Brahman, and offer thy adoration unto that Peerless Guru".

While remembering all my teachers, who have sown in me the desire to follow the path of knowledge and wisdom, first and foremost, I wish to express heartfelt gratitude for my thesis supervisor **Prof. P. K. Garg** at Civil Engineering Department, Indian Institute of Technology, Roorkee, India (now Vice Chancellor, Uttarakhand Technical University, Dehradun). His continuous encouragement and pedagogical expertise has helped me to absorb those technical and research insights which brought this study to its logical format. His support to arrange for resources and guidance in expanding my publication profile had been the core to reinforce the structure of my research. He exposed me to the various horizons of service to the society by integrated use of remote sensing technology for planning and development works. He has been very generous in providing me the necessary resources to carry out my research. All skills, we achieve have always a continuous scope of improvement. I have no doubt that under guidance of Prof. Garg, my way of analytical thinking, software programming, writing and presentation has lifted my confidence to a different level. Falling short of words, I bow my head to express 'Thank You Sir' for being my mentor.

My sincere thanks to my co-supervisor, **Dr. Mahesh K. Jat**, for his ever enthusiastic spirit, valuable suggestions and unconditional support and encouragement. His support during my stay at Jaipur had made convenient and possible for me to and re-evaluate the method of analysis. His efforts to coordinate with Prof. P.K. Garg has vastly contributed to the successful completion of this research document.

As an institution, I would like to acknowledge UGC (University Grants Commission), Government of India, New Delhi, for granting me scholarship during my research period as JRF (Junior Research Fellow) and SRF (Senior Research Fellow) in Engineering and Technology.

I extend my thanks to the Head of the Department and faculty members, Department of Civil Engineering, Indian Institute of Technology, Roorkee for the administrative support and academic encouragement. I specially thank my research committee members for their patience

during discussions and evaluations of my work. I am thankful to my SRC (Student Research Committee) members: **Prof. M. J. Nigam**, Department of Electronics Engineering, IIT Roorkee, Roorkee and **Prof. S. K. Ghosh**, Geomatics Engineering Group, Department of Civil Engineering, IIT Roorkee, Roorkee, for their valuable comments and suggestions to streamline and improve of my research work since beginning. Critical analysis had always inspired me to improve upon which also opened new door for me to look for things in a different way and remain open minded.

I take this privilege to thank all the Civil Engineering Department office staff for their support and tirelessly helping in the much needed paper work. A special thanks to Mrs. Chitra and Mr. Gupta for their ever contagious smile and quick response to the academic problems. I also thank Mr. Pratap and Mr. Vinod, staff members at the Geomatics lab, who have always supported in the best of their capacities.

I would like to thank several anonymous reviewers whose constructive comments and suggestions on the work from time to time since its initial stages helped me in improving the quality of the work and manuscript substantially.

My heartfelt thanks to all my friends and colleagues: **Etishree, Rajat, Priyadarshi, Rakesh Dwivedi, Gaurav** and **Kuldeep** for creating good research environment and sparing their valuable time by sharing their thoughts with me. A special thanks to my dear friend **Etishree** for many memorable moments amidst the stress of the work. I spent many enjoyable hours of working with her in the department. Without this friendly environment and freedom provided by my friends and colleagues, many of my ideas would not have come to fruition. I would also like to thank **Payal Chaudhary** for providing the joyful and friendly environment during my stay at A. N. Khosla Bhawan, I.I.T. Rooorkee.

My thesis appears in its current form due to the assistance and guidance of several people. I would therefore like to offer my sincere thanks to all of them.

There were few people outside the I.I.T. campus who always kept me connected with the rest of the world. I owe thanks for the love, care and support extended by **Virender, Nidhi, Shilpi, Urmil, Geeta and Yasholata.** A special thanks goes to **Shilpi**, who tirelessly kept scolding me throughout my research phase, so as to bring out something better out of my work.

A very special and heartiest thanks goes to my dear friend **Dr. Ekta Singh** and her husband **Dr. D. P. Singh** for unconditionally standing by my side and making me feel at home during my

entire stay at Roorkee. Their children **Ananya** and **Vasu** always made me and my kids feel special. I am really happy to mention that I have done the final compilation of my research work at Ekta's place with her help which will always remain a memorable experience.

I owe my existence as it stands today to the love and care that I received from my family and friends. I am indebted to my dear husband, **Manoj Dahiya**, for giving me constant encouragement and support without which I would not have been able to come this far. His sacrifices for me and kids can only be expressed in feelings. I also would like to express love and thanks to my kids; **Daksh** and **Ran Vijay**, for giving me their affection and those playful and fun-filled years which will remain as a treasure for me throughout my mortal life. Putting my heart back to order, I dedicate my work to them.

God understands our prayers even when we cannot find words to say them. I am indebted to the Almighty for making my life meaningful even outside the confines of this Ph.D. candidature. I thank God for everything I am blessed with.

Above all Maa DURGA had been a constant source of power and this Ph.D. work in its entirety is devoted to her.

Susheela

CONTENTS

LIST OF FIGURES

LIST OF TABLES

LIST OF ABBREVATIONS

2D	-	2-Dimension
3D	-	3-Dimension
AML	-	Arc Macro Language
AP	-	Accuracy Percentage
BEP	-	Building Extraction Percentage
BGIS	-	Ball Aerospace's Global Imaging System
BLRs	-	Building Like Regions
CAD	-	Computer Aided Design
CBRs	-	Candidate Building Regions
CIE	-	Commission Internationale de l'éclairage
CPK	-	Camy-Petrou-Kittler
DEM	-	Digital Elevation Model
DMP	-	Differential Morphological Profiles
DSM	-	Digital Surface Model
ECHO	-	Extraction and Classification of Homogeneous
ENVI	-	ENvironment for Visualizing Images
ERDAS	-	Earth Resources Data Analysis System
EROS	-	Earth Resources Observation Satellite
ESRI	-	Environmental Systems Research Institute
FAST	-	Features from Accelerated Segment Test
FN	-	False Negative
FP	-	False Positive
FSG	-	Fuzzy Stacked Generalization
GIS	-	Geographical Information System
GLCM	-	Gray Level Co-occurrence Matrix
GLSM	-	Gray Level Surface Model
GMSR	-	Gradient Magnitude based Support Regions
HSI	-	Hue-Saturation-Intensity
HMT	-	Hit or Miss Transform
ID	-	Identification
InSAR	-	Interferometry Synthetic Apeture Radar
IRS	-	Indian Remote Sensing Satellite
ISODATA	-	Iterative Self Organizing Data Analysis
L*a*b	-	Lightness-A-B

LAB	-	Lightness-A-B
LIDAR	-	Light Detection and Ranging
MATLAB	-	Matrix Laboratory
MF	-	Miss Factor
MLC	-	Maximum Likelihood Classifier
MM	-	Mathematical Morphology
MPEG	-	Moving Picture Experts Group
MRF	-	Markov Random Field
MS	-	Multi-Spectral
MSS	-	Mean Shift Segmentation
NDMA	-	National Disaster Management Authority
nDSM	-	normalized Digital Surface Model
NDVI	-	Normalized Difference Vegetation Index
NIR	-	Near Infra-Red
OAP	-	Overall Accuracy Percentage
PAN	-	Panchromatic
RAG	-	Right Angle Graphs
RGB	-	Red-Green-Blue
SF	-	Split Factor
SIFT	-	Scale Invariant Feature Transform
SPOT	-	Satellite Pour l'Observation de la Terre means "satellite for observation of earth"
SVM	-	Support Vector Machine
SWI	-	Shadow Water Index
THR	-	Threshold
TM	-	Thematic Mapper
TP	-	True Positive
VB	-	Visual Basics
YCbCr	-	Luminance; Chroma: Blue; Chroma: Red

CHAPTER 1 INTRODUCTION

1.1. BACKGROUND TO THE RESEARCH PROBLEM

Building extraction refers to the process of extracting the building or its features from a high resolution satellite images using various approaches. Depending on the level of human intervention involved, the building extraction approaches may be classified as being manual, semi-automatic or automatic. The process of building extraction from high resolution satellite images finds various applications that are crucial to both public and private sectors. Some of the interesting applications of building extraction include development and management of a Graphical Information System (GIS), Urban Planning, Urban Development and Management, Revenue Collection, Tracking Unauthorized Construction, Census Calculation, Military Operations, Transportation Planning, Assessment of loss due to Natural Hazard and likewise many others (Muttitanon and Tripathi, 2005; Ramasamy et al., 2005; Bariar et al., 2006; Roychowdhury et al., 2010; Huy and Kappas, 2010; Roychowdhury et al., 2011).

In the initial years of remote sensing technology development only coarse resolution image were available, due to which extraction of individual buildings was not possible. The information about natural and man-made resources was extracted through manual digitization and classification (Dadhwal, 1999; Gupta et al., 2002; Bhatti and Tripathi, 2014). Digitization involved the process of converting analogously produced graphical maps to the machine readable vector or raster formats (Sahin et al., 2004). Further, classification is done to sort out pixels into a finite number of categories, of data based on their reflectance values (Mozumder and Tripathi, 2012). If a pixel satisfies a certain criteria, it is assigned to the class, which meets the criteria (Chilar, 2000). Supervised and unsupervised are two techniques of classification. Of which supervised classification is mainly used to prepare the landuse/landcover (LULC) map of urban areas (Shaban and Dikshit, 1998; Shaban and Dikshit, 1999; Shaban and Dikshit, 2001; Shaban and Dikshit, 2002). Using this LULC map, change detections are carried out to analyse changes over time (Srivastava and Gupta, 2003), for the assessment of loss due to Natural Hazard (Ramasamy et al., 2006; Ramasamy et al., 2010;Thach et al., 2007; Kumar et al., 2010; Thach et al., 2011; Sengar et al. 2013) and for environmental studies (Erasmi et al., 2005). However, these methods of

information extraction proved to be very time consuming, tiresome, costly, and required human intervention and expensive equipment.

However, with the advancement in imaging technologies and availability of commercial high-resolution satellite imaging sensors such as Cartosat (2.5 m), SPOT5 (Satellite Pour l'Observation de la Terre means "satellite for observation of earth") (panchromatic mode, 2.5 meters), EROS (Earth Resources Observation Satellite) (panchromatic mode, 1.8 meters), IKONOS (panchromatic mode, 1 meter; multispectral mode 4 meters), QuickBird (panchromatic mode, from 0.61 meters; multispectral mode from 2.44 meters) and LIDAR (Light Detection and Ranging), there has been a paradigm shift in the process of Earth Observation (Wang et al., 2010).The resolution of an image describes the details that the image holds. In other words, a higher resolution shows more number of pixels making the same image which leads to a more detailed view of the image. As such, the greater the resolution, the better is quantifying phenomena. The high spatial resolution of the imagery obtained with the above mentioned advanced sensors provides a synoptic view of a large area of the Earth's surface in a single image with very fine details that facilitate the extraction of urban objects such as buildings and roads. These sensors differ in the kind of output and/or images and the details that can be obtained from them. LIDAR gives 3-D images that provide more details about the objects. The output obtained from LIDAR is in the form of a huge point cloud data that require extensive processing and editing which needs specific image processing software for further analysis. As a result, the building extraction using LIDAR becomes expensive, labor intensive, and time-consuming. However, the images obtained with IKONOS and QuickBird also capture good details of the objects like roads, vegetation, buildings, water bodies etc., existent in the piece of land or area, and available at a relatively lower price. Because of this reason, these images are most commonly used for object extraction.

The development of a fully automated process especially for building extraction from high resolution satellite imagery is more in demand in the era of fast-pace urbanization and state of art infrastructure development. However, any automated process of building extraction faces several challenges while analyzing or processing the satellite images. These difficulties include scenarios where parts of the building may be obstructed from view by surrounding objects (such as trees) and shadows, fuzzy edges of the building (similar to the surrounding surfaces or due to sun-illumination issues), varied building shapes (footprint of the roof), sizes, and colors (not solid color

within the roof).The appearance of buildings is diverse from different perspectives and much of the 3D information is omitted in a 2D image. The texture of building may appear to be similar to other objects present in the image, like road, open ground etc., and buildings may also contain islands of other object with different colors, such as vents and AC units. Thus, the identification of all the characteristics of buildings cannot be fully automated but requires a human involvement.

Over the last decade, a significant amount of work has been done on the development of efficient algorithm for automatic or semi-automatic extraction of buildings. Several semi-automated approaches have been established that efficiently perform the tough task of building extraction. However, the full automation of the building extraction process is still in its infancy. Many automated approaches have been proposed over the last decade, but their applications are greatly limited to specific cases and scenarios. Developing a fully automated building extraction process that can be applied to extract and analyze buildings with irregular shapes, unplanned urban growth, complex infrastructures etc. is still a challenge. The fully automated approaches are liable to fail whenever a new situation is encountered. In semi-automated approaches, human and computer have a complementary role to play. Humans perform high-level tasks more reliably while the computers do the low-level tasks faster and efficiently. This mutuality of roles, makes semi-automated processes more viable and valuable than fully automated approach. Therefore, semi-automated approaches are currently gaining more attention, catering to the persistent need of precision and reliability.

1.2. INDIAN CONTEXT

There is vast spatial diversity, in same category of buildings, at different locations and geographies in planned and unplanned settlement in India. The diversity in quality, combination, application of combination of materials in the range of buildings makes it difficult to come up with a standard data of the typology of buildings.

The only and most recent (2013) attempt has been made by National Disaster Management Authority (NDMA), India to compile the typologies of buildings in India for seismic assessment. Though the document covers most of the visible typologies for different parts of the country, but do not claim it to have covered all types. The reason attributes to the innumerable combinations of the standard and locally available materials and customized construction methods. However, the

heterogeneity in various aspects of Indian living, leads to spatial diversity in similar and different geographies. Even the slums which are the outcome of similar economic conditions are spatially different from each other located in same city (Kit et al. 2012).

The catalogue prepared by NDMA ("Seismic Vulnerability Assessment of Building Types in India," 2013) categorized the buildings with five broad categories of material application in buildings. They are Masonry, Structural concrete, Steel, Wood and Bamboo. Of these Masonry is classified in 18 masonry subtypes and 3 types of load bearing systems (Vertical/lateral). Structural concrete is classified in 12 subtypes and 3 types of load bearing systems. Steel is classified in 9 subtypes and 4 types of load bearing systems. Wood is classified in 14 subtypes and only 1 type of load bearing systems. Bamboo is classified in 1 subtypes and only 1 type of load bearing systems. All these categories have been surveyed on the basis of four parameters No. of stories, irregularity (horizontal, vertical or both), quality of construction and ground level (level ground or sloping ground). As the outcome of this compilation, 14 building typologies were found to be common in all regions of the country. On regional basis, 54 typologies were identified in northern region, and almost similar numbers in each for north-east region, eastern region, western region, and southern region. The identification of these typologies on the basis of study specific parameters (which will be different for specific studies) will bring a huge number of the types of buildings in Indian context. Since no fully automatic building extraction program is devised for such a diverse typology of buildings in Indian context, this forms the basis for the rationale of the research to develop such program.

1.3. PROBLEM STATEMENT

From the earlier discussion, it can be suggested that recent building extraction systems can extract a wide range of buildings, yet they are still inadequate to efficiently extract the buildings in Indian scenario. In India, urban buildings are comparatively more irregular in shape, size, and lack consistency in texture. Most of the building extraction processes in Indian context are based on classification approach which employs only low level parameters. However, the use of only low-level parameters is not sufficient for precise building detection, therefore high-level parameters must be used along with low-level parameters to increase the accuracy of building extraction process. In view of the foresaid constraints, the present research attempts to develop a new building extraction method where both low-level and high-level parameters are used.

Normally, urban area extraction from satellite images gives a cluster of buildings but does not provide any statistical information, details or size estimates about the building. However, such statistical details if obtained can be useful in several utilitarian scenarios such as revenue collection, population estimation and identification of unauthorized constructions. Furthermore, a detailed classification of the infrastructure is required for making a master plan of an area. In order to achieve this, high resolution data and a method to pick boundary of the buildings is required. On reviewing the literature, it was realized that no such software exists that is capable of extracting all kinds of buildings. Accordingly to fill this gap, the present research was carried out to study various building characteristics and develop a software that requires minimum human intervention to extract all types of buildings.

1.4. OBJECTIVES OF STUDY

In the proposed methodology, an attempt has been made to extract individual buildings of different shapes and sizes with varying orientations. The main objectives of the research work are:

i. Identification and analysis of important parameters required for automatic extraction of buildings from high resolution satellite images.

ii. Development of an automatic approach for the extraction of buildings from high resolution satellite images using these parameters.

iii. Testing the proposed approach for types of buildings typically found in Indian scenario so that it can be verified that the proposed approach is a fully automated approach which works for all types of buildings.

1.5. ORGANISATION OF THESIS

This thesis includes six chapters. In the following chapter (chapter 2), an extensive literature review is provided about the different building extraction methods and the parameters used for building extraction. The past studies are grouped in accordance with the used parameters and methodologies for gap identification.

Chapter 3 describes the study area and detailed information of the data and software used in the research. This includes the programming, digitization and classification of the sample.

Chapter 4 is the layout of the procedure (methodology) adopted to conduct the research in the structured format. This explains the approaches adopted to target the research gaps in building extraction for the Indian scenario tested in specifically identified study area (sample).

Chapter 5 presents the results obtained by the application of the 'developed code' designed for the proposed approaches. Subsequent analysis of the results is also presented in this chapter.

Chapter 6 concludes the outcome of the study of chapter 5. This chapter also suggests the future research possibilities as an extension of this research.

1.6. CONCLUSION

The preliminary chapter has presented a background note for the present research study. It identifies the problem against which the researcher intends to propose a new building extraction process. It is understood that application of high level parameters in building extraction is still in nascent stage in Indian scenario. However, the role of these techniques and processes is on the rise for development and governance issues. The adaptability of such processes depends on the value in terms of usability and reliability against the cost, time, and human interference.

In the following chapter, researcher has attempted to identify the research gap by discussing different building extraction methods along with the parameters used for building extraction.

CHAPTER 2 LITERATURE REVIEW

In the present chapter, existing literature for extracting buildings from high resolution satellite images is reviewed. The review of literature is categorised as follows:

- Studies based on classification of remote sensing data
- Studies conducted on segmentation
- Studies conducted using both classification and segmentation
- Studies employing the use of active contours
- Graph based building extraction studies
- Neural network based building extraction studies
- Studies conducted using neural network

Further, the essential features, data used for building extraction and the accuracy assessment methods are also discussed.

In urban areas, buildings are primary objects and play an essential role in the field of urban development, urban planning, climate studies and disaster management (Xia et al., 2008; Shen and Guo, 2014). Accurate knowledge of buildings serves as a primary source for interpreting complex urban characteristics and provide decision makers with more realistic and multidimensional scenarios for urban planning and management. Also, building boundaries or footprints are one of the fundamental GIS data that can be used to estimate the quality of life, urban population, property taxes (Jensen, 2000) etc. Detailed and accurate information about the boundary of the building is also essential for the construction of urban landscape models, estimation of natural disaster risk, study of urban heat island and earthquake damage assessment (Davis, 2005; Miliaresis and Kokkas, 2007). The precise knowledge of building boundary can serve as a primary source for interpreting complex urban characteristics (Zhou et al., 2009).

2.1 TYPES OF BUILDING EXTRACTION METHODS

2.1.1. Conventional Methods of Building Extraction

The initial works in building extraction from monocular aerial images were based on line extraction, edge detection and building polygon generation (Herman and Kanade, 1986; Huertas and Nevatia, 1988; Irvin and McKeown, 1989; Mohan and Nevatia, 1989; Matsuyama and Hwang, 1990; Venkateswar and Chellappa, 1991; Tripathi and Tripathi, 1993; McGlone and Shufelt, 1994; Krishnamachari and Chellappa, 1996; Shufelt, 1996; Lin and Nevatia, 1998; Kim and Nevatia, 1999; Mayer, 1999; Gereke et al. 2001; Persson et al. 2005 and Peng and Jin, 2007). However, these methods had their own flaws. They mostly employed a large set of heuristic rules and were computationally expensive. These methods were not well-equipped to locate exact lines or edges, consequently the obtained results showed deviations from the expected. Also, they were content dependent and only buildings having straight edges (rectangular, square buildings) could be extracted using these methods. In brief, it can be said that these methods were not capable of handling all the challenges in the field of building extraction.

2.1.2. Modern Methods of Building Extraction

The availability of very high spatial and spectral resolution satellite images, with multispectral information, had motivated researchers to develop new approaches for building extraction. Many researchers focused on the use of spectral reflectance values or spectral information for building extraction. The studies of Muller et al. (1997), Baltsavias et al. (2001) and Sohn and Dowman (2001) extensively discussed the effect of resolution on the building extraction. The building extraction methods that used very high resolution satellite images, increased the generic characteristic of the methods. Generally, the building extraction methods were considered in two phase tasks: low-level and high-level tasks. First, the low-level tasks concentrated on determining the region of interest. Second, the high-level tasks (feature extraction for buildings) were performed by using classification under supervision or by clustering in the absence of supervision. Different types of features defined and used for building extraction in the literature were geometric, structural, contextual and photometric (Pesaresi, 2000; Benediktsson et al. 2001; Tatem et al. 2001; Haverkamp, 2004; Zhen et al. 2004; Jin and Davis, 2005; Thach and Canh, 2012). They are defined as follows:

- Features that define the basic geometrical properties of buildings such as area, circumference, roundness, right angles, corners, straight lines are called geometric features.
- Features related to the colour information of buildings are called photometric features.
- Features that provide information to hypothesize the position of buildings such as shadow are called contextual features.
- Features that refer to the connectedness of neighbours, according to some similarity measures are called structural features.

2.2 REVIEW OF BUILDING EXTRACTION METHODS

Several researchers have recommended classification methods for the extraction of buildings while many others advocated for segmentation methods. A few researchers used a combination of both classification and segmentation methods for building extraction. Also, there are researchers who have used active contours, graph based methods and neural networks for extracting buildings.

2.2.1. Classification Based Methods

Zhang (1999), proposed a two-level framework for extraction of urban buildings. At the first level, unsupervised classification was performed on a fused Iterative Self Organizing Data Analysis (ISODATA) clustering. At second level, filtering based on a modified co-occurrence matrix was applied to improve the classification results of the first level. The method was applied on the merged near-natural-colour TM–SPOT image of the Shanghai city, China. The study reported approximately 26% improvement in the performance when compared with the results obtained from normal texture filtering. But, the results presented were not sufficiently detailed for the investigation of urban buildings.

Benediktsson et al. (2003), used differential morphological profiles (DMPs) for the classification of panchromatic high resolution Indian remote Sensing (IRS) 1-C from Athens, Greece and IKONOS-2 Reykjavik, Iceland as image data sets. In the proposed approach, DMPs were defined by the opening and closing morphological transforms and the features were extracted on the basis of these DMPs. Then a neural network was used to classify the urban areas. A good overall accuracy was achieved for both datasets, but since only one significant derivative-maximum was used for the morphological profile of a structure. The method proved to be ineffective in complex environments.

Shackelford and Davis (2003), proposed an object-based approach which relies on pixel-based fuzzy classification, to classify the dense urban area, using pan-sharpened multispectral IKONOS-2 imagery. Applying the fuzzy pixel-based classifier, they integrated both spectral and spatial information to distinguish between spectrally similar urban land classes for roads and buildings. Subsequently, both spectral and spatialheterogeneity were used to segment the image. After that, an object-based fuzzy logic classifier was applied to complete the classification of the segmented image. The accuracy assessment results showed that 24% of the building reference pixels were misclassified as roads and impervious surfaces.

Inglada (2007) used a different Support Vector Machine (SVM) classification approach to extract man-made objects from SPOT-5 THR image. In this work, the objects were identified on the basis of their geometric descriptions, i.e., geometric invariants and Fourier–Mellin descriptors, and then a supervised SVM classification method was applied to learn and separate various classes, including the isolated buildings. However, this approach was not customized to detect the building regions in an image, but only to detect the patches having a certain size that were labelled as buildings.

San et al. (2010) developed an approach for the automatic extraction of the rectangular and circular shaped buildings from the high resolution PAN imagery using Hough Transform. In this approach, first, the candidate building patches were detected using the binary SVM classification technique. The classification was performed on ENVI (ENvironment for Visualizing Images) 4.3. In the classification process, the bands NDVI (Normalized Difference Vegetation Index), and nDSM (normalized Digital Surface Model) were also used along with the original image bands. After classifying the building patches, MATLAB 7.1 programming environment was used for implementing canny edge detection algorithms for extracting the edges of the building patches. The resultant images were converted into vector images and on the basis of perceptual grouping, the lines and edges were grouped to construct the building boundaries. The proposed method was applied to the residential and industrial urban buildings of the Batikent district of Ankara (the capital city of Turkey) captured by the IKONOS satellite. The proposed building extraction procedure can be effectively used to extract the boundaries of the rectangular and circular shaped buildings, but the accuracy of the developed approach is dependent on the success of the detection

of the building patches. If the building patches are not detected accurately due to the characteristics of the land use classes, the buildings may not be delineated correctly.

Sumer and Turker (2013) proposed an approach for building detection using an IKONOS-2 satellite image based on an adaptive fuzzy-genetic algorithm. In this method, two feature classes, building and non-building were selected as training samples. Then image processing operators (basic mathematical, logical, thresholding, texture, spectral and filtering) were calculated for finding out the temporary output bands. In the next step, a traditional classification method (Fisher's linear discriminant) was applied to reduce the temporary output bands into one band. Finally, the adaptive fuzzy logic controller operation was performed to identify the fuzzy rules to detect buildings. The proposed approach was applied on ten image patches selected from the IKONOS-2 image of Batikent district of the city of Ankara, Turkey. The building detection performances achieved were in the range of 50–91%. It was observed that the building detection process was highly dependent on the selection of parameters to achieve the best detection results.

Most of the work done on building extraction was based on monocular images, but a few researchers also developed 3D building extraction methods by using stereo/multiple aerial and high resolution satellite images. Based on the literature review, the methods developed by using stereo/multiple images can be classified into two groups:

(i) Methods which are extensions of monocular methods, and
(ii) Methods that are originally designed to work with stereo/multiple images.

In the methods of first group, the potential buildings hypothesis was generated in a similar manner as in the methods used for building extraction from monocular satellite images, and the additional stereo /multiple images were used for verifying the buildings hypothesis (e.g., Collins et al., 1998; Noronha and Nevatia, 2001; Suveg and Vosselman, 2004; Xiao et al., 2012). In the second group methods, 3D object modeling and processing was done to extract the buildings from the stereo/multiple images at the earliest stages of the processing and then it is coupled with the 2D image to complete the extraction process (Fischer et al., 1998; Cord and Declercq, 2001; Cord et al., 2001; Fradkin et al., 2001; Kim and Nevatia, 2004).

2.2.2. Segmentation Based Methods

Pesaresi and Benediktsson (2001) proposed a new morphological segmentation method. In the proposed method, morphological characteristics were defined on the basis of theoretical definitions of morphological levelling and morphological spectrum, and then these characteristics were used to perform multi-scale segmentation, for extracting buildings. This method was tested on IRS-1C panchromatic image of a densely built-up area of Milan, Italy. The results obtained showed that the method performed well for building extraction from test image. However, the performance depended upon selection of the range of increasing opening and closing by reconstruction operations, which lead to a heavy computational burden.

Wei et al. (2004) proposed an algorithm for building extraction from high resolution PAN QuickBird images using clustering and edge detection. Initially, the image was clustered into a number of classes using histogram peak selection. Also, shadow of the buildings was extracted from the lowest gray class. The shadow side was determined by the sun angle of the image. The shadow and shadow side were used as verification for the buildings and candidate buildings objects were detected from every cluster except for the shadow cluster. In the next step, the canny edge detector was used to detect edges of the candidate buildings and Hough transform was applied to detect straight edges of the candidate buildings. The drawback of this algorithm was that it extracts only big buildings having a shadow and also that the performance of extraction depended on clustering results.

Ünsalan and Boyer (2005) proposed a system to simultaneously detect houses and street networks using IKONOS-2 multispectral images of residential areas of North America. In this approach, k-means that clustering process was introduced, in which clusters were made by using the spatial information (NDVI and shadow-water index). After that, a shape-based strategy was applied to emphasize on the houses and street areas. This method successfully extracted the houses with 94% extraction rate. However, because of the assumptions involved during the extraction process, the proposed strategy was only applicable for the type of house and street formations observed in North America.

Jin and Davis (2005) proposed a method for identifying buildings in 1- meter resolution PAN satellite imagery of urban areas. In the proposed method, buildings were extracted using structural,

contextual, and spectral information. Firstly, a series of geodesic opening and closing operations were used to build a DMP that provided image structural information. Subsequently, building hypotheses were generated and verified through shape analysis applied to the DMP. Secondly, shadows were extracted using the DMP to provide reliable contextual information to hypothesize position and size of adjacent buildings. Seed building rectangles were verified and grown on a finely segmented image. Next, bright buildings were extracted using spectral information. The extraction results from the different information sources were combined after independent extraction. Performance evaluation of the building extraction on an urban test site using IKONOS satellite imagery of the City of Columbia, Missouri, was reported. With the combination of structural, contextual, and spectral information, 72.7% of the building areas were extracted with an accuracy of 58.8%.

Liu and Prinet (2005) proposed a method for extracting building objects from high-resolution panchromatic image in dense urban area by using a probability model. Initially, the input image was segmented into regions as building candidates, using cut-and-merge approach. Entropy (texture), gray level average value, standard deviation, shapes and shadow features that characterize buildings were computed for the candidate buildings. On the basis of these features, probability estimation was done and the buildings were extracted on the basis of the probability value. The application was performed on QuickBird images over Beijing city. The method was able to extract most of the buildings, but the position and shape of the buildings obtained was not correct. It was noticed that shadow feature was insufficient since it cannot be generalized from one image to another.

Hai-yue et al. (2006) proposed a new solution of automatic building extraction and mapping from remote sensing images. Firstly, they used a potential function clustering method to segment the image effectively, thus the candidate building regions could be extracted. Then, the real building regions were verified by firstly getting its edges by applying the canny operator, and then the dominant line segments were found by applying Hough transform and finally by judging the length of dominant line. Finally, the grid matching method was used to map the target buildings into regular polygons. The experimental results prove that this solution had a good precision and robustness.

Theng (2006) proposed a circular cast active contour initialization algorithm by using corner detection method (Harris and Stephens, 1988). The proposed active contour initialization method was prototyped for extracting buildings. The prototyped model involved two steps of image pre-processing, and building extraction. In a preprocessing step, the noise around the buildings was normalized by using a non-linear anisotropic diffusion model (Weickert, 1999). The corners present in this noise normalized image are obtained and active snake contours are generated. The user can accept or reject the snake contours. For each accepted contours, iterative minimization function is invoked. This iteration process is stopped when active contours lock a building outline, which results in extraction of building outlines. This method was tested on urban buildings of Burlington city captured by QuickBird satellite. This method successfully extracted the regular and irregular shaped rectangular buildings.

Song et al. (2006) proposed an approach for building detection from densely built-up areas using texture and shape features. The shadow was also used for verification of buildings. Initially, a training building set was prepared by manually selecting 120 rectangular buildings from urban areas. Then energy histogram was plotted for the training buildings as texture feature. Rectangular ratio and contour descriptor ratio were used as shape feature. After that Building Like Regions (BLRs) were obtained for the input satellite image by performing over segmentation and then these BLRs were combined by using the seed based region grouping method to obtain Candidate Building Regions (CBRs). Finally, rectangular shapes were generated for each CBRs, and these rectangular shapes were verified as building on the basis of associated shadow. The proposed method successfully extracted rectangular buildings, but was not able to correctly extract buildings with complex shape and structures.

Lefevre (2007) proposed a method for building extraction in very high resolution panchromatic (PAN) remote sensing images. Initially, the PAN image was converted into a binary image by applying a histogram analysis based clustering method. After that erosion and dilation binary mathematical morphological (MM) operators were applied on the binary image to remove objects having size lower than the minimum size of the buildings in the raw image. After filtering the noisy objects, Hit or Miss Transform (HMT) was used for selecting the area belonging to buildings and the area not belonging to buildings. As a result of HMT, the buildings were detected with their respective positions. But to retain the actual shape of the buildings, geodesic reconstruction

followed by conditional dilation were applied as a post-processing step. This method was able to extract the buildings having linear or composite rectangular shape. Since this method was applied on PAN images, some undesired objects having similar spectral signature were also extracted as buildings.

Cui et al. (2008) proposed a method for building detection and recognition from high resolution remotely sensed imagery. It was a semi-automatic method based on region-based segmentation combining the Hough transform and computation of convex hull of the pixels contained in the building areas. The proposed method successfully extracts the boundary of flat roofed rectangular buildings and gave precise result when the contrast between flat building rooftop and the background was high enough.

Liu et al. (2008) proposed semi-automatic method for extracting well separated rectangular building rooftops. In this method, both region based and feature based building extraction were performed. In region based building extraction, buildings are extracted by using seeded region-growing-segmentation and multi scale object-oriented-segmentation. In feature based building extraction, buildings were extracted by using corners, edges, lines and orthogonal corners information. Then, Hough transform was applied to remove the irrelevant orthogonal corners. After that, shape reconstruction was performed for the output of both of the extraction processes. This method was only able to extract buildings having a regular rectangular shape.

Senaras et al. (2013) proposed a decision fusion approach to detect building regions from a single VHR optical satellite image. In this approach a Fuzzy Stacked Generalization (FSG), a two-layer hierarchical ensemble learning architecture was used. First, the input image was segmented using Mean-shift segmentation and the parameters of Mean-shift segmentation were optimized and the segments belonging to the vegetation and shadow regions were eliminated from the image. The features were extracted on the basis of their shape, colour and texture. Area, rectangularity and axis length were calculated for extracting shape information. The standard deviation of the intensity values was calculated for extracting colour information. Gray Level Co-occurrence Matrix (GLCM) was applied for extracting texture information. Then decision of individual base layer classifiers was computed by using the features and decision fusion was done by using FSG. After that, the output decision spaces of each classifier were fused in a hierarchical manner by using FSG. The approach was tested on 10 different test patches selected from a single QuickBird image

of Ankara and an overall performance of 84% was reported. Nevertheless, their approach assumes the statistical stability of the training and test data, and if this was not the case, the performance values would have decreased dramatically due to the changes in the terrain structures and building variations. Also, the computational complexity of the proposed decision fusion architecture was extremely dependent on the number of segments.

2.2.3. Classification and Segmentation Based Methods

Lee et al. (2003) used ECHO (Extraction and Classification of Homogeneous) classifier and ISODATA segmentation to extract buildings from IKONOS-2 multispectral images. In this method, the ECHO classifier was used for performing supervised classification for detecting the approximate locations and shapes of buildings, while ISODATA segmentation method was applied for performing unsupervised classification followed by Hough transformation to extract the building boundaries. The results showed that 64.4% of the buildings were detected, and accurately formed through this process. As, the detection step was completely based on the results of the ECHO classifier, this method resulted in high false detection rate due to the misclassification of road and building classes.

Liu et al. (2005) developed a building extraction system from high resolution satellite images based on multi-scale object-oriented classification and probabilistic Hough transform. This system involved two different phases. In the first phase, bottom up region-merging segmentation was performed and the pixels were clustered using spectral information, tone, texture, shape and context information. After this, object-oriented classification by using eCognition 3.0 software was conducted to extract building rooftops. In the second phase, progressive probabilistic Hough transform was adopted to delineate the building rooftops and subsequently, a building squaring algorithm based on the rectilinear fitting of building boundary was applied. This system was able to extract rectangular buildings successfully, but buildings not having rectangular shape were not extracted.

Benedek et al. (2010) introduced a robust, marked point process model and a probabilistic approach based on shape, colour and shadow for building extraction in remotely sensed images. To cope with the data heterogeneity, they constructed a flexible hierarchical framework which could create various building appearance models from different elementary feature based modules (shape,

colour and shadow). A global optimization process attempted to find the optimal configuration of buildings, considering simultaneously the observed data, prior knowledge, and interactions between the neighboring building parts. The proposed method was evaluated on various aerial image sets containing more than 500 buildings, and the results were matched against two state-of-the-art techniques.

2.2.4. Active Contour Based Methods

A different approach used to extract buildings from single images was based on active contours. Peng et al. (2005) developed a different method to extract buildings from monocular aerial images. The proposed method was based on active contours. In this method, on the basis of regional features, the image was segmented into sunshine part of high objects, sunshine ground and shadow regions. Then the direction of the cast shadows was estimated without prior knowledge of illuminating direction or viewing angle and was used to verify the segments. Then the building contours were refined by combining contexts with the modified partial snake model using the direction of the cast shadows. The developed method was applied to the aerial images of a Chinese city with a resolution of 0.2 m/pixel. The assessment of the performance of the developed method was done only on the basis of the quality of the shapes of the buildings detected, and no quantitative assessment was done for the extraction process.

Karantzalos and Paragios (2009) introduced a framework for building extraction by incorporating the prior shape knowledge of buildings into segmentation process. An objective function was designed for minimizing the multi-reference shape and similarity measure. The objective function selected both, the most appropriate prior building model and the transformation that could relate the model to image. The proposed framework was applied both on aerial images and to high resolution images. The authors reported 88% overall detection accuracy when applied on high resolution satellite images and 82% overall detection accuracy when applied on aerial images with approximately 0.7m ground resolution. But the proposed framework is unsuccessful, if the data term is not able to detect possible building regions, as no recognition process had been integrated into the segmentation process.

Ahmadi et al. (2010) developed a new approach for building extraction based on level-set formulation using active contours. In the proposed model, initially the sample data from the

buildings and background was selected and the developed active contour model was applied to detect the building boundaries. After that, the building boundaries were generalized to eliminate the redundant points which resulted in the extraction of buildings. The developed model was tested on a single aerial image acquired on August 2005 from Lavasan (central Iran) having 0.5m spatial resolution. The results indicated a mean shape accuracy of 85%, completeness ratio of 80% and correctness ratio of 96%. However, the number of building and background classes should be precisely known on priority to achieve the best results. However, the developed model was independent of additional data, such as height information, usually required for the extraction of buildings.

2.2.5. Graph Based Methods

Graph-based approaches were also introduced in several works and were tested with monocular optical images. In the work, presented by Krishnamachari and Chellappa (1996), Markov Random Fields (MRFs) were used to group the straight line segments for delineation of rectangular shaped buildings from aerial images. Lastly, the shapes of the partially grouped line segments were completed with deformable contours (active contours). The presented method was tested on aerial images for extracting rectangular and L-shaped buildings, but no quantitative results were provided to assess the accuracy of the presented method.

Katartzis and Sahli (2008) also used MRFs in a stochastic framework for the identification of building rooftops. The authors combined both 2-D and 3-D contextual information of the imaged scene to extract buildings from synthetic and airborne images. In the proposed method, MRFs were used to describe the dependencies between the building hypotheses with regard to a globally consistent interpretation. Verification of these hypotheses was done by a stochastic optimisation process that operates on the whole grouping hierarchy to find the globally optimal configuration for the locally interacting grouping hypotheses, also providing an estimate of the height of each extracted rooftop. The tests were conducted on a set of aerial image patches covering a few isolated buildings, and the approach yielded good detection and reconstruction performances. However, the approach was valid only for building rooftops with low inclination.

Kim and Muller (1999) developed a building extraction method from aerial images. The method was developed in four stages: line extraction, line-relation-graph generation, building hypotheses

generation, and building hypotheses verification. In the first stage, lines were extracted by firstly detecting the edge elements by a Canny-Petrou-Kittler (CPK) edge filter and then connecting the detected edges using a connected edge labelling algorithms. After extraction of lines, in the second stage, line-relation-graph was generated by setting thresholds for the length of a line and the angle between lines. In the third stage, building hypotheses were generated by searching closed loops in the line-relation-graph. Building hypotheses were verified by the presence of the shadow. The results indicated 92.30% accuracy for industrial buildings and 62.46% accuracy for residential buildings. But considering geometric relationships between line segments during building hypotheses generation stage, the applicability of the approach was limited to certain building shapes.

In another study proposed by Croitoru and Doytsher (2003), Right-Angle Graphs (RAG) were used to detect right-angled flat roof buildings from aerial images. The right-angle corners that would have been associated with the buildings present in the image were extracted. The graph was generated by considering the Hough space and the extracted right-angle corners. Because a prior knowledge of the building models is necessary to initialize the approach, this approach is more useful for urban areas with regular rectangular shaped building layouts.

The system developed by Ünsalan and Boyer (2005) also used a graph to detect houses and streets from IKONOS multispectral images. While developing the system, general house and street characteristics of North America were taken into account. On the basis of these characteristics, the vertices of the graph were generated from binary balloons used to represent a house or street segments. This approach had its limitation to the detection of the house and street formations observed in North America.

Sirmacek and Unsalan (2009) used point features for the detection of buildings. In this approach, the scale invariant feature transform (SIFT) key points of the template building images and the test images were obtained. The urban area in the test images was obtained by applying multiple sub-graph matching between the SIFT key-points of the template and test images. From the detected urban area, separate buildings were detected by using a graph cut method. This approach was tested on a large set of panchromatic IKONOS-2 images of regularly developed urban areas, and the results showed that 88.4% buildings are successfully extracted. Nonetheless, this approach was

designed mainly for the extraction of isolated buildings, yet specific building templates were the preliminary requirement for initiating the proposed building detection method.

In the method proposed by Cui et al. (2011), the parallel and perpendicular lines were extracted by region growing segmentation followed by Hough transformation and then irrelevant edges were filtered out and a building structural graph was constructed by using the edges obtained after filtering process. On the basis of the building structural graph, cycles in the graph were detected and building hypotheses were formed. The proposed approach was tested on an image of north part of Chiba in Japan acquired by Leica ADS40 digital sensor with a ground sampling distance of 0.2 meters. The experimental results showed that the proposed approach was quite effective for flat rectangular building roofs. As a limitation, the output of this approach was completely based on the quality of segmentation steps done to identify the building locations.

In an approach developed by Izadi and Saeedi (2012) image primitives (lines and line intersections) were used to deduce a set of building rooftop hypotheses, using a graph-based search. 20 QuickBird image patches were used to test the approach. 95.2% accuracy was achieved, which shows good detection and reconstruction results. However, this approach only worked for flat or flat-looking roofs and the assumption of smoothness of the rooftops may be valid only for certain roof shapes.

Another study, on graph-cut method for image classification done by Schindler (2012) had emphasised the importance of smoothness. The output of this work represented that the assumption of smoothness applied during the classification may improve the performances up to 33%. However, note that the proposed framework was capable of solely handling the images, the obtained results took benefit of the height data used during the classification.

2.2.6. Neural Network Based Methods

Lari and Ebadi (2007) proposed an automatic building extraction method from high resolution multispectral images based on neural networks. The method was developed using C# programming language. The proposed method works in two phases: learning phase and an application phase. In learning phase, the neural network in the method was trained with the help of test data and in the application phase, the developed program extracted the buildings on the basis of trained data. Initial image processing was done for preparing the test data. In initial image processing, first seeded region growing segmentation algorithm was applied on the image, then opening and closing

operators were applied on the segmented image. Subsequently, features, present in the image were extracted on the basis of geometric features (area and perimeter), structural features (roundness, compactness and specific angles) and photometric features (mean, colour and intensity). Then tree-layer neural network was trained by randomly selecting the different regions and using the numeric features calculated in the image processing step. The training process worked well when all weight coefficients were selected truly. The proposed method was tested on the IKONOS images of the urban area of Kashan in Iran. The proposed method was able to extract approximately 80% of the buildings present in the image. The accuracy of the proposed method depends on the training data that requires knowledge of neural networks.

Sirmacek and Unsalan (2011) proposed a method for building detection by using a probabilistic framework depending on four different local feature vector extraction methods. These local feature vector extraction methods were Harris corner detection, gradient-magnitude-based support regions (GMSR), Gabor filtering in different orientations, and Features from Accelerated Segment Test (FAST). These four local feature vectors indicated a building to be detected. Also, the possible spatial coordinates of building locations were represented as discrete joint random variables and their probability density function (pdf) was estimated on the basis of the local feature vectors. On the basis of the estimated pdf, a probabilistic framework was introduced. In the probabilistic framework, the effects of local feature vectors were adjusted w.r.t. their orientation and weight that resulted in building detection. The proposed method was tested on Ikonos satellite images and on aerial images of Istanbul and nearby villages. This method detected buildings with an accuracy of 93.4% with false detection rate of 17.9% for satellite images, and an accuracy of 100% with false detection rate of 31.3% for aerial images. In this method, the building detection rate was good, but the false detection rate was quite high. Also, this method was not able to extract the actual shape of the buildings.

Wang et al. (2015) presented an automatic approach for the extraction of rectangular buildings from very high resolution optical satellite images. First, pre-processing was done to reduce the noise and enhance the contrast of building edges by using histogram equalization and edge-preserving bilateral filter. Then EDLines line segment detector was used to detect the line segments present in the image. Then, the collinear lines were grouped by using perceptual grouping considering the overlap length, lateral distance, separation and angle between the lines. After

linking the lines, their relationship was examined using graph search and then a path completion for rectangular buildings considering the right angle structure was done. Also, the perceptual contour search was done to remove the multiple boundaries of the same rooftop. This method resulted in detection of rectangular building rooftops with an accuracy of 80.9%. This method was not applied to extract buildings with complex shapes, and as a drawback extracting the buildings using edges resulted in the extraction of other land-cover features as roads, parking areas etc.

2.2.7. Methods Developed for Stereo/Multiple Images

Besides the above discussed methods, some other methods have also been developed for building extraction from stereo images. Kim and Muller (1998) proposed a robust combination of the results of 2D building detection technique and a 3D height extraction technique. The combination was done by inserting the heights into the buildings extracted by 2D building boundary detection technique. The proposed approach had been tested on airborne images, and the results obtained indicate that 3D building reconstruction can be achieved successfully.

Jaynes et al. (2003) presented an approach in which segmentation was done for building reconstruction. The digital elevation map (DEM) generated from stereo/multiple images was used for building reconstruction. The findings suggested that the present approach was capable of reconstructing a wide variety of building types including peaked, flat, multi-level flat, and curved surfaces.

In the work presented by Baillard et al. (1998) and Baillard and Maitre (1999), a stereo-based DSM was used to extract buildings from stereo aerial images. Along with DSM, region-based Markovian classification algorithm was used to distinguish between ground and above-ground objects and then a textural characterization was performed to distinguish natural and man-made parts, which finally resulted in building extraction. The DSMs are generally used to extract raised structures, and for that purpose, many other different approaches were applied in the literature, such as thresholding (Rüther et al., 2002), local evidence (Paparoditis et al., 1998), automated segmentation and classification (Cord and Declercq, 2001; Cord et al., 2001), marked point processes (Lafarge et al., 2008; Tournaire et al., 2010) or an existing Digital Terrain Model (DTM) (Vestri, 2006; Koc-San and Turker, 2012).

Lafarge et al. (2006) conducted a study of a dense urban area using high resolution data and presented an automatic 3D city model of the same. In this method, researchers have used structural approach, to construct complex buildings, by merging simple 3D parametric models with rectangular ground footprint. In order to achieve rectangular building extraction footprints, an automatic building extraction method, relying on marked point processes was used. Next, a Bayesian framework, including both prior knowledge of models and their interactions, and then a likelihood fitting them to the DEM, was applied. The main drawback of this model was the presence of artifacts due to a non-optimal rectangle overlapping.

A fully automated algorithm model was developed by Shackelford et al. (2004). This model utilized commercial high-resolution satellite imagery for the extraction of building footprints. The buildings and their shadows were identified in the DMP of 1-m resolution panchromatic IKONOS imagery. Then, a variety of shape-based features were utilized to extract buildings and their shadows from the DMP. Six different parameters were employed to differentiate building from the building shadow. This algorithm when applied to an IKONOS image test site, produced an accurate image. However, the building extraction was incomplete in the image.

2.3 DATA USED FOR BUILDING EXTRACTION

Building boundary (footprint) provides primary information about a building, as the boundary shows the exact position and the potential shape of a building. Many studies have been conducted regarding building extraction from remote sensing imagery (Ahmadi et al., 2010; Champion et al., 2010; Lafarge et al., 2008; Michaelsen et al., 2010; Tournaire et al., 2010). Different data sources were used for building boundary extraction. Various data included early aerial images (Huertas & Nevatia, 1988; Irvin & McKeown, 1989), Interferometry Synthetic Aperture Radar (InSAR) (Gamba et al., 2000), recent high-resolution IKONOS and QuickBird satellite imageries (Lee et al., 2003), related DSM (Lafarge et al., 2008), light detection and ranging (LiDAR) and point clouds (Forlani et al., 2006; Zhang et al., 2006), and terrestrially sensed images (Pu and Vosselman, 2009). To exploit the respective advantages of each data source, data combination was also widely used for building footprint extraction (Simonetto et al., 2005; Sohn & Dowman, 2007; Tupin & Roux, 2003; Turlapaty et al., 2012).

2.4 CONCLUSION

This chapter provides a review of earlier researches done in the last few years, in the area of building extraction. Based on this review, it may be concluded that there is a dearth of studies on extraction of buildings from high resolution satellite images, particularly in the Indian context. A significant amount of the existing literature limits to extraction of buildings from a single image having rectangular shape, same size and same orientation of buildings. Also, the accuracy assessment of the methods discussed in the literature had been done on the basis of TP, FP and FN. No accuracy assessment is done on the basis of the area. The present review of studies highlight the need to develop an approach, using which all types of buildings can be extracted irrespective of their type, shape, size, and orientation. Also, the approach should be able to perform an accuracy assessment on the basis of the count along with the area of the extracted building. The case of research needs to be tested for the sample area containing various typologies of buildings in complex urban environments as in Indian scenario. In the present thesis, an attempt is made to fill the gaps identified in this review.

CHAPTER 3 STUDY AREA AND DATA USED

3.1 INTRODUCTION

This chapter provides a detailed description of the satellite data and study area which have been used to achieve the research objectives as discussed in Chapter 1. The general information about the study area such as geographical location, geology, demography, climate conditions etc. has also been provided in this chapter.

3.2 THE STUDY AREA

In order to test the developed methodologies for different types of buildings found in the Indian scenario, we need high resolution satellite images of an Indian city containing all types of urban infrastructure/buildings/built structures i.e., planned, unplanned, slum, industrial, business and educational buildings having different shapes, sizes and orientations. In the present study, Jaipur City, Rajasthan, India, has been chosen as the study area which are located between the latitudes 26° 55' N to 26° 92' N and longitudes 75° 49' E to 75° 82' E. Jaipur, the capital of Rajasthan state in India was founded on 18 November 1727. Jaipur is popularly known as the Pink City of India. As, Jaipur city is the district headquarter, largest city and state capital of Rajasthan, it is one of the well-planned cities in India. The city is planned on a network of gridded streets and probably has all types of urban structures and infrastructure i.e., planned, unplanned, slum, industrial, business, and educational buildings. This diversified urban character of Jaipur eventually led it to be the choice as a study area to test the building extraction approach developed in the present research. The location of the study area is shown in Figure 3.1.

3.2.1. Geographic Extent

Jaipur district is positioned at an altitude of 1417 feet above the sea level. On three sides, the city is enclosed by Aravali hills. The Aravali hills safeguard the city from the rough desert conditions. The district shares its border with Ajmer and Nagaur district to the west, Alwar, Dausa and Sawai Madhopur district to the East, Sikar district to the North and Tonk district to the South. Jaipur is in 509 meters to 264 meters elevation range. There are 13 subdivisions, 16 Tehsils, 2369 Villages, 15 Panchayat Samitis, 489 Gram Panchayat, 10 Nagar Palikas and 1

Nagar Nigam in Jaipur district ((http://jaipur.rajasthan.gov.in/content/raj/jaipur/en/about-jaipur/history.html).

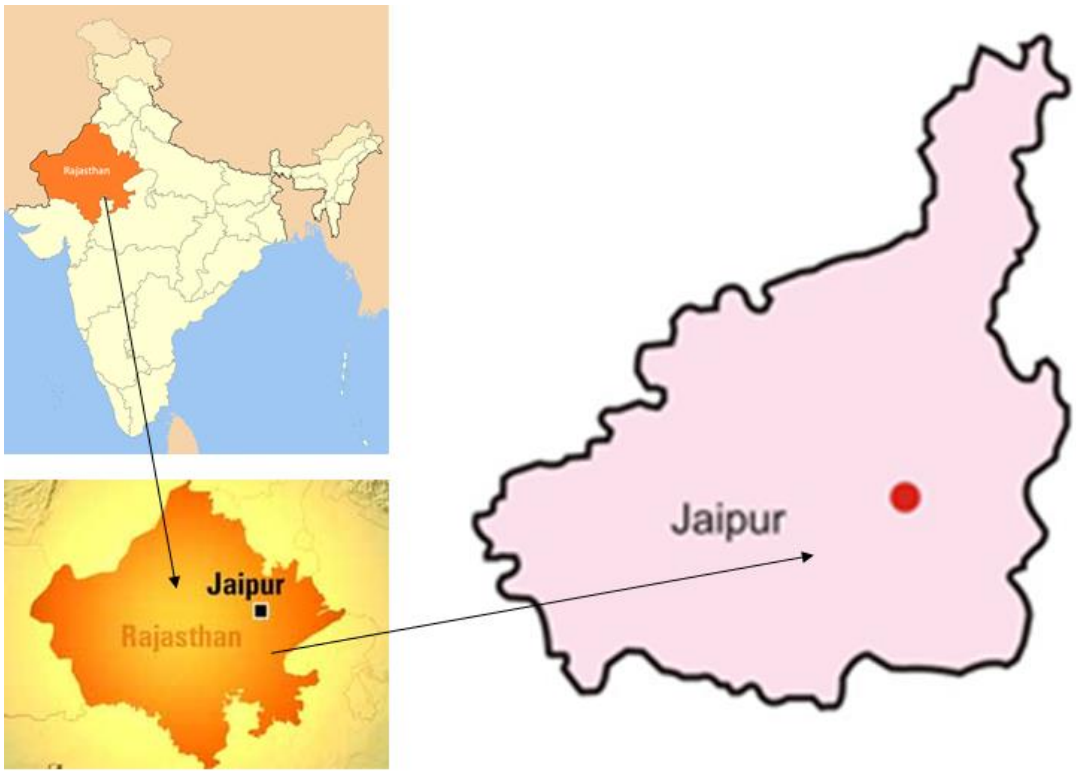

Figure 3.1: Location of Study Area

3.2.2. Population Description

According to the 2011 District Census (Census, 2011), it is the tenth most populous district in India (out of 640). Jaipur district has an area of 11,152 km² with a population of 6,626,178. The district has a population density of 598 inhabitants per square kilometer. Its population growth rate over the decade 2001-2011 was 26.19%. Jaipur has a literacy rate of 75.51%. It is the largest district in the state by population, 12th largest district in the state by area, 10th largest district in the country by population, 2nd highest district in the state by literacy rate and 234th highest district in the country by literacy rate. (http://www.mapsofindia.com/maps/rajasthan/districts/jaipur.htm).

3.2.3. Climate

Jaipur has a semi-arid climate under the Koppen climate classification, receiving over 650 mm of rainfall annually, but most rains occur in the monsoon months between June and September. The temperature remains relatively high throughout the year, with the summer months of April to early July having average daily temperatures of around 40 °C. During the monsoon there are

frequent, heavy rains and thunderstorms, but flooding is not common. The winter months of November to February are mild and pleasant, with an average temperatures ranging from 15-18 °C (59-64 °F) and with little or no humidity though occasional cold waves lead to temperatures near freezing (http://www.imd.gov.in/).

3.3 DATA USED

The high resolution satellite images of Jaipur city (Rajasthan, India), used in this research belong to QuickBird-2. QuickBird-2 is a high resolution commercial earth observation satellite, owned by Digital Globe. QuickBird-2 was launched on 18 Oct 2001. The last picture acquired by QuickBird-2 was on 17 December 2014. QuickBird-2 re-entered in Earth's atmosphere on 27 January 2015. It was the first satellite in a constellation of three scheduled to be in orbit by 2008. QuickBird used Ball Aerospace's Global Imaging System 2000 (BGIS 2000) ("Ball Aerospace: QuickBird"). The satellite collected panchromatic (black and white) imagery at 0.61 meter and multispectral imagery at 2.44 meter spatial resolution ("Digital Globe Data Sheet: QuickBird," 2014).

At this resolution, many objects such as buildings, trees, roads and other infrastructure are visible. However, this resolution is insufficient for working with smaller objects, such as mud buildings, buildings hidden by tree cover. These images can also be used as a framework for mapping applications, such as Google Earth and Google Maps.

QuickBird-2 collects data in four multispectral bands including 450nm to 520nm (blue), 520nm to 600nm (green), 630nm to 690nm (red) and 760nm to 890nm (Near Infra-Red). The image data used for this study was acquired on June 2008, and includes two spectral bands (Red and Green) from the visible spectrum and one band from the near-infrared spectrum (NIR).

3.4 DETAILS OF THE TEST IMAGES USED

Sixteen different regions are selected from the QuickBird-2 satellite imagery of Jaipur city to test the proposed approach. Each region has different type, density, shape and orientation of buildings. Also, the building rooftop surface material varies with respect to the type of buildings. For example, some buildings have different building rooftops, such as concrete, brick and metal. Also, some buildings have a similar intensity reflectance to the roads which normally causes interference of the roads and the buildings.

Figure 3.2 (a): Image 1

Figure 3.2 (b): Image 2

Figure 3.2 (c): Image 3

Figure 3.2 (d): Image 4

Figure 3.2 (e): Image 5

Figure 3.2 (f): Image 6

Figure 3.2 (g): Image 7

Figure 3.2 (h): Image 8

Figure 3.2 (i): Image 9

Figure 3.2 (j): Image 10

Figure 3.2 (k): Image 11

Figure 3.2 (l): Image 12

Figure 3.2 (m): Image 13

Figure 3.2 (n): Image 14

Figure 3.2 (o): Image 15

Figure 3.2 (p): Image 16

Figure 3.2: Test Images selected from QuickBird Satellite imagery of Jaipur City. The test images 1 and 2 covers educational buildings. The test image 3, 4 and 5covers business buildings. The test image 6 and 7 covers industrial buildings. The test Image 8, 9 and 10 covers planned residential buildings. The test image 11, 12 and 13 covers unplanned residential buildings. The test image 14, 15 and 16 covers buildings from slum area.

Test images selected from QuickBird Satellite imagery of Jaipur are depicted in Figure 3.2. All selected test images pose different kinds of challenges for the building extraction process. The location and size of the test regions is listed in Table 3.1.

Table 3.1: Locations and Size of the Test Regions

Image No.	Location	Size (in meter)
1	Rajasthan University Campus, Jaipur	178.2×175.2
2	Jaipur Engineering College and Research Centre, Jaipur	199.8×142.8
3	Appolo College of Veterinary Medicine, Agra Jaipur Highway, Jaipur	203.4×214.2
4	Bambala, Pratap Nagar, Jaipur Govardhan Nagar, Tonk Road, Jaipur	109.8×103.2
5	Sitapura, Tonk Road, Jaipur	109.8×118.2
6	Kanha Ki Dhani, Diggi Malpura Road, Muhana, Jaipur	309.6×330
7	Indian Oil Corporation Limited (IOCL) Inferno, Jaipur	298.2×158.4
8	JDA Colony, Paldi Meena, Jaipur	420.6×339.6
9	Telecom Colony, Model Town, Jagatpura, Jaipur	139.8×151.8
10	Morning Mist, Kumbha Marg Chauraha, Pratap Nagar, Jaipur	130.2×160.8
11	Sevaram Nagar, Gokulpura, Jaipur	175.8×232.8
12	Kesar Vihar Colony, Sawal Gaitor, Jagatpura, Jaipur	78.6×70.8
13	Muhana Mandi, Diggi Malpura Road, Sanganer, Jaipur.	173.4×131.4
14	Near Tunnel Circle, Jaipur	95.4×109.2
15	Jawahar Nagar, Delhi Jaipur bye pass, Near Burmeese Colony, Jaipur	75.6×182.4
16	Jawahar Nagar, Delhi Jaipur bye pass, Near Burmeese Colony, Jaipur	91.2×164.4

3.5 SOFTWARE USED

The software used in this research are given in Table 3.2.

3.5.1. Matlab 8.1

The main software used in this study for writing the code for building extraction is MATLAB 8.1. MATLAB (Matrix Laboratory) is a high-level language and interactive environment for numerical computation, visualization, and programming. The MATLAB is used for analyzing the data, developing the algorithms, and creating the models and applications. The language,

tools, and built-in math functions enable the users to explore multiple approaches, and reach a solution faster than with spreadsheets or traditional programming languages, such as C/C++, FORTRAN, Python and Java. The MATLAB is used for a wide range of applications, including signal processing and communications, image processing, video processing, control systems, test and measurement, computational finance, and computational biology.

Table 3.2: Software used in the Present Research

Software	Version	Explanation
MATLAB	8.1	MATLAB is a high-level language and interactive environment for numerical computation, visualization, and programming. MATLAB is used for analyzing the data, developing the algorithms, and creating the models and applications
ERDAS Imagine	11	ERDAS Imagine is a broad collection of software tools for digital image processing and related applications.
ArcGIS	10.2	ArcGIS is the name of a group of GIS software modules developed by Environmental Systems Research Institute (ESRI) (ESRI, 1994). ArcGIS provides full advanced analysis and data management capabilities, including geostatistical and topological analysis tools.

3.5.2. ERDAS Imagine 2011

The software used for performing supervised classification on QuickBird imageries is ERDAS Imagine 2011.ERDAS Imagine is developed by Leica Geosystems (USA). It is a remote sensing based software for geospatial applications with raster graphics editor abilities. It is a toolbox which primarily allows the user to perform geospatial raster data processing operations, like radiometric and spectral enhancement, supervised, unsupervised and hybrid classification of remote sensing data. The digital images prepared, displayed and enhanced are used for mapping in GIS or in computer-aided design (CAD) software. The ERDAS imagine also have many easy to use GIS analysis capabilities. It also has many surface analysis capabilities, such as generation of Digital Elevation Model (DEM) and slope map. Its Imagine Objective module provides a framework to automate the process of feature extraction from high resolution imageries. With the help of ERDAS (Earth Resources Data Analysis Systems) Imagine, it is possible to see the features that would not usually be visible. It also helps in locating geo-positions of those features that would otherwise be graphical. Other usage examples of ERDAS Imagine are linear feature extraction, generation of processing work flows

by using the Spatial Modeler module, import and export of data to and from a wide variety of image formats, ortho-rectification, mosaicking of imagery etc.

3.5.3. ArcGIS 10.2

ArcGIS is a group of GIS software modules developed by ESRI. ArcGIS is the industrial standard software used for GIS, and is also widely used in educational institutions, government organizations and private industries. The license of ArcGIS suite is available at three license levels: Basic, Standard, or Advanced. Each higher level provides the user with more advanced features to perform a variety of querying on a data set. ArcInfo is the highest level of licensing, and provides full advanced analysis and data management capabilities such as 3D Analyst, Spatial Analyst, and the Geostatistical Analyst module. It includes the features of ArcReader, ArcView, and ArcEditor, adding geoprocessing functionality. It is a vector data based software. However, it can be used for raster data analysis using the Spatial Analyst Module.

ArcInfo comprises of three basic modules: ArcMap, ArcCatalog, ArcGlobe and ArcScene. ArcMap is very simple to use. In ArcMap, users can create and manipulate the data set. Also, a variety of information, like arrows, scale bars, titles, legends etc. can be included in the data sets to make it more revealing. Its capabilities of switching on the required module e.g., Spatial Analyst, 3D Analyst etc., made it computationally very efficient. ArcMap is also used for digitization of the objects present in an image. ArcMap is used to develop custom map applications, display and query maps and perform several other map-based tasks. ArcMap's layout composer is used to prepare cartographic quality maps for presentation. ArcCatalog is used to explore and manage the spatial data stored in folders on local disks or in relational databases that are available on the network. ArcCatalog is also used for database designs, recording and viewing the metadata. ArcGlobe and ArcScene are used for specialized 3-D visualization and analysis. ArcInfo has very powerful customizations capabilities using Arc Objects and Arc Macro Language (AML), Visual Basics (VB) and C++ programming languages.

CHAPTER 4 METHODOLOGY

4.1. INTRODUCTION

In this chapter, a detailed description of the methodology developed to achieve the research objectives discussed in Chapter 1 has been provided. Figure 4.1 outlines the overview of methodology adopted in the research work conducted for the extraction of buildings from high resolution satellite images. The detailed description of the methodology proposed in the research work has been provided in the subsequent sections.

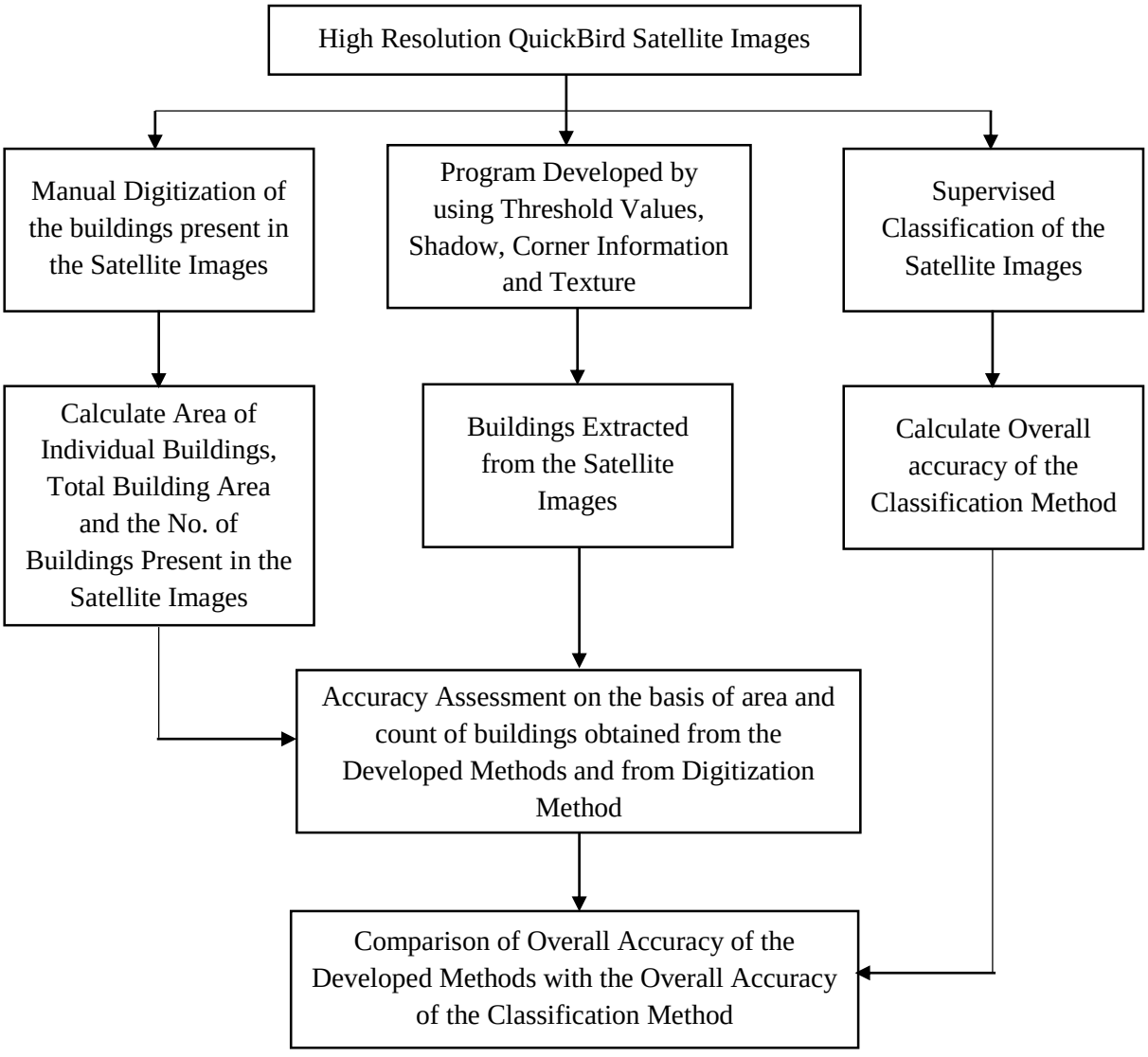

Figure 4.1: Overview of the Methodology Adopted in the Research Work

4.2. SELECTION OF THE PARAMETERS REQUIRED FOR BUILDING EXTRACTION

From review of the literature, it was found that threshold value (pixel value), colour, texture, shadow, size, shape and height are the parameters required for building extraction from high resolution MS satellite images. For developing a fully automatic building extraction method, we need to select those parameters that are very essential for building extraction and at the same time can be calculated from the pixel values of the input image. It has been analyzed that height parameter play an important role only when the information about storey of the buildings needs to be extracted. However, calculation of height parameter requires the exact time and date of acquisition, which was not available for the test images used in the present research. Since, the aim of the proposed work was to extract buildings of varying heights hence, height feature was not included in the development of proposed work. The shape parameters have also been omitted because the aim of the research is to extract all types of buildings irrespective of their shapes.

The features used for the proposed work were:

i. Threshold Value
ii. Colour
iii. Texture
iv. Shadow and
v. Size

The threshold value has been used for masking out the pixels not belonging to the building class. Colour feature has been used to change FCC of input test image into the colour space required for that particular process. Texture has been used to obtain the texture feature at pixel level, to cluster the pixels belonging to building class separately. The shadow has been used to validate, the extracted object (having shadow) as a building. Size feature has been used, as a constraint value, to remove the false positives extracted as a building, by the proposed methods.

4.2.1. Color Spaces Used

From the established procedures, it is also found that the color space (also called color model or color system) presents colour information in a way that make certain calculations more convenient. They provide a way to identify colours that is more intuitive. And, color space

conversion is meant to convert the colour data from one colour space to another through a mathematical transformation. Following color spaces were used for the program development of this research:

(i) YCbCr

(ii) HSI

(iii) CIE L*a*b

YCbCr: In YCbCr color space, Y represents luminance, Cb represents blue chromaticity and Cr represents red chromaticity. This color model is used in MPEG (Moving Picture Experts Group) video compression Standards. YCbCr is related to RGB (Red-Green-Blue) by the following way:

$$\begin{bmatrix} Y \\ Cb \\ Cr \end{bmatrix} = \begin{bmatrix} 0.257 & 0.504 & 0.098 \\ -0.148 & -0.291 & 0.439 \\ 0.439 & -0.368 & -0.071 \end{bmatrix} * \begin{bmatrix} R \\ G \\ B \end{bmatrix} + \begin{bmatrix} 16 \\ 128 \\ 128 \end{bmatrix} \quad \textbf{Eq. 4.1}$$

HSI (Hue Saturation Intensity): HSI color space is based on the characteristics of the human's visual system. H denotes the hue that indicates the measure of color purity, S is the degree of a color permeated the white color, I denotes light intensity. HSI provides independent control over hue, saturation and intensity. HSI is related to RGB by the following way:

$$\mathbf{H = polar\ hue\ angle} \quad \textbf{Eq. 4.2}$$

$$S = 1 - \frac{3}{(R+G+B)}\ [\min(R + G + B] \quad \textbf{Eq. 4.3}$$

$$I = \frac{I}{3}(R + G + B) \quad \textbf{Eq. 4.4}$$

The value of H is greater than equal to zero and less than 360. The value of S and I should be greater than equal to zero and less than equal to one.

L*a*b (Lab): This color space was proposed by Commission International del'Eclairage (CIE). In this color space, L represents the lightness component, a component shows the degree green to red and b component shows the degree from blue to yellow.

4.2.2. Texture Analysis Methods Used

Texture is defined as providing information about the spatial arrangement of the colours or intensities in an image. Texture is described qualitatively, by its coarseness under the same viewing condition, and its association to the recurrence of the local spatial patterns. Although coarseness is an important parameter to describe texture, but some other textural parameters commonly used are contrast, density, roughness, directionality, frequency, regularity, uniformity, orientation, and many others (Tamura *et al.*,1978). To define, the texture accurately, is the most critical part of texture analysis.

Two important approaches, which are generally used in texture analysis, are structural and statistical approaches. In structural approach, texture is defined as a set of primitive texels in some systematic or recurring relationship. In statistical approach, texture is a quantifiable measure of the arrangement of intensities in a region. The structural approach works well for man-made and regular patterns, whereas the statistical approach is wide-ranging and easier to compute, and is used more often in practice. The example of statistical methods is Grey Level Co-occurrence Matrix (Haralick et al., 1973), while the example of filter techniques includes Laws' method (Laws, 1980) and Gabor.

Recently, few techniques have been proposed which are based on wavelet decomposition. The texture features that are extracted, from high resolution remote sensing imagery, provides a corresponding source of data which is used in applications that have insufficient spectral information for identification and classification of spectrally heterogeneous landscape units. The methods, such as statistical methods, filter techniques and other techniques are now widely used to perform texture analysis with different criteria, for feature extraction. Following texture methods have been used for the program development of this research:

1. LAWS
2. Wavelet
3. Gabor
4. GLCM
5. Tamura

Laws' texture energy (LAWS):

K. I. Laws (Laws, 1980) developed a texture energy approach that measures the amount of variation within a fixed-size window. This approach has been used for many diverse applications. These measures are computed, by first applying small convolution kernels to a digital image, and then performing anon-linear windowing operation. The 2-D convolution kernels typically used for texture discrimination are generated from the following set of one dimensional convolution kernels of length three and five, as given below:

L3 = [1 2 1], E3 = [-1 0 1], S3 = [-1 2 -1]

L5 = [1 4 6 4 1] E5 = [-1 -2 0 2 1]

S5 = [-1 0 2 0 -1] W5 = [-1 2 0 -2 1]

R5 = [1 -4 6 -4 1]

These mnemonics stands for Level - average grey level, Edge - extract edge features, Spot - extract spots, Wave - extract wave features, and Ripple - extract ripples.

Wavelet Transform:

The use of wavelet transform was first proposed for texture analysis by Mallet (1989). This transform provides a robust methodology for texture analysis at different scales. The wavelet transform allows for the decomposition of a signal using a series of elemental functions, called wavelets and scaling, which are created by scaling and translations of a base function, known as the mother wavelet:

$$s \in R^{+} \qquad u \in R \qquad \textbf{Eq. 4.5}$$

$$\varphi_{s,u}(x) = \frac{1}{\sqrt{s}}\,\varphi\left(\frac{x-u}{s}\right) \qquad \textbf{Eq. 4.6}$$

Where "*s"* governs the scaling and "*u"* the translation. The wavelet decomposition of a function is obtained by applying each of the elemental functions or wavelets to the original function:

$$Wf(s,u) = \int_R f(x)\frac{1}{\sqrt{s}}\varphi^{*}\left(\frac{x-u}{s}\right)dx \qquad \textbf{Eq. 4.7}$$

In practice, wavelets are applied as high-pass filters, while scalings are equal to low-pass filters. As a result, wavelet transform decomposes the original image into a series of images at different scales, called trends and fluctuations. The former are averaged versions of the original image,

and the latter contain the high frequencies at different scales or levels. Since the most relevant texture information gets lost in the lowpass filtering process, only fluctuations are used to calculate texture descriptors. If the inverse transform is applied to the fluctuations, three reconstructed images, or details, are obtained; horizontal, vertical and diagonal. This process is called multi-resolution analysis.

Regarding previous work in image texture analysis using wavelet decomposition, different texture features have been extracted; sometimes from the fluctuations and in other cases from the details, subjective to the authors. Sometimes, basic features directly extracted from the histogram were used, suchas the local energy (Randen and Husoy, 1999) or variance filter (Ferro and Warner, 2002). However, Simard et al. (1999) used wavelet histogram signatures, while Van de Wouwer et al. (1999) compared the energy wavelet histogram signatures and co-occurrence features.

Gray Level Co-occurrence Matrix (GLCM):

Gray-scale image is used for GLCM creation. The different parameters which are used for the construction of GLCM are as follows:

i. *Contrast:* Contrast is defined as a measure of intensity contrast between a pixel and its neighbour over the entire image. The contrast value is 0 when the image is constant, and contrast value is the largest for the random intensity image. Also, the pixel intensity and neighbour intensity are very different when the image is of random intensity. The equation of the contrast is shown below:

$$\text{Contrast} = \sum_i \sum_j |i - j|^2 p(i, j) \qquad \textbf{Eq. 4.8}$$

ii. *Energy:* Energy is defined as a degree of uniformity and its value is maximum when the image is constant. The equation of the energy is shown below:

$$\text{Energy} = \sum_i \sum_j p(i, j)^2 \qquad \textbf{Eq. 4.9}$$

iii. *Homogeneity:* Homogeneity is defined as the spatial closeness of the distribution of the co-occurrence matrix. For uniform distribution of the co-occurrence matrix, the value of homogeneity is equal to 0, and when the distribution is only on the diagonal of the matrix, its value is 1. The equation of the homogeneity is shown below:

$$\text{Homogeneity} = \sum_i \sum_j \frac{p(i,j)}{1+|i-j|} \quad \textbf{Eq. 4.10}$$

iv. *Entropy:* Entropy is defined as the degree of randomness of the elements of the co-occurrence matrix. When elements in the matrix are equal, then the value of entropy is maximum. When all elements in the matrix are dissimilar then its value is zero. The equation of the entropy is shown below:

$$\text{Entropy} = \sum_i \sum_j p(i,j) \log(p(i,j)) \quad \textbf{Eq. 4.11}$$

v. *Correlation:* It is also defined as the local variation of the intensity and computed using the following equation:

$$\text{Correlation} = \sum_i \sum_j \frac{(i-\mu_i)(j-\mu_j)\, p(i,j)}{\sigma_i \sigma_j} \quad \textbf{Eq. 4.12}$$

Tamura Features*:*

Coarseness, contrast, directionality, line-likeness, regularity and roughness are the six features of Tamura. Coarseness, contrast and directionality correlate strongly with the human insight, and therefore, these are of prime importance.

4.3. SELECTION OF TYPES OF BUILDINGS

In Indian context, the National Building Code of India (NBC, 2005), categorise the types of buildings that includes; Residential, Educational, Institutional, Assembly, Business, Mercantile, Industrial, Storage and Hazardous buildings. In the proposed methodology, the concern is about the shape, size and orientation of the types of buildings rather than the functional aspect of the buildings. On verification of satellite images by field survey, it was observed that Residential, Educational, Business and Industrial categories tend to have more variation in shape, size and orientation of the buildings. Also, the shape, size and orientation of remaining categories of the building were more or less similar. This formed the basis for limiting the categories of buildings in methodology adopted for research mentioned as:

1. Residential Buildings
2. Educational Buildings
3. Business Buildings and
4. Industrial buildings.

Residential Buildings: These shall include any building, in which sleeping accommodation is provided for normal residential purposes, with or without cooking or dining or both facilities. Residential buildings are further classified into the following categories:

- Planned Buildings
- Unplanned Buildings
- Slum Buildings

Educational Buildings: These shall include any building used for school, college or day-care purposes involving assembly for instruction, education or recreation.

Business Buildings: These shall include any building or part of a building which is used for transaction of business for keeping of accounts and records and similar purposes, professional establishments, service facilities, etc. City halls, town halls, court houses and libraries shall be classified in this group so far as the principal function of these is transaction of public business and keeping of books and records.

Industrial Buildings: These shall include any building or part of a building or structure, in which products or materials of all kinds and properties are fabricated, assembled, manufactured or processed, for example, assembly plants, laboratories, dry cleaning plants, power plants, pumping stations, smoke houses, laundries, gas plants, refineries: dairies and saw-mills.

4.4. PROGRAM DEVELOPMENT

Four different methods for extracting individual buildings from high resolution MS images have been developed in Matlab 2013a environment. The methods have been based on:

1. Threshold Value
2. Shadow and Corner Information
3. Texture
4. Threshold, Texture and Shadow

The detailed description of these methods has been provided in the subsequent subsections. The basic details of the computer on which the proposed methods have been implemented are listed in Table 4.1.

Table 4.1: Details of Computer used to run the developed Methodology

Windows Edition	Windows 7 Home Premium (Service Pack 1)
Processor	Intel(R) Core™ i3 CPU M330@2.13GHz
RAM	3.00 GB
System Type	32-bit Operating System

4.4.1. Building Extraction based on Threshold Value

Initially, high resolution MS QuickBird satellite image has been taken as input. Then, vegetation mask has been prepared by first making two difference images obtained by subtracting Red band from the NIR band (NIR-R) and Green band from the NIR band (NIR-G), respectively. The data points have been created using these two difference images. K-means clustering has been used to cluster the data points into two classes (vegetation and background). Mean value is calculated for each cluster. The cluster having largest mean value has been selected as vegetation cluster, and saved as vegetation mask.

After preparing vegetation mask, non-building mask has been prepared from the input image by first converting the image into YCbCr colour space. A difference image of Cb and Cr has been created and the pixel identifications (IDs) having value less than 10, have been selected. An array has been created having the same dimensions as the input image with all values having value one for the pixel IDs selected in the previous step, and for all other pixel values equal to zero. Again, the input image has been converted into LAB colour space. All pixel IDs with values less than zero in A component of LAB and greater than zero in B component of LAB have been selected. Another array has been created having the same dimensions as the input image with all values having value one for the pixel IDs selected in the previous step, and for all other values equal to zero. A union operation has been performed on the pixel IDs having value one in 1st and 2nd array. A 3rd array has been created having value 1 for those pixels which we get from the union operation and having the pixel value zero for all other pixel IDs. This array results in a non-building mask.

After preparing vegetation and non-building mask, shadow mask has been prepared from the input image by first plotting a histogram of green band. Thereafter, a local minima has been

calculated. The value of local minima has been taken as the threshold for extracting shadow. The pixels having values less than the threshold values are the shadow pixels. So, another array has been created having zero value for all pixel IDs for which the value in green band has been greater-than-equal-to the threshold value and having pixel value one for all other pixel IDs.

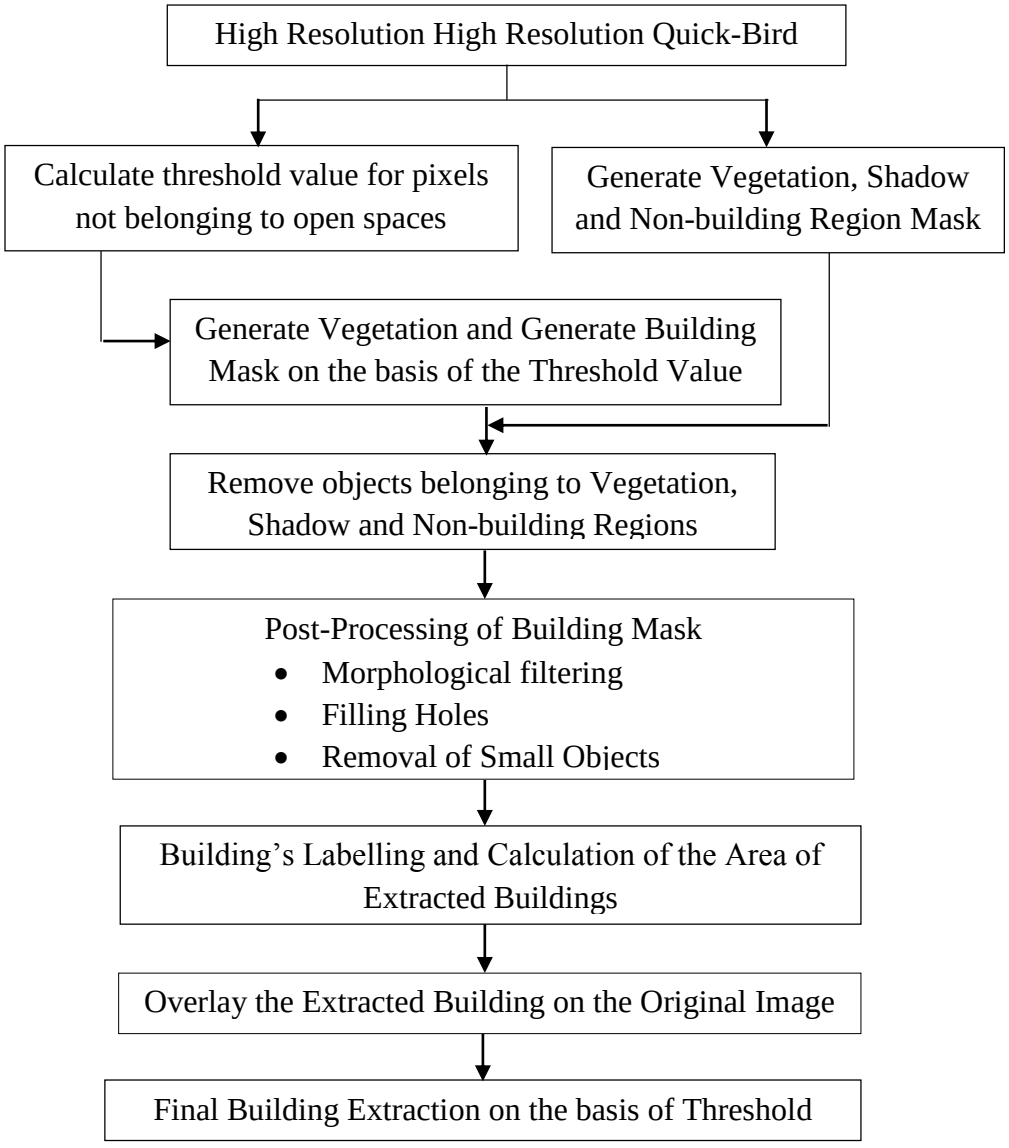

Figure 4.2: Methodology Developed for Building Extraction using Threshold Value

After preparing these masks, a threshold value for the pixels which do not belong to open spaces has been calculated on the basis of weight, mean and variance. By using this threshold value, a building mask has been prepared. Vegetation, shadow and non-building areas have been masked out from the input image if any of them have been extracted as building. Post-

processing has been carried out on resulting image to smoothen the edges and for filling the small holes present in the extracted buildings. After this step, labelling of the extracted buildings have been done and the area has been calculated for each building. Then the buildings having area less than the threshold value (specified by the users) have been masked out which finally results into individual building extraction on the basis of threshold values. After removing the small objects, again, labelling of the buildings have been done and the area have been calculated. The extracted buildings are overlaid on the input image for a better visualisation of the extracted buildings. Flow chart of the proposed methodology is shown in Figure 4.2.

4.4.2. Building Extraction based on Shadow and Corner Information

Initially, high resolution MS QuickBird satellite image has been taken as input. Then, vegetation mask, shadow mask and non-building area mask were prepared as described in previous section. The existing corners in the input satellite image have been detected by using Harris corner detection method (Harris and Stephens, 1988). According to Harris corner detection method, the corner points can be easily recognized by looking at intensity values within a small window. For a flat region, there will be no change in the intensity values in all directions. For an edge, there will be no change in the intensity values along the edge directions. For corner points, shifting the window in any direction should yield a large change in appearance. Thereafter, the corners have been overlaid on the shadow mask and the corners which are closer to shadow but do not fall into shadow have been extracted. These corners belongs to the buildings present in the image. By using this corner information, a probable threshold value for building areas has been calculated and a rough building mask has been prepared. After that non-building mask, vegetation mask and shadow mask have been applied to mask out the non-building area, vegetation and shadow, in case any of the feature have been extracted as a building. Finally, post-processing has been carried out on resulting image to smoothen the edges and for filling the small holes present in the extracted buildings. After this step, labelling of the extracted buildings have been done and the area has been calculated for each building. Then the buildings having area less than the threshold value (specified by the users) have been masked out which finally results into individual building extraction on the basis of threshold values. After removing the small objects, again, labelling of the buildings has been done and the area has been calculated. Flow chart of the developed methodology is shown in Figure 4.3.

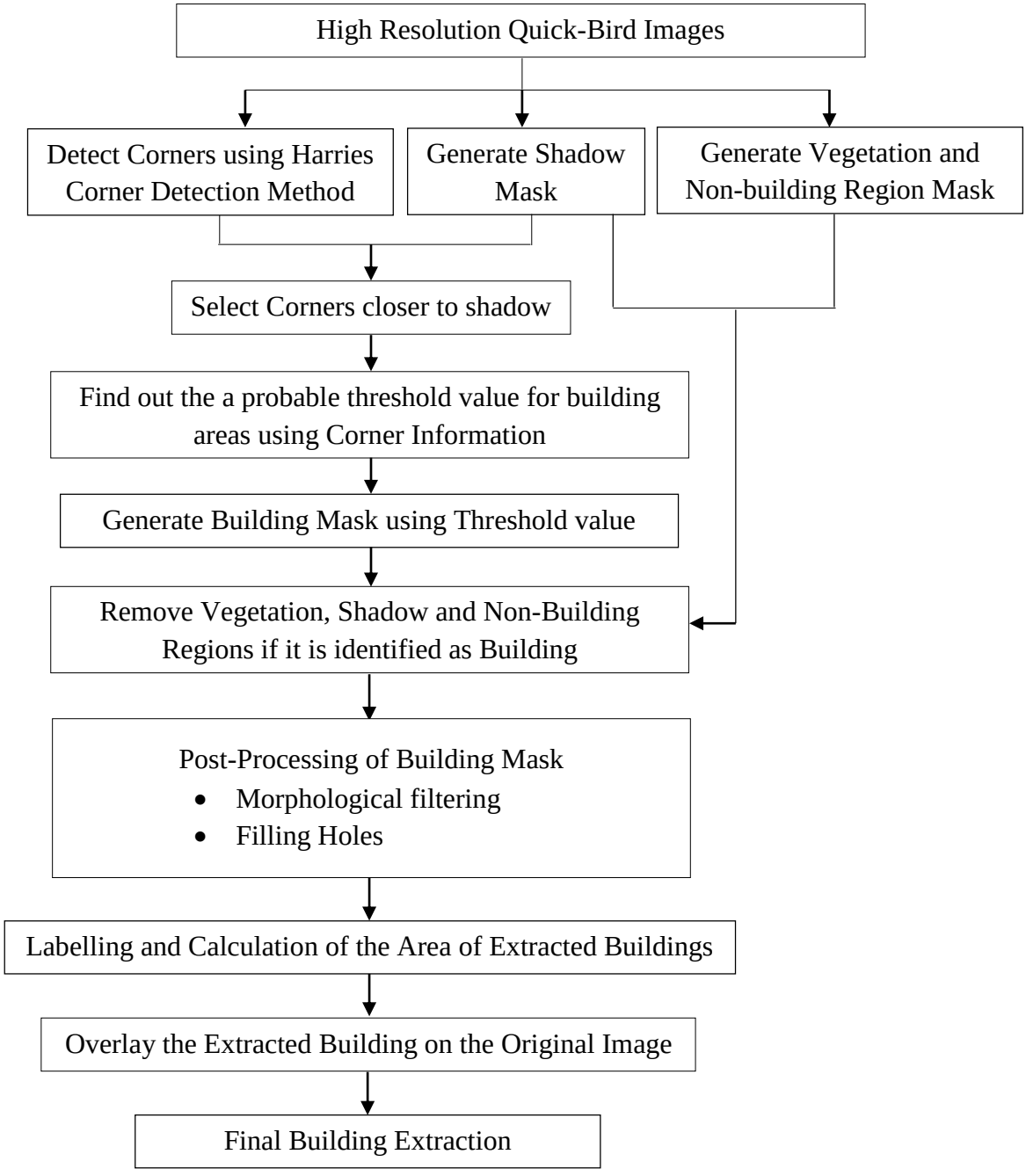

Figure 4.3: Methodology for extracting Buildings using Shadow and Corner Information

4.4.3. Building Extraction on the Basis of Texture

Laws, Wavelet, GLCM, Gabor and Tamura texture methods are selected for extracting buildings from high resolution satellite images. The user has to select which texture method or a combination of the texture methods to be used for extracting texture features for each pixel of the test images. Then K-means clustering method has been applied for generating a building mask from the texture generated pixel values. After this step, some post-processing has been carried out on resulting image to smoothen the edges and for filling the small holes present in the extracted buildings. After this step, labelling of the extracted buildings has been done and the area has been calculated for each building. Then the buildings having area less than the threshold value (specified by the users) have been masked out. After removing the small

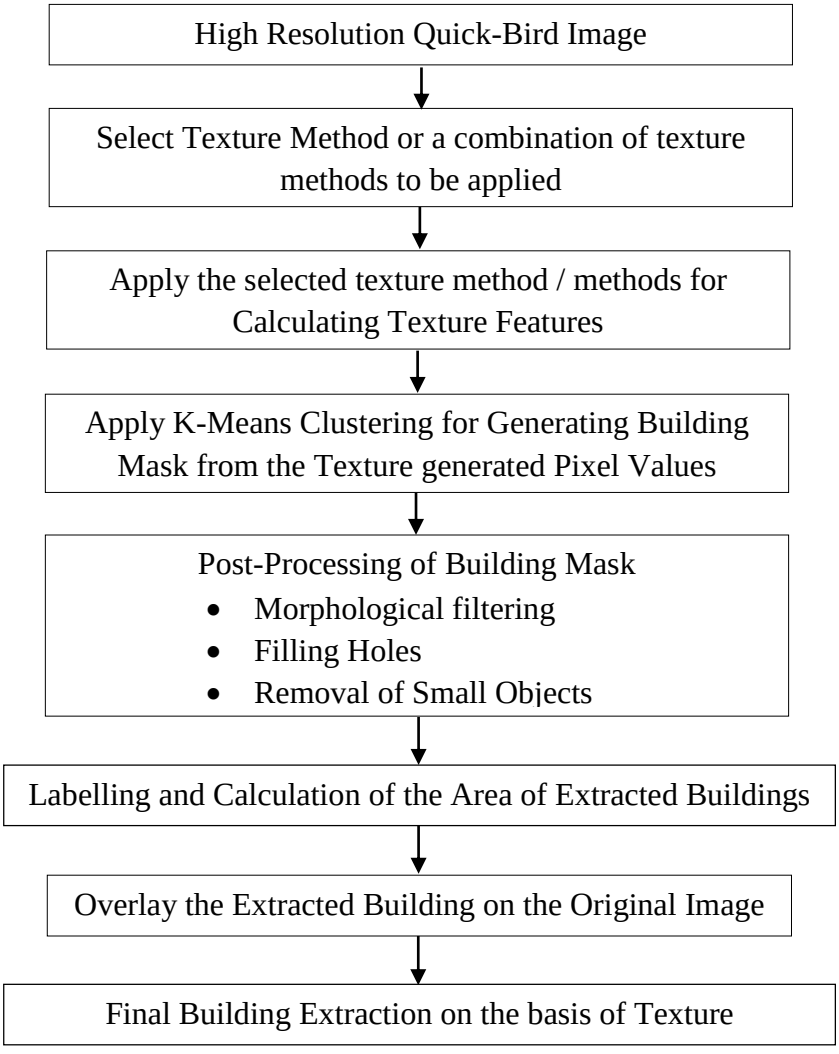

Figure 4.4: Methodology for Extracting Buildings using Texture

objects, again, labelling of the buildings has been done and the area has been calculated. Flow chart of the proposed methodology is shown in Figure 4.4.

4.4.4. Building Extraction on the Basis of Threshold, Texture and Shadow

This method involved the combination of threshold method and texture method. Initially, two building masks have been generated, one by using threshold value and another one by using

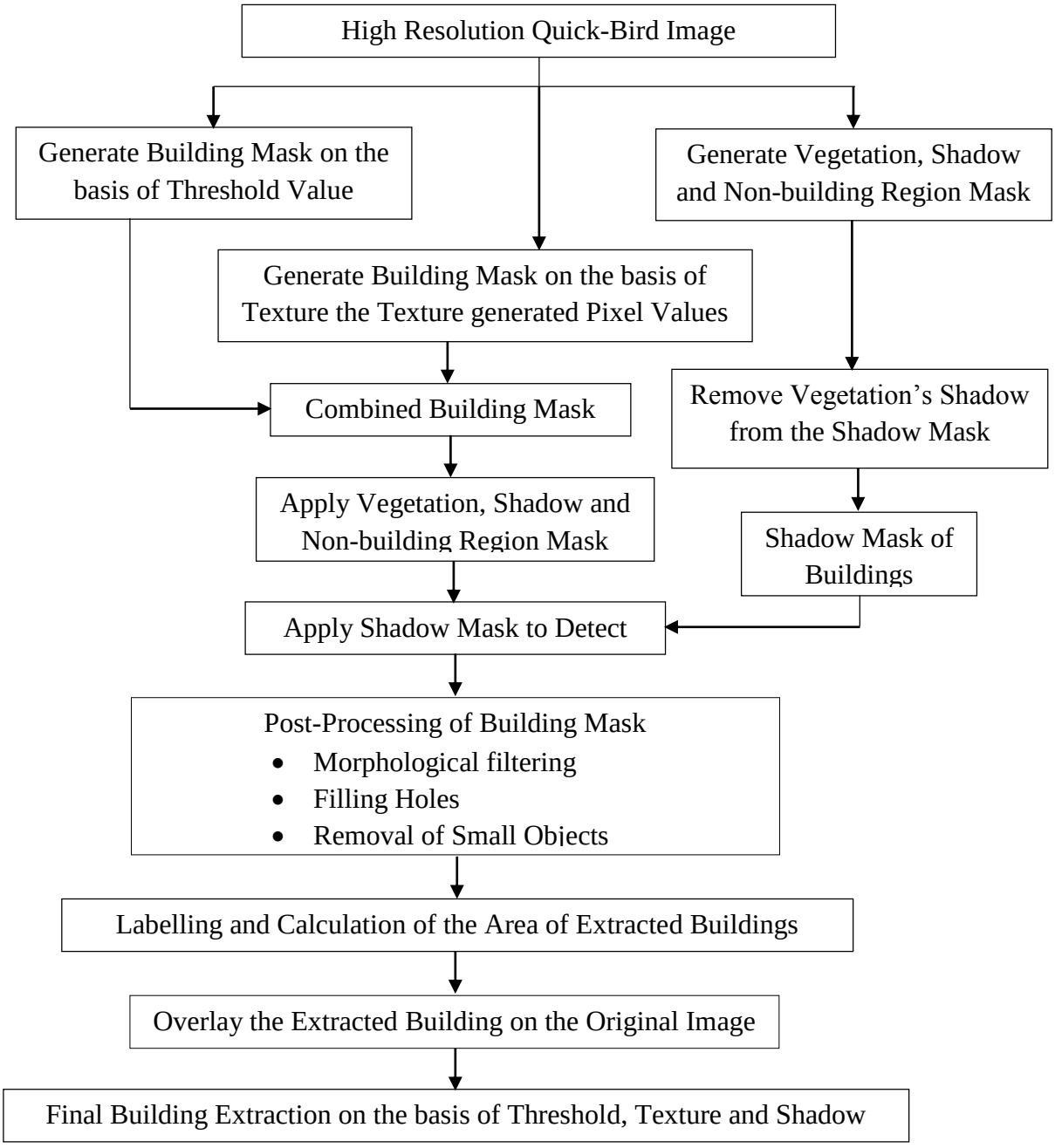

Figure 4.5: Methodology for Extracting Buildings using Threshold, Texture and Shadow

texture. These building masks have been combined to make another building mask based on both texture and threshold. Thereafter, non-building areas, shadow and vegetation were masked out if any of them are extracted as a building. A shadow mask of buildings has been generated by removing the shadow of vegetation from the earlier generated shadow mask. Then the verification of the extracted buildings has been done by applying the shadow mask on the extracted buildings to detect true buildings and remove false positives. After this step, some post-processing has been carried out on resulting image to smoothen the edges and for filling the small holes present in the extracted buildings. After this step, labelling of the extracted buildings has been done and the area has been calculated for each building. Then the buildings having area less than the threshold value (specified by the users) have been masked out which finally resulted into individual building extraction. After removing the small objects, labelling of the buildings has been done and the area has been calculated. Flow chart of the proposed methodology is shown in Figure 4.5.

4.5. PREPARATION OF DATASET

The data set used plays an important role in its development, analysis and accuracy assessment of the research. The dataset should be prepared in a way that it can check, whether the developed methods are achieving the desired objectives or not. To test the building extraction methods developed in the present research, we need high resolution satellite images of an Indian city containing all types of urban infrastructure/buildings/built structures i.e., residential (planned, unplanned and slum), industrial, business and educational buildings having different shapes, sizes and orientations. Due to the economical availability and desired features of having all types of urban infrastructure, the high resolution QuickBird satellite imageries of Jaipur, Rajasthan have been selected for testing the developed building extraction methods.

For analyzing the results of the building extraction approach developed in the present research, the dataset has been prepared by manual digitization of the buildings present in the test images. The accuracy obtained from the developed building extraction methods has been compared with the accuracy obtained from the supervised classified test images. The details of the manual digitization and supervised classification are provided in the succeeding sections.

4.5.1 Digitization

All buildings present in the test images were manually digitized in the form of polygon feature class to get the exact count and area of buildings present. In Polygon Feature Class, Polygons are represented by a closed set of lines and are used to define features, such as administrative boundaries. The buildings were digitized at a map scale of 1:300. The buildings were also manually digitized by using ArcGIS 10. The digitized buildings have been used as a reference set for comparing the extracted buildings. The labelled digitized buildings overlaid on input images, are shown in Figure 4.6.

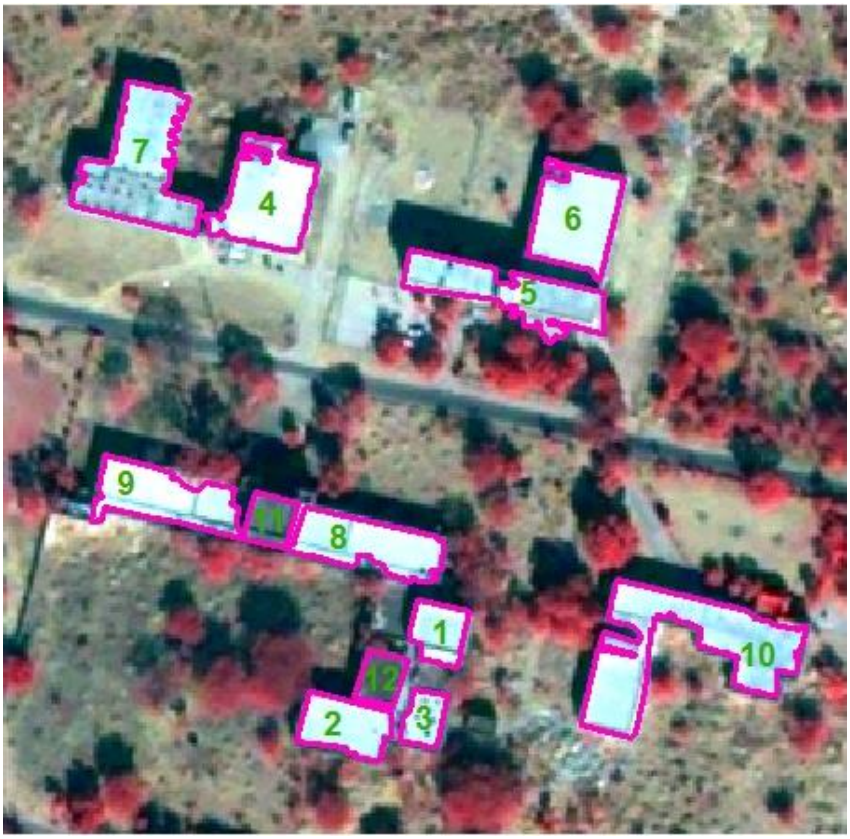

Figure 4.6 (a): Image 1

Figure 4.6 (b): Image 2

Figure 4.6 (c): Image 3

Figure 4.6 (d): Image 4

Figure 4.6 (e): Image 5

Figure 4.6 (f): Image 6

Figure 4.6 (g): Image 7

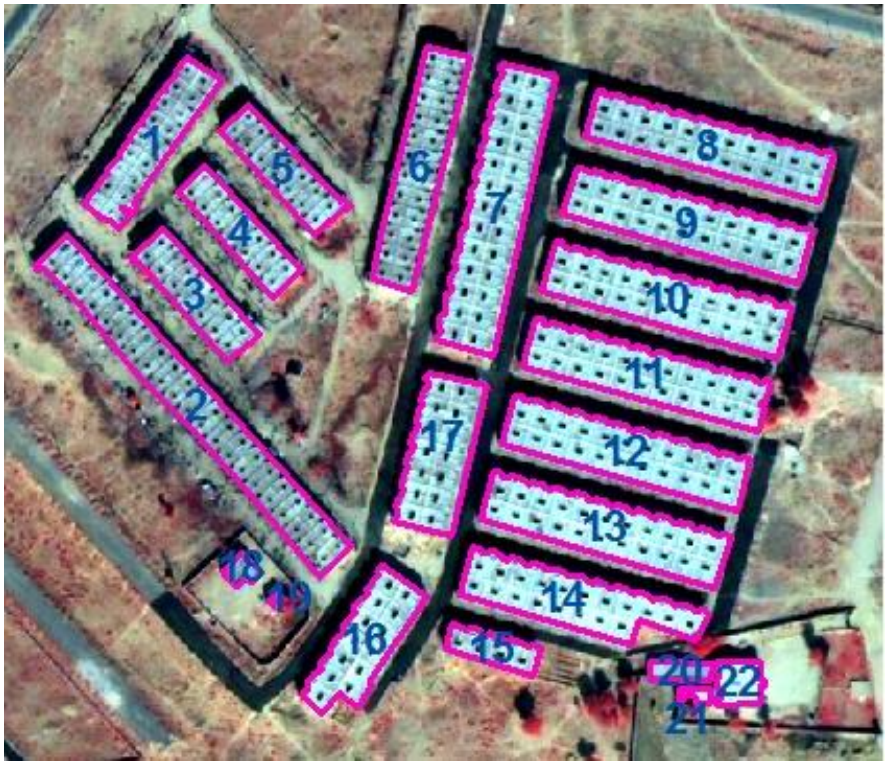

Figure 4.6 (h): Image 8

Figure 4.6 (i): Image 9

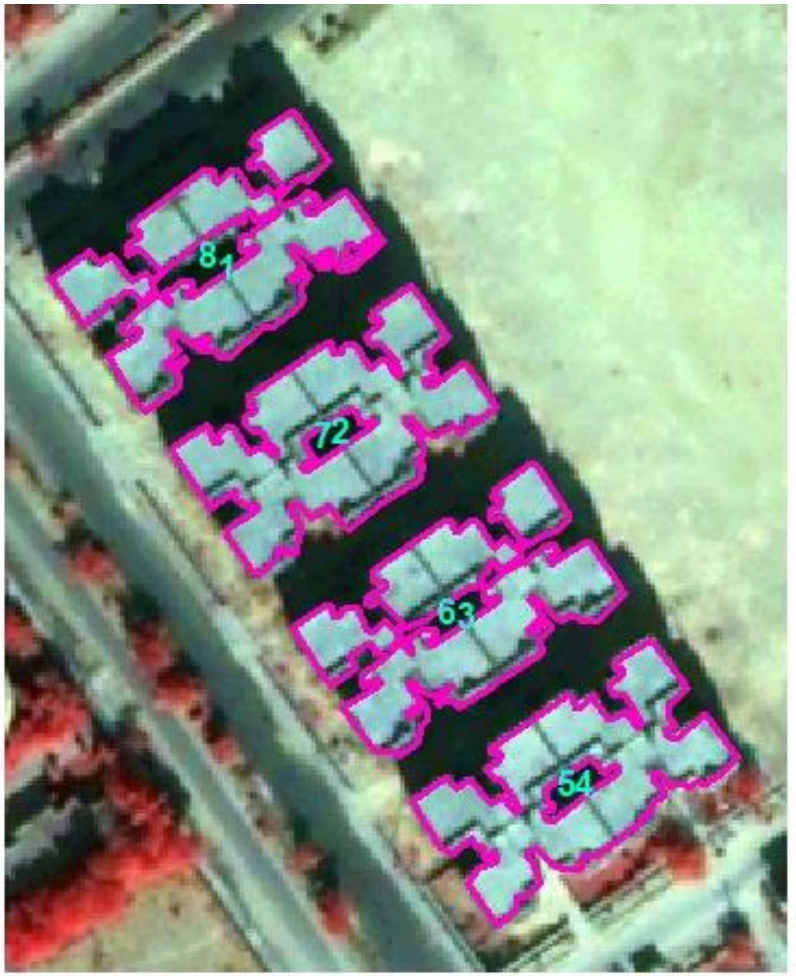

Figure 4.6 (j): Image 10

Figure 4.6 (k): Image 11

Figure 4.6 (l): Image 12

Figure 4.6 (m): Image 13

Figure 4.6 (n): Image 14

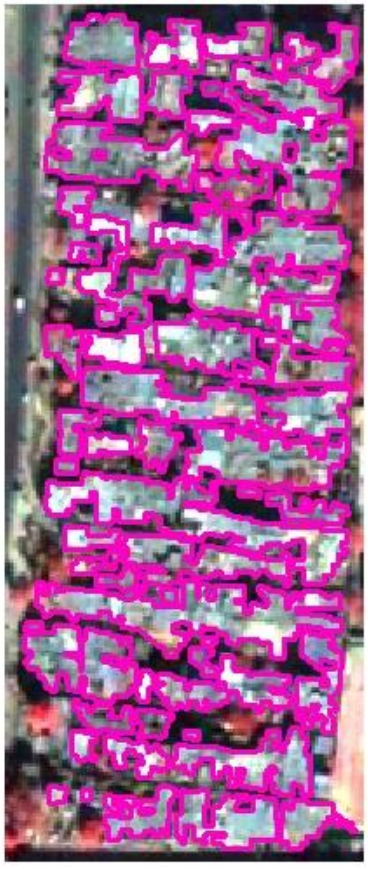

Figure 4.6 (o): Image 15

Figure 4.6 (p): Image 16

Figure 4.6: Digitized Images overlaid on the input images.

4.5.2 SUPERVISED CLASSIFICATION

Supervised classification is a tool used for extracting information from satellite images. In the present study, supervised classification has been performed using Maximum Likelihood Classifier (MLC). MLC algorithm is one of the most popular supervised classification methods (Boloorani et al., 2006; Kumar et al., 2006(a); Kumar et al., 2006(b); Dikshit and Behl, 2009;Guo et al. 2012). The MLC algorithm is based on probability that a pixel belongs to that particular landuse/landcover class. The important steps carried out for conducting supervised classification of the test image are as follows:

- Deciding the set of classes into which the image has to be segmented. The classes selected were: buildings, roads, vegetation, barren/open land and shadow.
- Extracting the spectral features of landcover classes from the image. These are known as training data. Training data consists of appropriate pixel from each of the desired set of classes. Training sets have been be decided using maps and visiting fields.
- Using the training data, the parameters of the MLC algorithm were estimated. These set of parameters for a particular class is called the signature of that class.
- Then, classification of the image data, into appropriate defined classes was done.
- Accuracy assessment of classification has been carried out. It compares the classification results with the ground-truth data which is assumed to be true in order to determine the accuracy of classification.

The details of training sets selected on the images for building classification are given in Table 4.2. The supervised classified images are given in Figure 4.7. In the supervised classified images, pink colour represents buildings, green colour represents vegetation, grey colour represents roads and brown colour represents open/barren land.

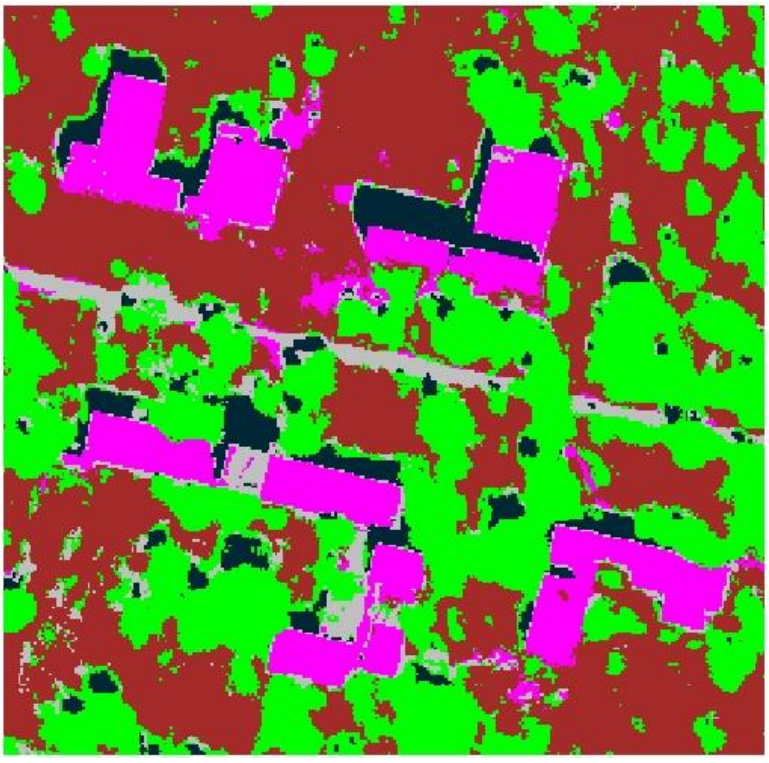

Figure 4.7 (a): Image 1

Figure 4.7 (b): Image 2

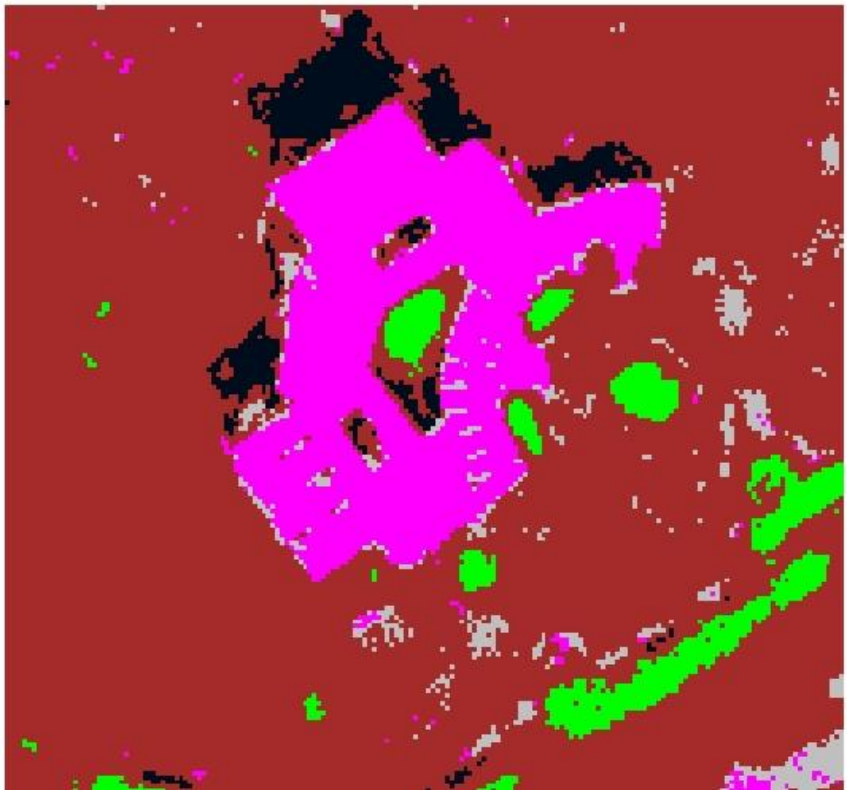

Figure 4.7 (c): Image 3

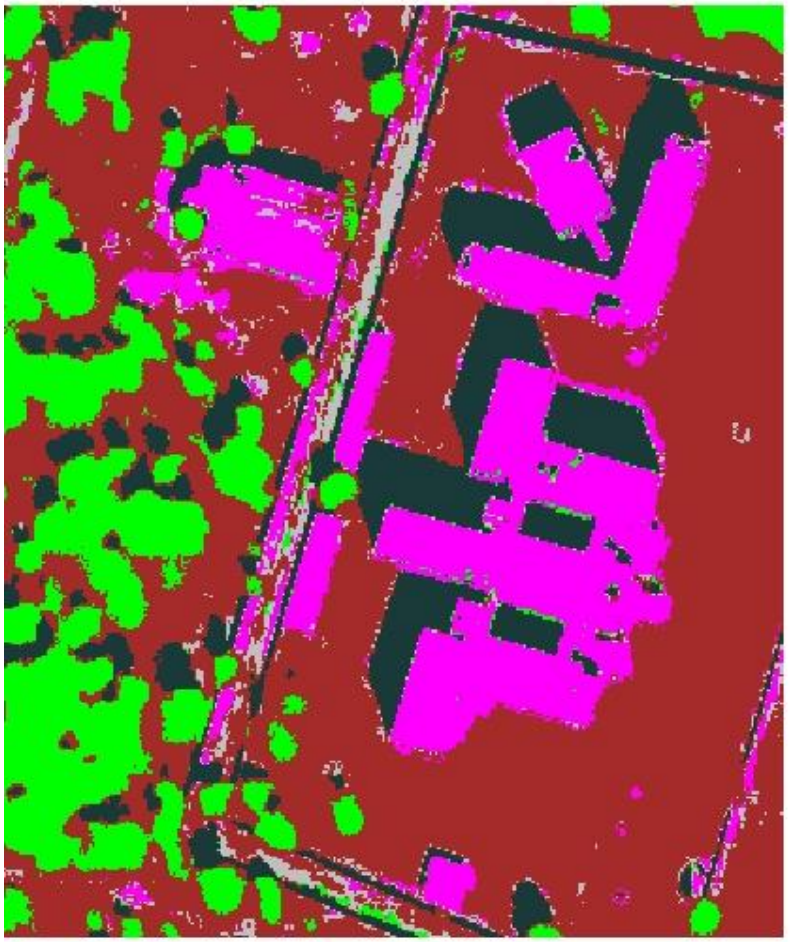

Figure 4.7 (d): Image 4

Figure 4.7 (e): Image 5

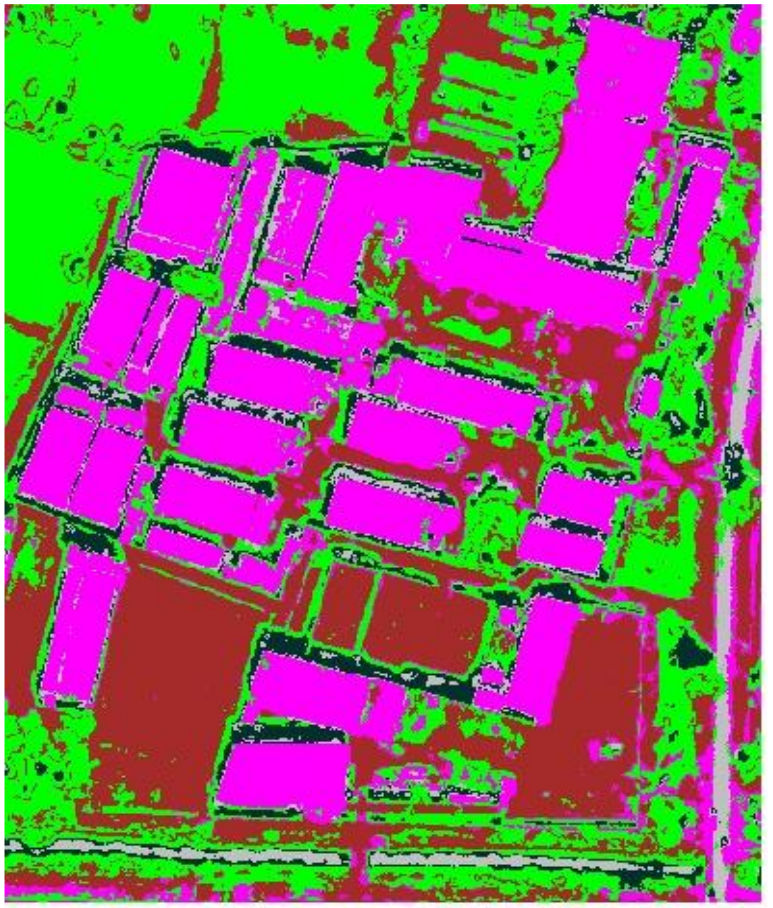

Figure 4.7 (f): Image 6

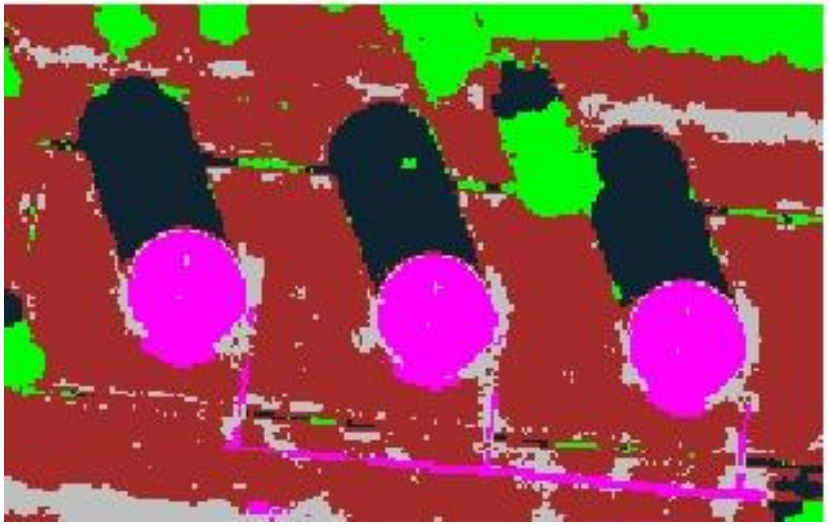

Figure 4.7 (g): Image 7

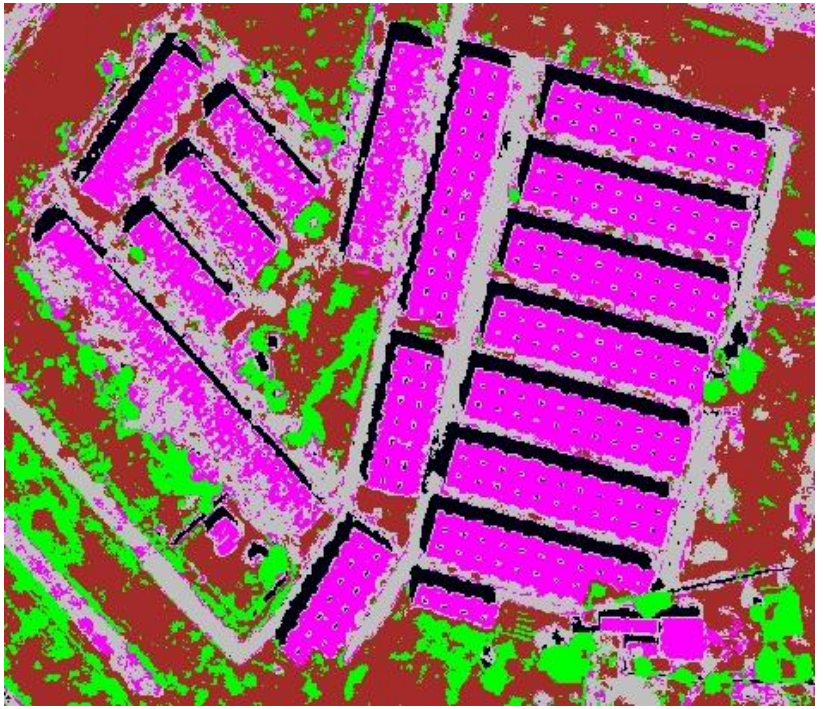

Figure 4.7 (h): Image 8

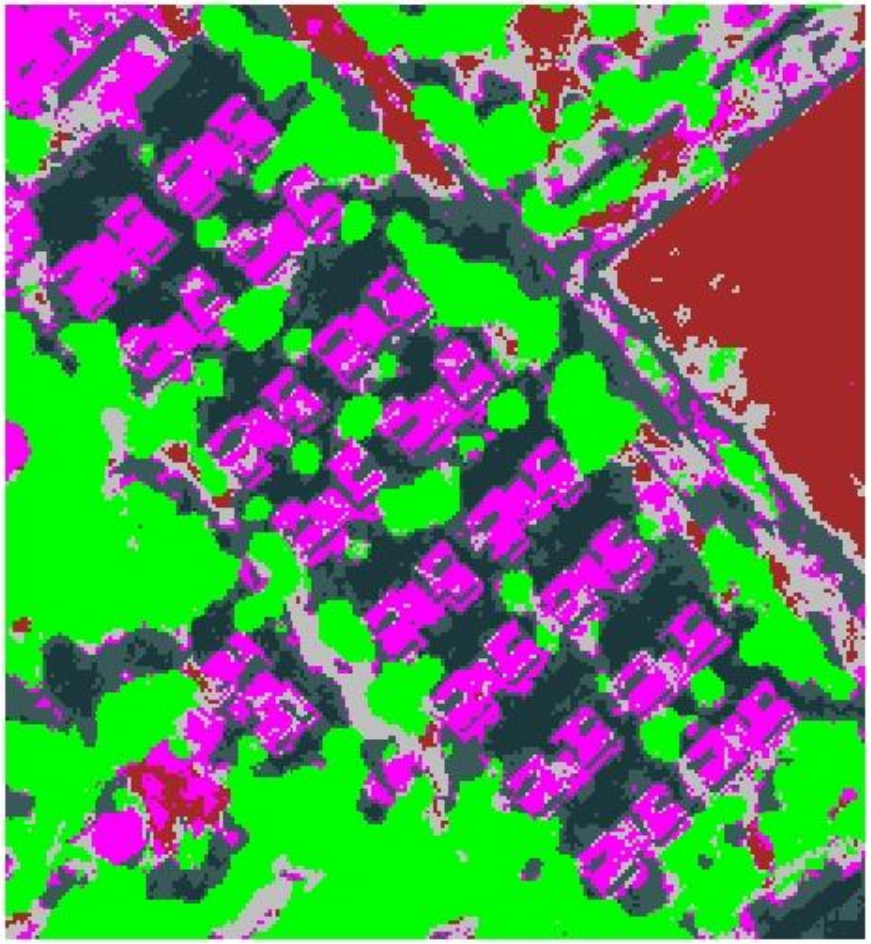

Figure 4.7 (i): Image 9

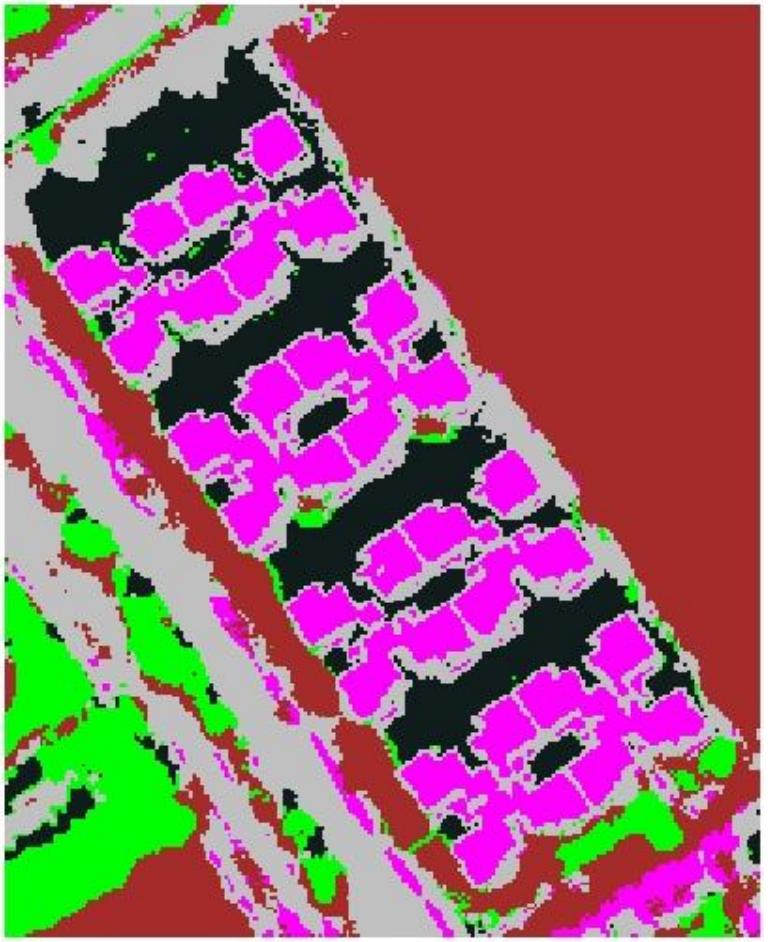

Figure 4.7 (j): Image 10

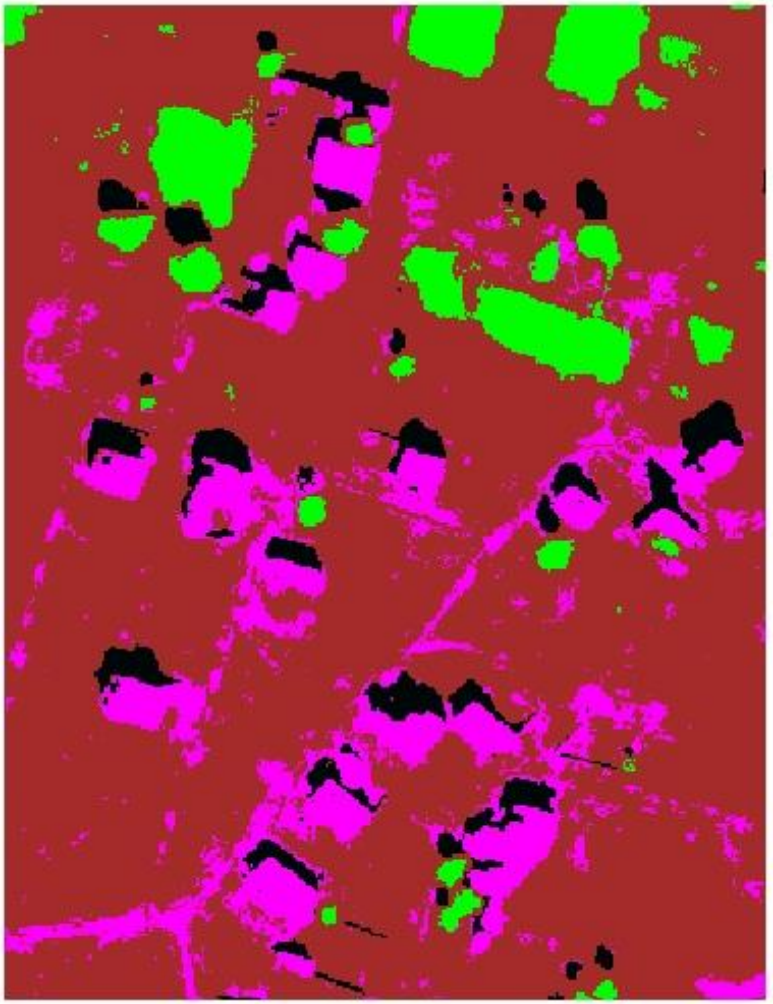

Figure 4.7 (k): Image 11

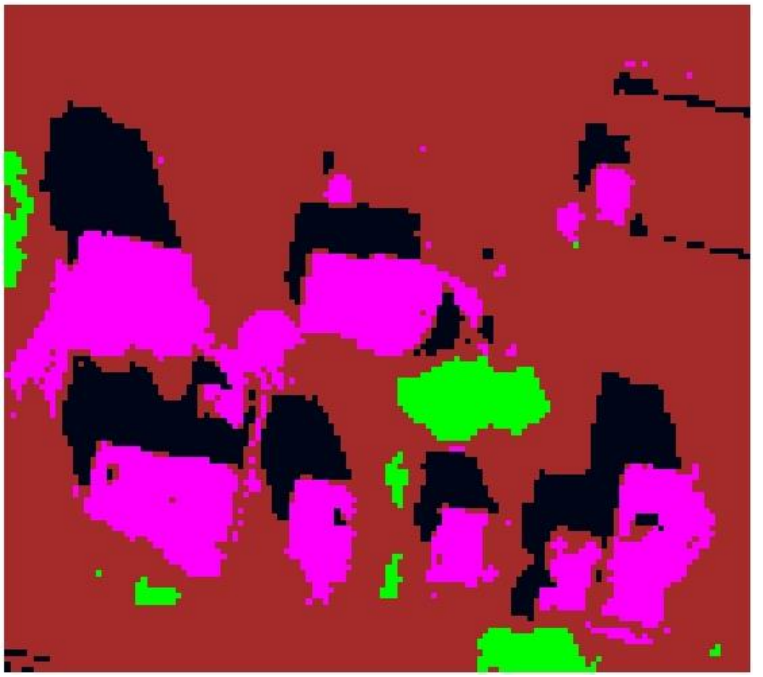

Figure 4.7 (l): Image 12

Figure 4.7 (m): Image 13

Figure 4.7 (n): Image 14

Figure 4.7 (o): Image 15

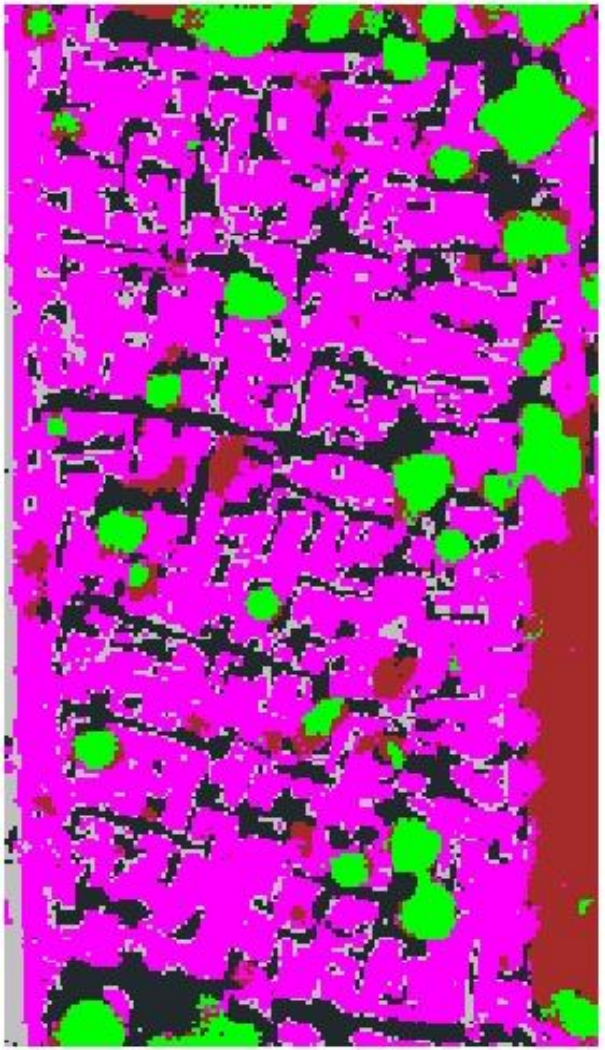

Figure 4.7 (p): Image 16

Figure 4.7: Supervised Classified Images

Table 4.2: Details of Training Samples taken for Supervised Classification

S. No.	No. of Training Samples taken for Building Class	No of Training Samples taken for Building Classes	No of Training Samples taken for Vegetation Classes	No of Training Samples taken for Barren Classes	No of Training Samples taken for Road Classes	No of Training Samples taken for Shadow Classes
Image 1	3	34, 40, 39	31, 20, 20	27, 21, 35	23, 25, 30	35
Image 2	3	40, 22, 30	37, 44	35	25, 17	35
Image 3	1	34	35,34	31, 31	48	35
Image 4	4	27, 31, 22, 32	25, 31	25, 27	7	6
Image 5	2	39, 41	19, 12	19, 36, 35	17	30
Image 6	3	41, 56, 60	32, 37	24, 31	10	7
Image 7	3	23, 28, 20	21, 25, 16	23, 34, 29	29	35
Image 8	4	29, 28, 31, 28	28, 21, 25	22,27	30	30
Image 9	3	31, 45, 33	29, 35	34	21	41
Image 10	4	37, 33, 39, 29	41, 54, 46	51, 58, 46	36	18
Image 11	2	51, 59	33, 42	26, 29	241-250	8
Image 12	2	24, 29	27, 28, 27	29, 27, 30	22, 17, 26	10
Image 13	5	21, 28, 23, 24, 20	29, 36	42, 66, 51	351-377	8
Image 14	2	23, 26	41, 34	29, 33, 27	13	30
Image 15	2	16, 19	23, 31	21, 23	135-148	9
Image 16	4	30, 31, 29, 30	28, 29, 29	30, 30	28,3 0	30

4.6. THRESHOLD VALUES USED

In the developed methods, non-building area, shadow and building mask have been generated on the basis of some threshold values. These threshold values can either be entered by the user or the algorithm will calculate from the images. The user can either enter threshold values by own choice or select from range of threshold values provided. The provided range of threshold values for masking non-building area, shadow and rough building mask does not have any continuity as they are dependent on the colorspace/colorband used. The colorspace and the

corresponding threshold values used in the developed method for extracting non-building area, shadow and rough building mask are listed in Table 4.3.

Table 4.3: Threshold values provided in the developed method

	Color Space / Color Band Used	**Range of Threshold Value**
Non-building Area	YCbCr	8-15
Shadow	Green Band	130-180
Building Mask	Decorrelation Stretched Green Band	0.3-0.9

In the developed methods, as a post-processing step, artifacts other than buildings were removed on the basis of their area. The threshold values for area, entered as input in the developed methods are listed in Table 4.4.

Table 4.4: Threshold values used for Area

S. No.	**Type of Buildings**	**Area (in sq. m.)**
1	Educational Buildings	100
2	Business Buildings	100
3	Industrial Buildings	50
4	Residential Planned Buildings	50
5	Residential Unplanned Buildings	20
6	Residential Slum Buildings	3

4.7. TEXTURE COMBINATIONS

The combinations of 5 texture methods have been used to develop the building extraction methods. The sequence in which the combination of texture methods used to test the developed methods is listed in Table 4.5.

Table 4.5: Texture Methods and the Combinations of Texture Methods Used

S. No	Texture Methods and the Combinations of Texture Methods Used	S. No	Texture Methods and the Combinations of Texture Methods Used
1	Laws	11	Laws, Wavelet, Gabor, Tamura
2	Laws, Wavelet	12	Laws, Wavelet, GLCM, Gabor, Tamura
3	Laws, Gabor	13	Wavelet
4	Laws, GLCM	14	Wavelet, GLCM
5	Laws, Tamura	15	Wavelet, Gabor
6	Laws, Wavelet, GLCM	16	Wavelet, Tamura
7	Laws, Wavelet, Gabor	17	Wavelet, GLCM, Gabor
8	Laws, Wavelet, Tamura	18	Wavelet, GLCM, Tamura
9	Laws, Wavelet, GLCM, Gabor	19	Wavelet, Gabor, Tamura
10	Laws, Wavelet, GLCM, Tamura	20	Wavelet, GLCM, Gabor, Tamura

4.8. ANALYSIS AND ACCURACY ASSESSMENT

The analysis and accuracy assessment of the developed methods has been done by:

i. Comparing the ground truth (number of buildings and area of buildings) which has been produced by manually delineating the building boundaries in the ArcGIS environment, with the buildings extracted by the developed methods.
ii. Comparing the area of individual buildings calculated by manually delineating the building, with the area of the buildings extracted by the developed methods.
iii. As the buildings in slum area were highly dense and adjacent to one another, it was not possible to extract them individually. So, for the accuracy assessment of slum buildings, rather than comparing the count of buildings and area of individual buildings; total area digitized as building area and total building area extracted by the developed methods have been compared.
iv. By comparing the OAP obtained by the supervised classification method, and the OAP obtained by comparison of the manually delineating building with the buildings extracted by the developed methods.

For comparing the manually delineated building boundaries with the output image obtained by the algorithm, the evaluation metrics (Lee et al., 2003; Shufelt, 1999), widely accepted for building extraction has been applied. Basically, the ground truth, which has been produced by

manually delineating the building boundaries in the ArcGIS environment, was compared with the output image obtained by the algorithm.

On the basis of extracted buildings and the manually delineated buildings, the performance is evaluated by first determining the values of True Positive (TP), False Positive (FP), False Negative (FN), and then by using these components, the "Split Factor", "Miss Factor", "Building Extraction Percentage " (BEP) and "Overall Accuracy Percentage" (OAP) which were calculated as follows:

$$\text{Split Factor} = \frac{FP}{TP} \qquad \textbf{Eq. 4.13}$$

$$\text{Miss Factor} = \frac{FN}{TP} \qquad \textbf{Eq. 4.14}$$

$$\text{Building Detection Percentage} = 100 \times \frac{TP}{TP + FN} \qquad \textbf{Eq. 4.15}$$

$$\text{Overall Accuracy Percentage} = 100 \times \frac{TP}{TP + FP + FN} \qquad \textbf{Eq. 4.16}$$

Where TP are the buildings extracted by the proposed methods which are also digitized as building area, FP are the buildings which are extracted only by the proposed methods, and FN are the buildings which are not extracted by the proposed methods but digitized are as a building area.

The 'SF' is a measure of commission error which indicates the rate of incorrectly labelled building areas, while the 'MF' measures the omission error which describes the rate of missed building areas. The 'BEP gives the percentage of building areas correctly extracted by the automatic process and the 'OAP' is the overall measure of performance of the automated extraction process and is the most stringent measure (San, 2007; Shufelt and McKeown, 1993). To obtain 100% quality, the extraction algorithm must correctly label every object (FN = 0) without mislabelling the background pixels (FP = 0) (Jin and Davis, 2005).

4.9. SUMMARY

This chapter presented a detailed description, of the features used for extracting buildings, types of buildings found in Indian scenario, and the methodology developed for extracting buildings. The process of data set preparation from the supervised classification and digitization was presented in the chapter. The accuracy assessment of the extracted buildings was conducted by using supervised classified images and digitized images. Well-structured flowcharts have been given for all of the developed methodologies. The detailed information of dataset prepared for analysis and accuracy assessment of the developed methods, by manual digitization and by supervised classification has also been provided in this chapter. The threshold values and the texture combinations used for obtaining the results have also been provided in this chapter. A detailed analysis of the results of developed methodologies has been given in next chapter. The next chapter presents the accuracy assessment of the results obtained w.r.t. the results obtained from digitization and the supervised classified images.

CHAPTER 5 RESULTS AND ANALYSIS

5.1 INTRODUCTION

This chapter presents the results obtained by using the developed methods on satellite images, as listed in chapter 3. The results have been analysed and discussed to accomplish the objectives mentioned in chapter 1. The results and their analysis have been presented in accordance with the methodologies defined in chapter 4. The next section 5.2, presents the results and analysis of the method based on threshold values. The section 5.3 provides the results and analysis of the method based on Shadow with Corner Information. The results and analysis of the Texture based method are discussed in section 5.4. The results and analysis of the method based on Threshold, Texture and Shadow are presented in section 5.5. Lastly, section 5.6 presents the comparative accuracy assessment of the developed methods.

5.2 RESULTS OBTAINED AND ANALYSIS OF THE METHOD BASED ON THRESHOLD VALUE

This section presents the results obtained after running the developed code for the method based on threshold value have been presented. In addition, the findings of both qualitative and quantitative analysis have been presented. Also, an accuracy assessment was obtained, based on the analysis.

5.2.1. Results obtained

The developed method was executed for extracting different types of buildings from QuickBird satellite images of Jaipur city, India. The results obtained after executing the developed program are shown in Figure 5.1.

Figure 5.1 (a): Image 1

Figure 5.1 (b): Image 2

Figure 5.1 (c): Image 3

Figure 5.1 (d): Image 4

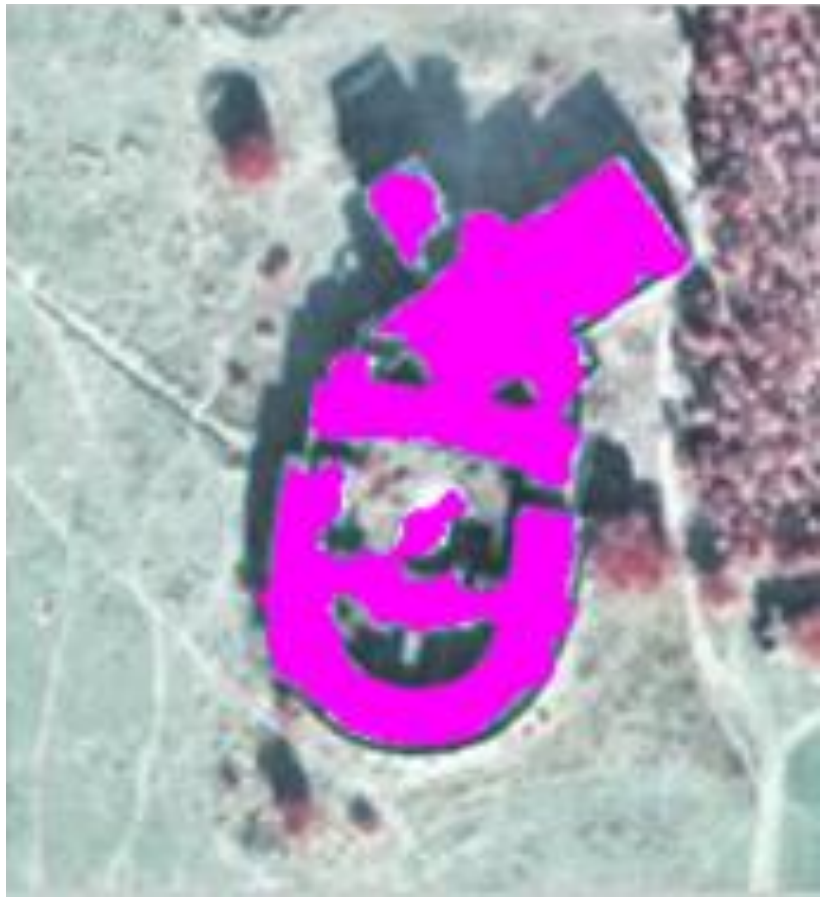

Figure 5.1 (e): Image 5

Figure 5.1 (f): Image 6

Figure 5.1 (g): Image 7

Figure 5.1 (h): Image 8

Figure 5.1 (i): Image 9

Figure 5.1 (j): Image 10

Figure 5.1 (k): Image 11

Figure 5.1 (l): Image 12

Figure 5.1 (m): Image 13

Figure 5.1 (n): Image 14

Figure 5.1 (o): Image 15

Figure 5.1 (p): Image 16

Figure 5.1: Results obtained after running the developed method based on threshold value on the QuickBird satellite imageries of Jaipur. (Reference Images 1 & 2: Educational Buildings, Images 3, 4 & 5: Business Buildings, Images 6 & 7: Industrial Buildings, Images 8, 9 & 10: Planned Residential Buildings, Images 11, 12 & 13: Unplanned Residential, Images 14, 15 & 16: Slum Residential Buildings)

5.2.2. Analysis of the Results

The results obtained by application of the developed method are analyzed and accuracy assessment was obtained for the same. The results were subjected to both, qualitative and quantitative analysis. The qualitative assessment has been done by visually analyzing the obtained results. The quantitative assessment has been done by object-based analysis and area-based analysis.

Qualitative Analysis:

After visually analyzing the results, it was found that:

i. This method performed well, for all types all types of buildings (i.e., planned, unplanned, industrial, business and educational buildings; image 1 to image 13) having different shapes, sizes and orientations, except slum buildings (image 14 to image 16).
ii. The buildings having either very bright or darker appearances were not extracted because the buildings having very bright appearance were considered as a part of non-building area and the buildings having very dark appearance were considered as a part of shadow area.
iii. The buildings adjacent to each other were grouped and extracted as one building by the developed algorithm.
iv. The corners of extracted buildings were quite sharp but the edges were not that smooth, so giving a look of free handed lines.
v. The non-building areas having same spectral reflectance value were also extracted as building area.

Object-based Analysis:

The object-based analysis has been done for all images (images 1 to 13), except the images belonging to slum area, as it was not possible to count the individual buildings present in the slums. For object-based analysis, Correct Extraction or TP, False Extraction or FP and Missed Extraction or FN have been calculated, and using these values SF, MF, BEP and OAP are computed for accuracy assessment, as per the procedure described in Chapter 4. The performance evaluation results are presented in Table 5.1.

Except for Image 7 and Image 10, low values for SF are observed ranging between 0–0.12, which indicates that the rate of incorrectly extracted buildings is low. For Image 7 (belonging to industrial area) and for Image 10 (belonging to planned residential area), a very high value of SF is observed as 1.67 and 1.75 respectively, because of the extraction of high FP having same texture as buildings. The values of MF are observed between 0–0.12, which indicates that rate of missed buildings is also very less. The BEP is observed between 88.89-100%, which indicates that this method is able to extract all types of buildings successfully. Except Image 7 and Image 10, the OAP is observed between 84.21-100%. For Image 7 (belonging to industrial area) and for Image 10 (belonging to planned residential area), a very low value of OAP is observed as 37.5% and 36.36% respectively, because of the extraction of high FP due to the same spectral reflectance values of bare land and buildings.

From the above observations, we can conclude that this method has been able to extract all types of buildings successfully, present in Indian scenario, but at the same time it also extracts some false positives, having same reflectance values as that of buildings, attributing to its limitation.

Table 5.1: Analysis of the Results of the Method based on Threshold Value

No. of Images	No. of Buildings Extracted by Manual Digitization	Threshold Method						
		TP	FN	FP	SF	MF	BEP	OAP
Image 1	12	12	0	0	0	0	100	100
Image 2	7	7	0	0	0	0	100	100
Image 3	7	7	0	0	0	0	100	100
Image 4	1	1	0	0	0	0	100	100
Image 5	2	2	0	0	0	0	100	100
Image 6	36	33	3	0	0	0.09	91.67	91.67
Image 7	3	3	3	5	1.67	0	100	37.5
Image 8	22	21	1	2	0.09	0.05	95.45	87.5
Image 9	21	21	0	1	0.05	0	100	95.45
Image 10	4	4	0	7	1.75	0	100	36.36
Image 11	26	25	1	3	0.12	0.04	96.15	86.21
Image 12	8	8	0	0	0	0	100	100
Image 13	36	32	4	2	0.06	0.12	88.89	84.21

Area-based Analysis:

Except for images of slum area (images 14, 15 and 16), the area-based analysis has been done by comparing the area of individual buildings calculated by both digitization method and extracted by the developed method. For slum buildings, the total area calculated by digitization method and extracted by the developed method has been compared as shown in Table 5.2. The graphs presented in Figure 5.2 gives a comparative view of the digitized area and the extracted area for each image.

Table 5.2: Area extracted by Digitization and Developed Threshold Based Method for Images belonging to Slum area

Image	Area calculated by Digitization Method	Area extracted by Threshold Value Method
Image 14 (I_{14})	6543	4258.75
Image 15 (I_{15})	4024	3884.58
Image 16 (I_{16})	5055	3141.75

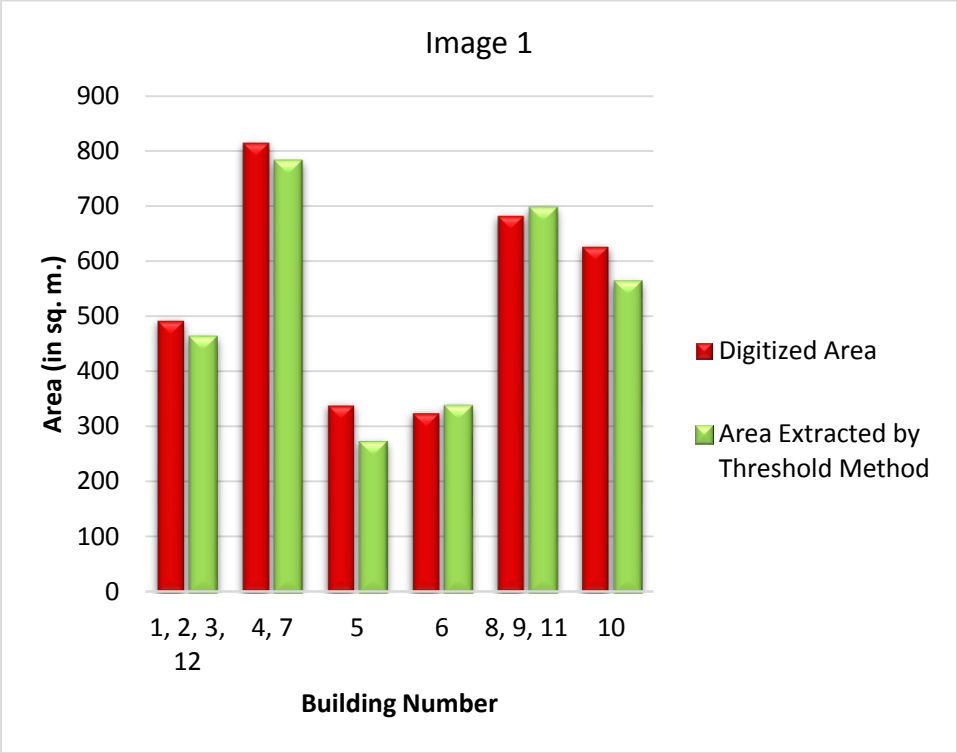

Figure 5.2 (a)

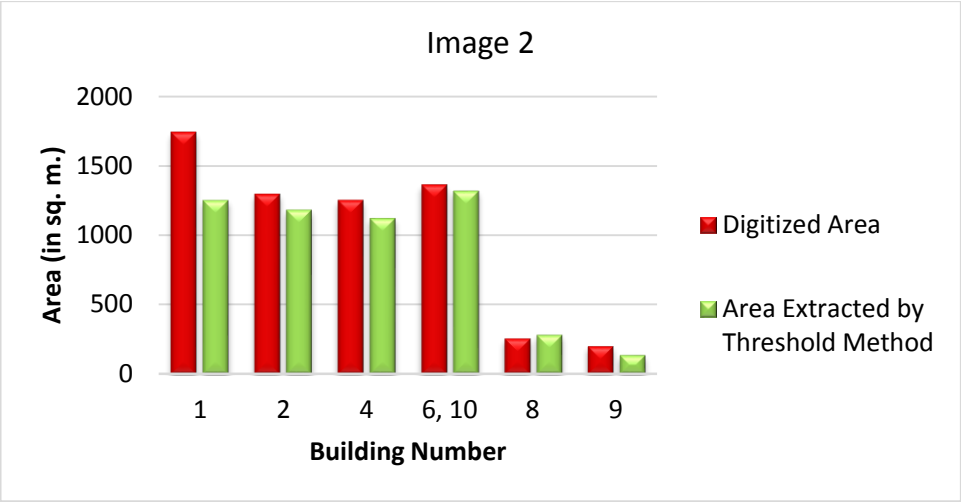

Figure 5.2 (b)

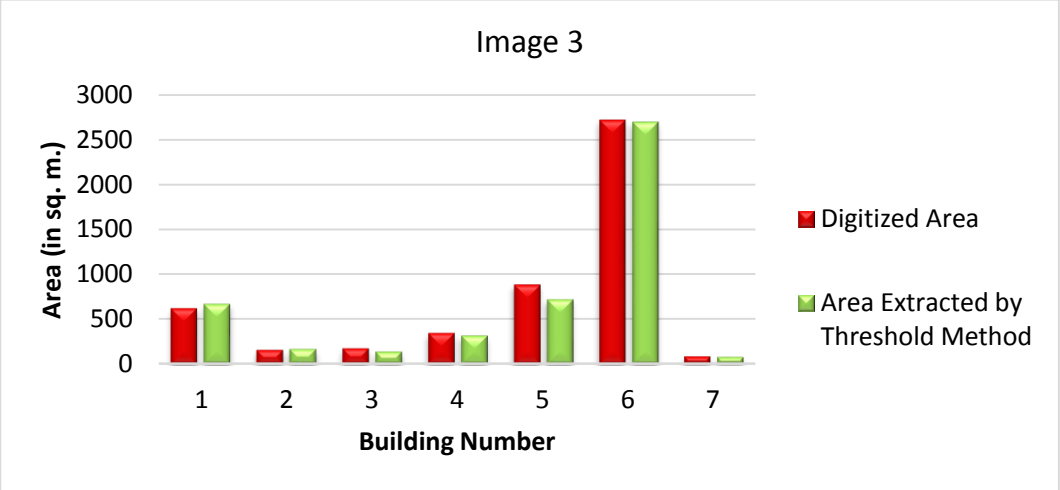

Figure 5.2 (c)

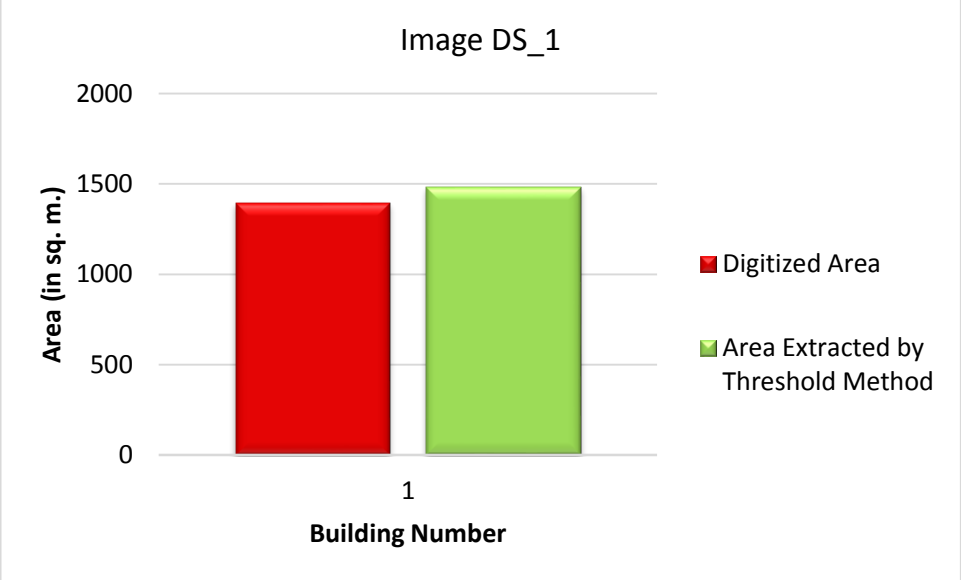

Figure 5.2 (d)

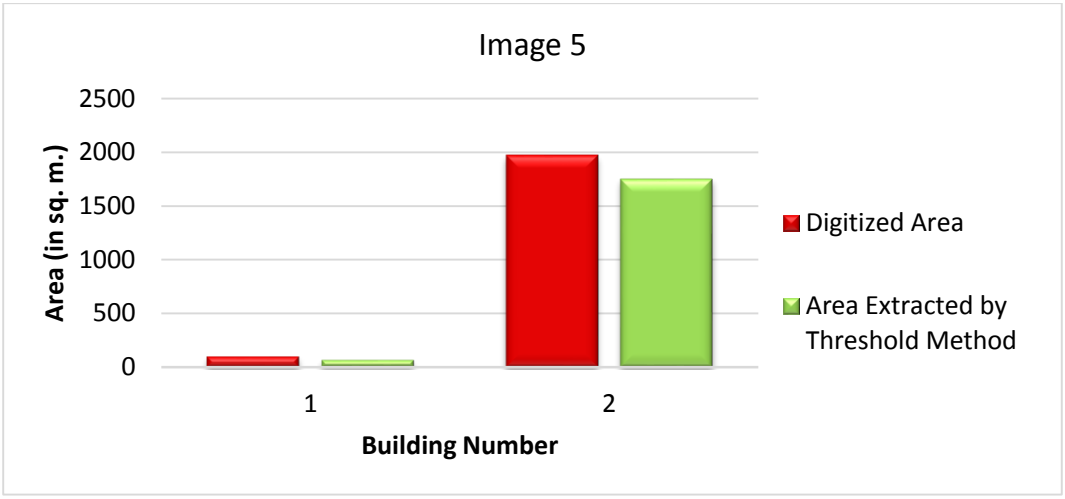

Figure 5.2 (e)

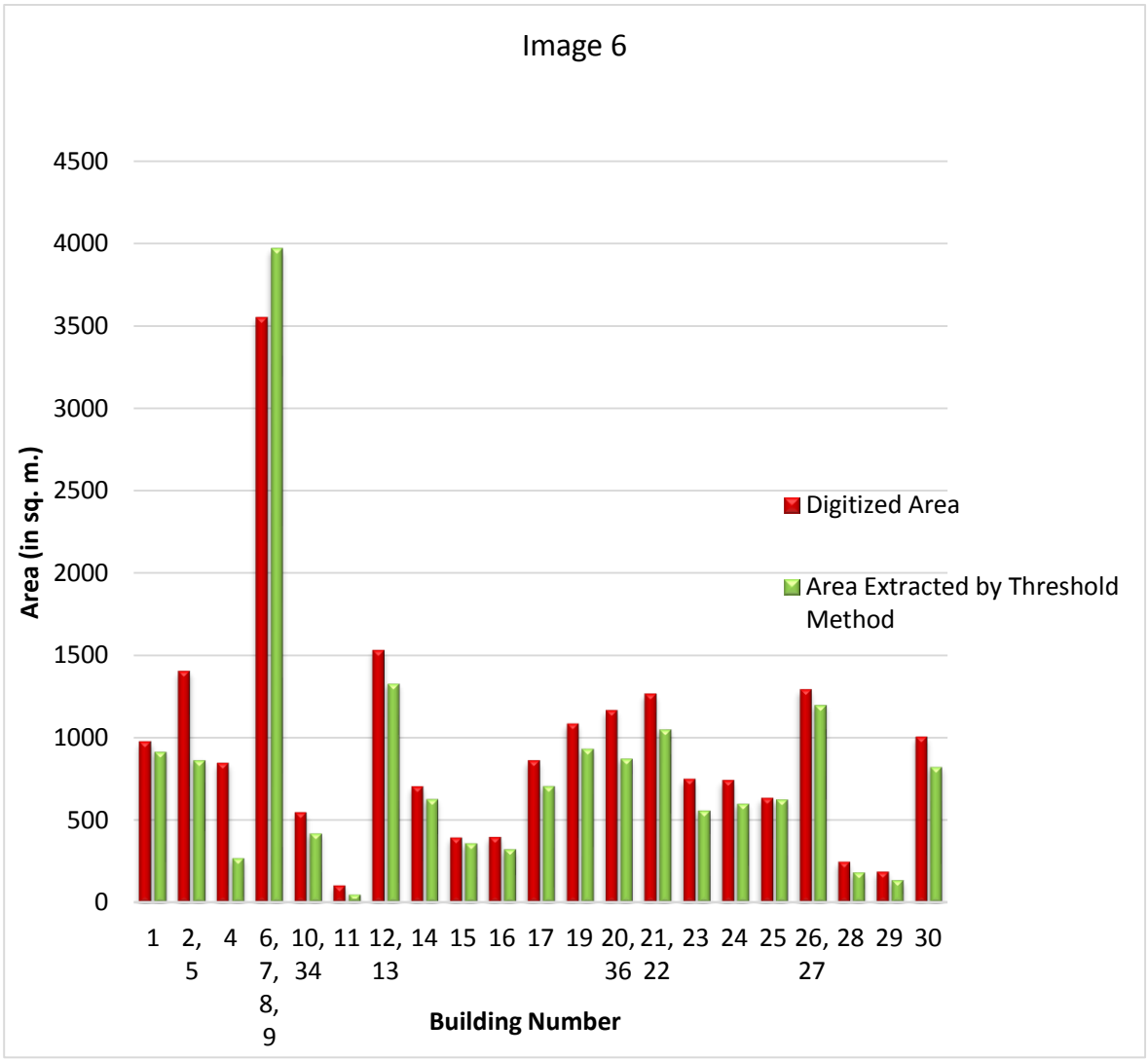

Figure 5.2 (f)

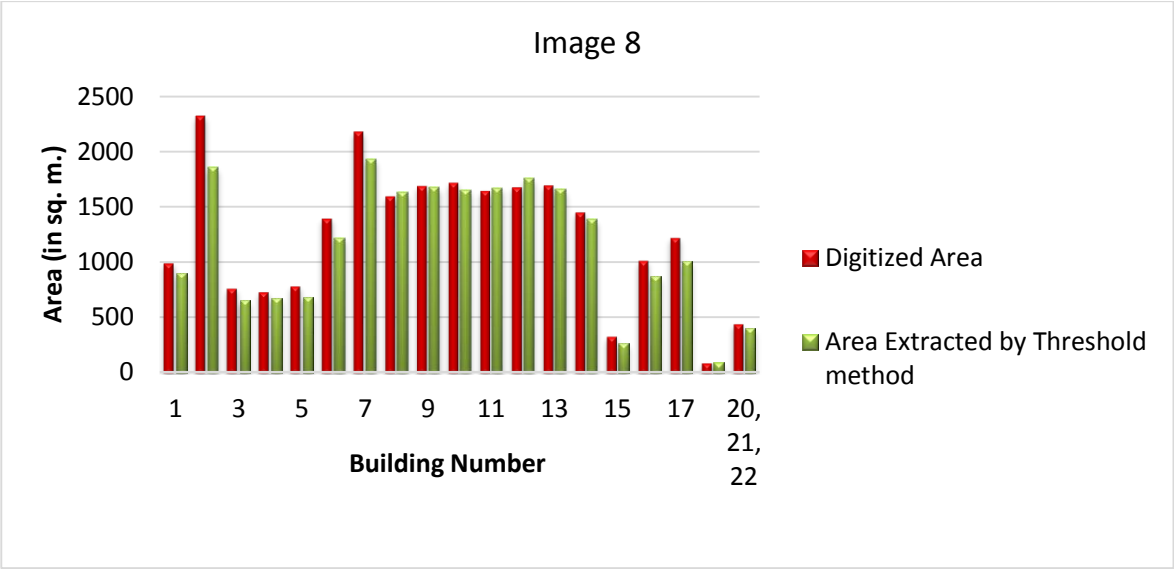

Figure 5.2 (g)

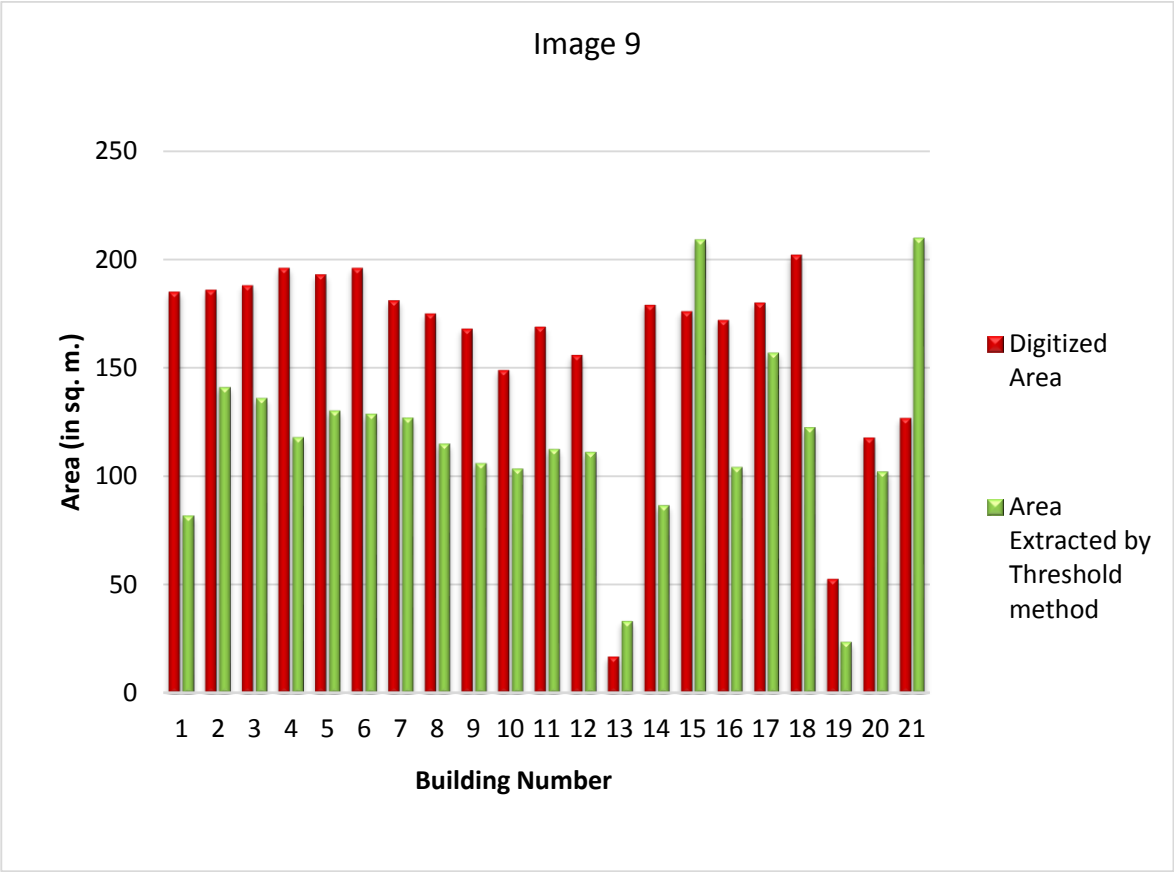

Figure 5.2 (h)

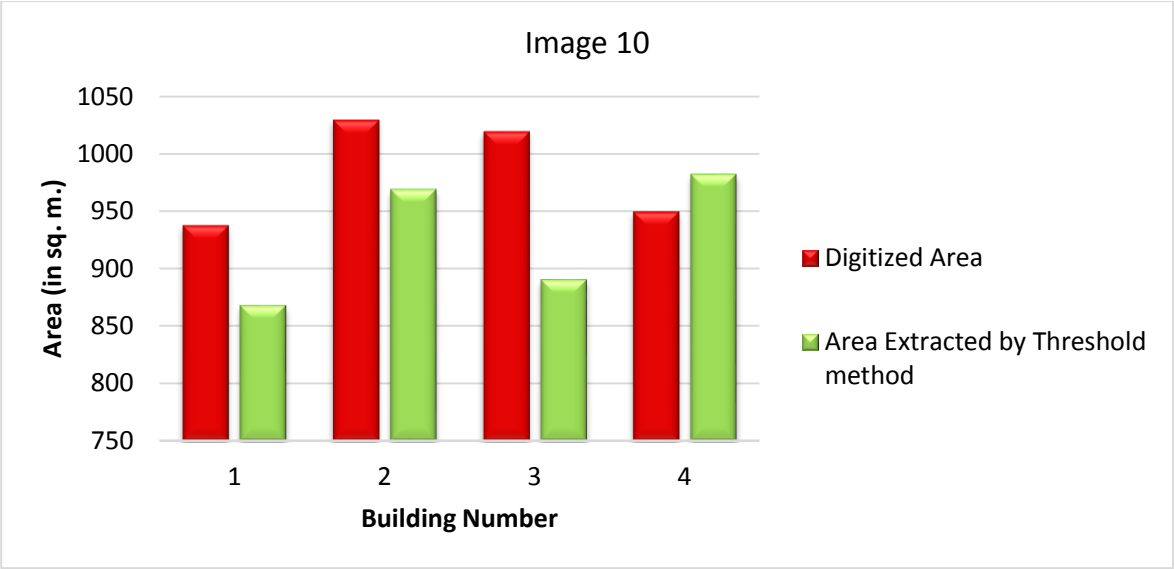

Figure 5.2 (i)

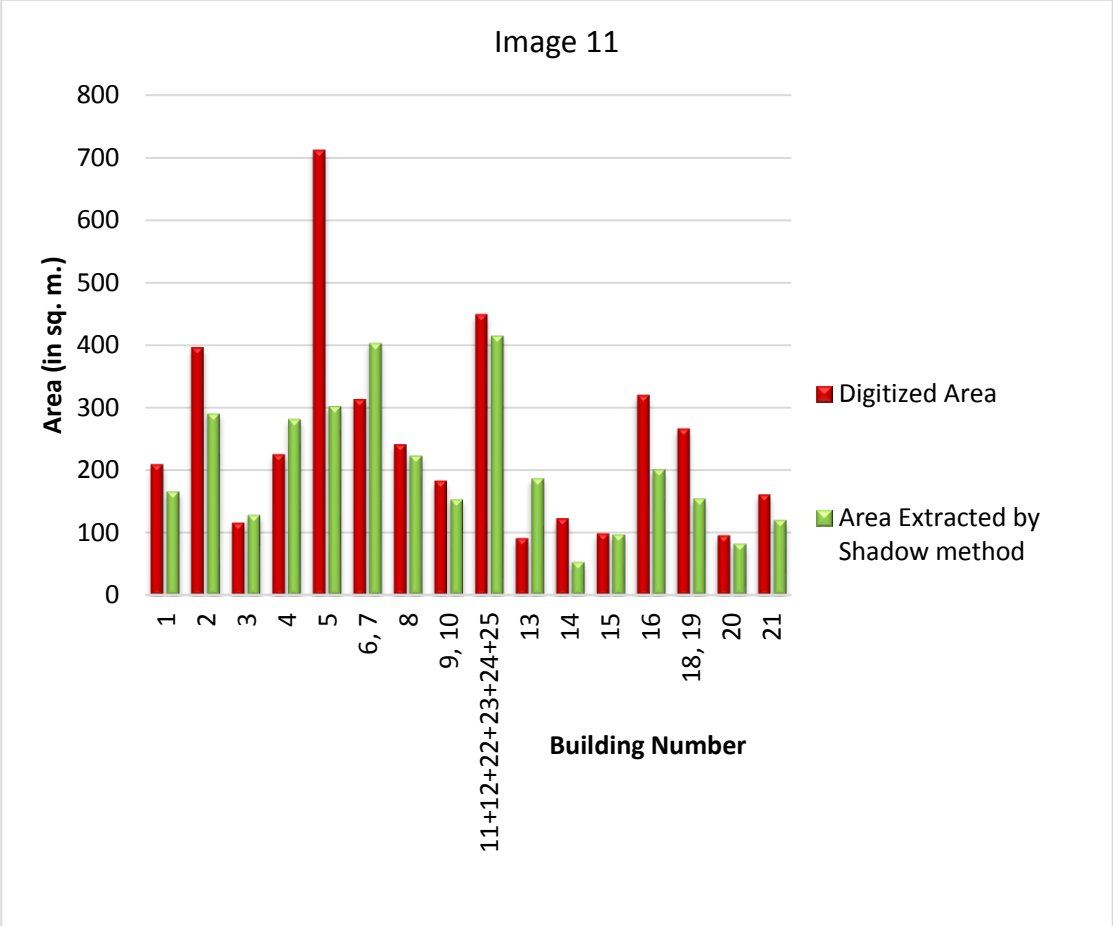

Figure 5.2 (j)

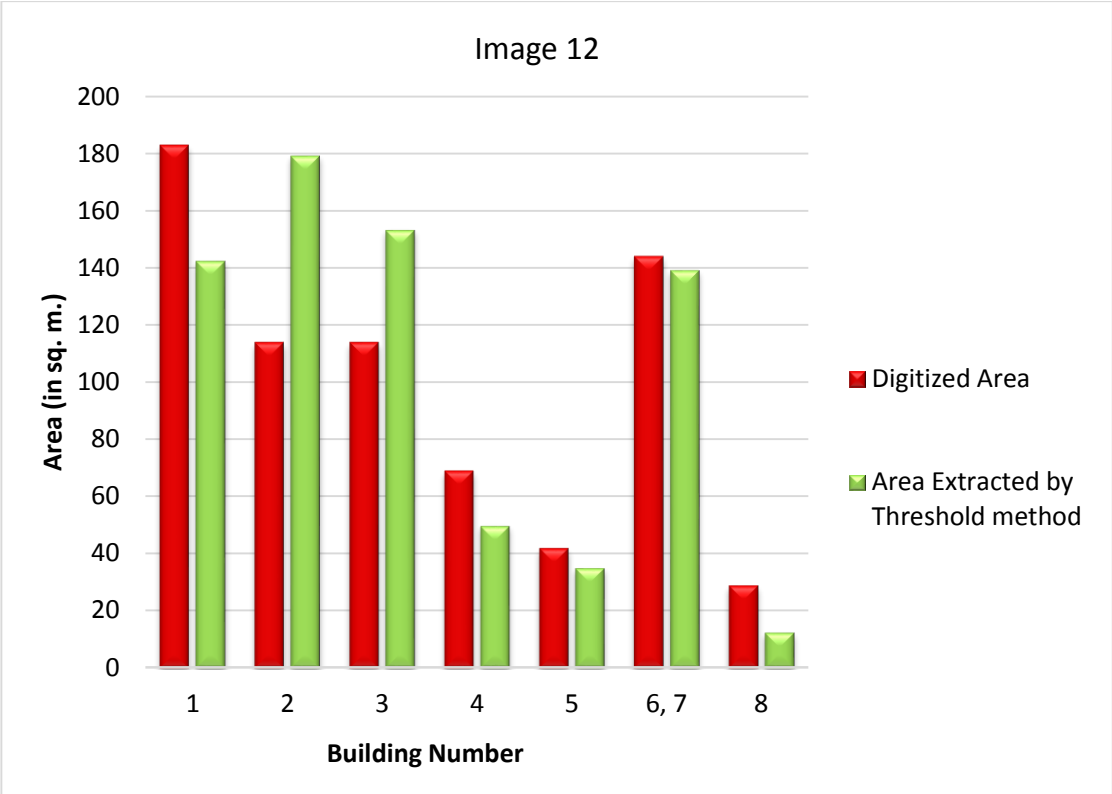

Figure 5.2 (k)

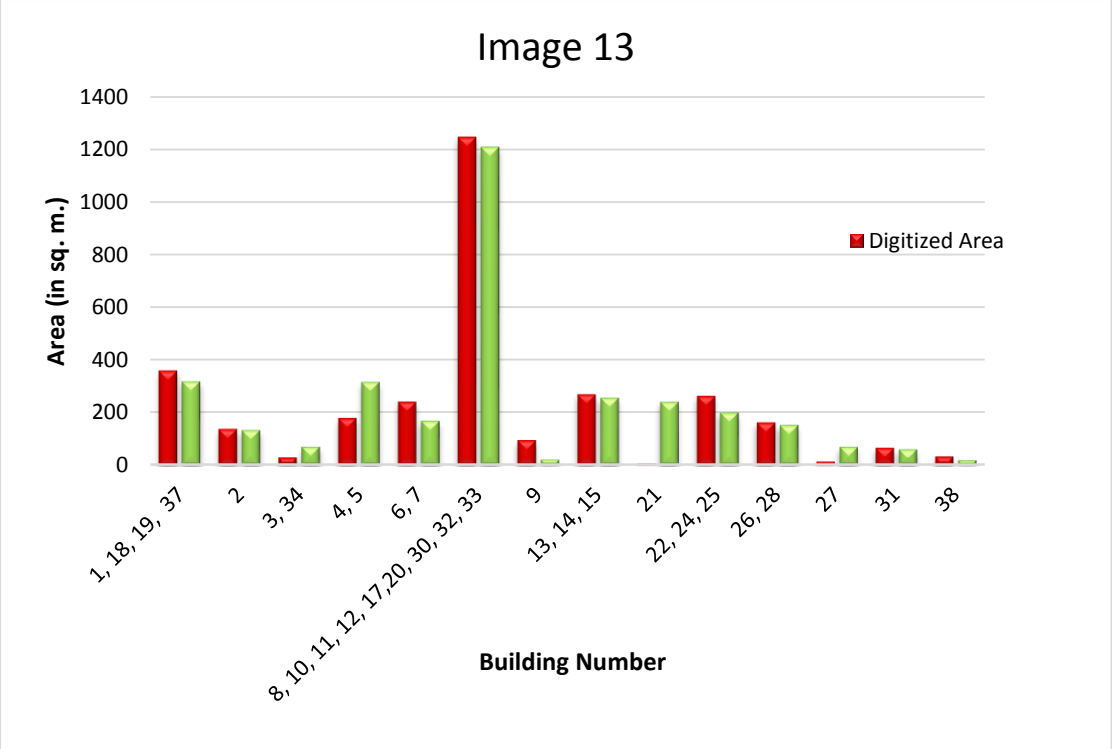

Figure 5.2 (l)

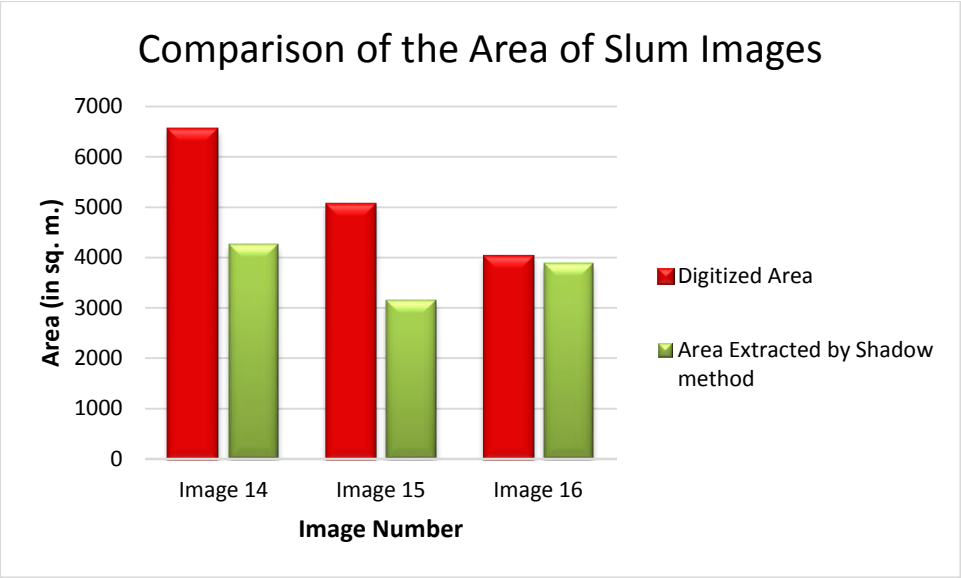

Figure 5.2 (m)

Figure 5.2: Comparison of Area extracted by the developed Threshold Based Method and the Area Extracted by Digitization Method.

The observations made from the plotted graphs are listed below:

i. For most of the extracted buildings, there is a slight variation between the area extracted from the developed method and the manually delineated area.

ii. The difference between the extracted and manually delineated area is mainly for those buildings having a variation between the reflectance values within boundary of rooftop of the buildings.

iii. For slum buildings, there is a huge variation in the calculated area and the extracted area for Images 14 and 15. The digitized area and the calculated area are almost same for Image 16, because of the extraction of FP having same reflectance value, as that of buildings.

5.3 RESULTS OBTAINED AND ANALYSIS FOR THE METHOD BASED ON SHADOW AND CORNER INFORMATION

This section presents the results obtained after running the developed code for the method based on shadow and corner information. The findings of both qualitative and quantitative analysis have been given, and accuracy assessment is done for the same.

5.3.1. Results obtained

The developed method was executed for extracting different types of buildings from QuickBird satellite images of Jaipur city, India. The results obtained after executing the developed program are shown in Figure 5.3.

5.3.2. Analysis of the Results Obtained

The qualitative and quantitative analysis of the results obtained by the application of developed program based on shadow and corner information has been done. The accuracy assessment is conducted for the analyzed results. The qualitative assessment has been done by visually analyzing the results obtained. The quantitative assessment has been done by object-based analysis and area-based analysis.

Figure 5.3 (a): Image 1

Figure 5.3 (b): Image 2

Figure 5.3 (c): Image 3

Figure 5.3 (d): Image 4

Figure 5.3 (e): Image 5

Figure 5.3 (f): Image 6

Figure 5.3 (g): Image 7

Figure 5.3 (h): Image 8

Figure 5.3 (i): Image 9

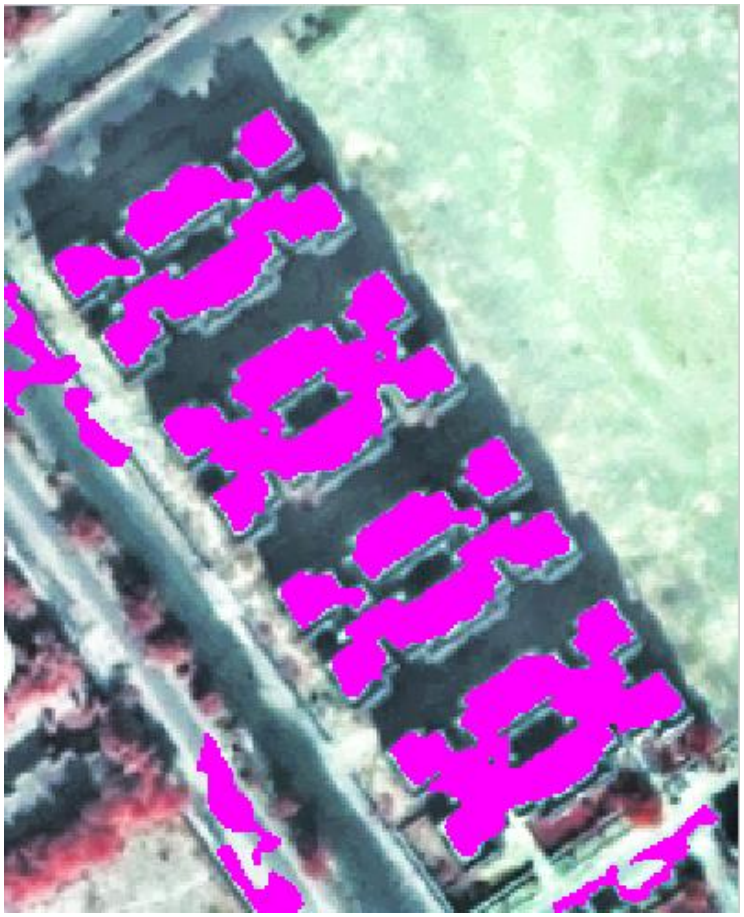

Figure 5.3 (j): Image 10

Figure 5.3 (k): Image 11

Figure 5.3 (l): Image 12

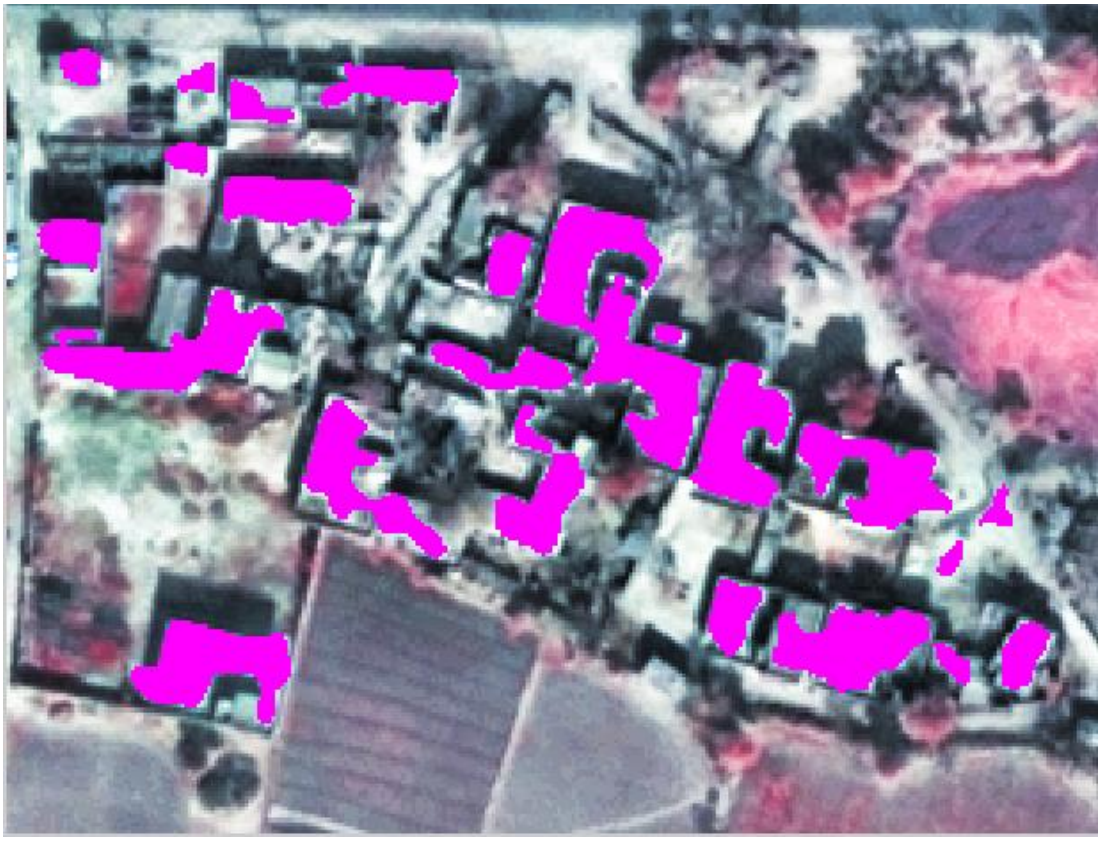

Figure 5.3 (m): Image 13

Figure 5.3 (n): Image 14

Figure 5.3 (o): Image 15

Figure 5.3 (p): Image 16

Figure 5.3: Results based on shadow and corner information on the QuickBird satellite images of Jaipur. (Reference Images 1 & 2: Educational Buildings, Images 3, 4 & 5: Business Buildings, Images 6 & 7: Industrial Buildings, Images 8, 9 & 10: Planned Residential Buildings, Images 11, 12 & 13: Unplanned Residential, Images 14, 15 & 16: Slum Residential Buildings)

Qualitative analysis:

After visually analyzing the obtained results, it was found that:

i. This method worked well, only for rectangular shaped buildings.
ii. The buildings, not associated with shadow, were not extracted well.
iii. The buildings adjacent to each other were not grouped, and extracted as separate buildings as in Image 6 and 13.
iv. The corners of the extracted buildings were not very sharp and edges were not smooth. Both gave a look of free handed lines.

Object-based Analysis:

The object-based analysis has been done for all images, except the ones belonging to slum area, as it was not possible to count the individual buildings present in the slums. For object based analysis, Correct Extraction or TP, False Extraction or FP and Missed Extraction or FN have been calculated and using these values SF, MF, BEP and OAP have been computed for accuracy assessment, as described in Chapter 4. The performance evaluation results are given in Table 5.3.

Except for Images 7 and 10, low values for SF have been observed between 0– 0.10 which indicates that the rate of incorrectly extracted buildings is very less. For Image 7 (belonging to industrial buildings) and Image 10 (belonging to planned residential area), high value of SF are observed as 2 and 1.25 respectively, because of the extraction of high FP having same spectral reflectance, as that of buildings. Also, except for Images 1, 5 and 9, low values of MF have been observed between 0–0.24, which indicates that the rate of missed buildings is also low. Except for Image 1, 5 and 9, the BEP is observed between 80.55- 100%, which indicates that this method is able to extract most of the building types successfully. For Image 9, belonging to planned residential area, a very low value of BEP is observed as 33.33%, because of the extraction of very less TP attributed to the absence of corners lying close to shadow.

For Images 2, 3, 4, 6, 8, 11, 12 and 13, the OAP is observed between 74.36-100%. For Images 1, 5, 7, 9 and 10, a very low value of OAP is observed between 33.3-66.67%, because of high FN and the extraction of high FP attributed to the same spectral reflectance values of bare land and buildings.

From the above observations, we can conclude that this methods is successfully able to extract all types of buildings present in Indian scenario, but at the same time extracts some false positives having same reflectance values as that of buildings.

Area-based Analysis:

Except for images of slum area (images 14, 15 and 16), the area-based analysis has been done by comparing the area of individual buildings calculated by both digitization method and extracted by the developed method. For slum buildings, the total area calculated by digitization method and extracted by the developed method has been compared as shown in Table 5.4. Graphs have been plotted between the digitized area and the extracted area as shown in Figure 5.4.

Table 5.3 Buildings extracted by the Developed Method based on Shadow and Corner Information

Images No.	No. of Buildings Extracted by Manual Digitization	Shadow with Corner Information Method						
		TP	FN	FP	SF	MF	BEP	OAP
Image 1	12	8	4	0	0	0.5	66.67	66.67
Image 2	7	7	0	0	0	0	100	100
Image 3	7	6	1	0	0	0.17	85.71	85.71
Image 4	1	1	0	0	0	0	100	100
Image 5	2	1	1	0	0	1	50	50
Image 6	36	31	5	0	0	0.16	86.11	86.11
Image 7	3	3	3	6	2	0	100	33.33
Image 8	22	19	3	0	0	0.16	86.36	86.36
Image 9	21	7	14	0	0	2	33.33	33.33
Image 10	4	4	0	5	1.25	0	100	44.44
Image 11	26	23	3	2	0.08	0.13	88.46	82.14
Image 12	8	7	1	0	0	0.14	87.5	87.5
Image 13	36	29	7	3	0.10	0.24	80.55	74.36

Table 5.4 Details of the output Buildings of Slum Area (in sq. m.)

Images No.	Area Extracted by Digitization	Area Extracted By Shadow Method
Image 14	6543	1241.50
Image 15	4024	1215.50
Image 16	5055	1036.17

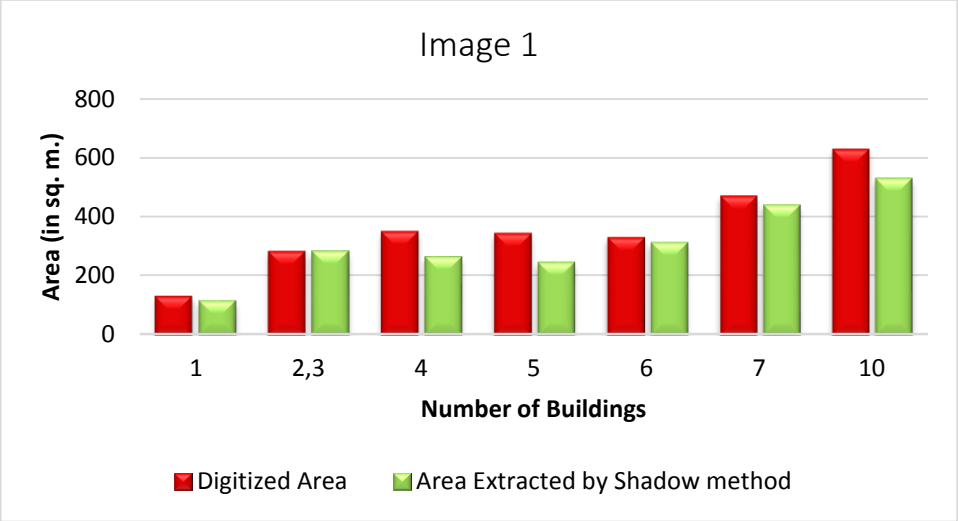

Figure 5.4 (a)

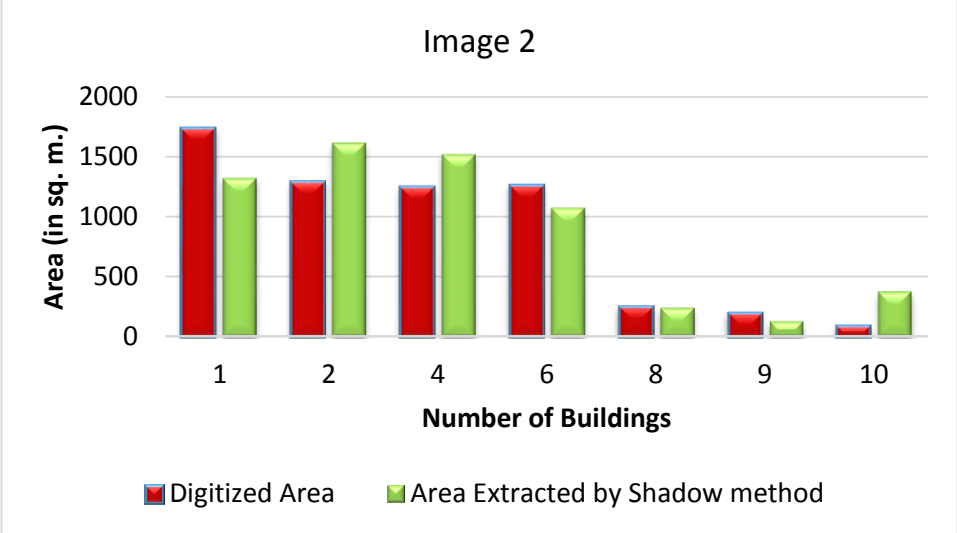

Figure 5.4 (b)

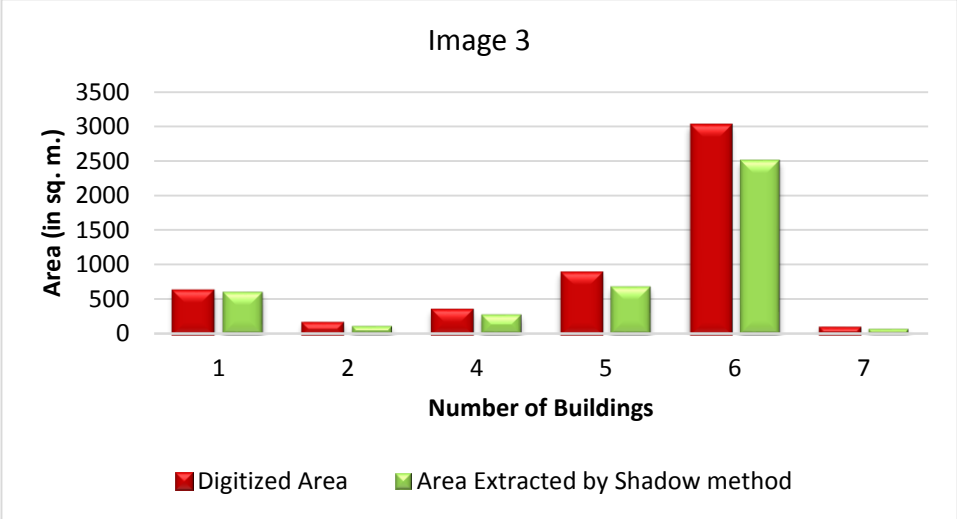

Figure 5.4 (c)

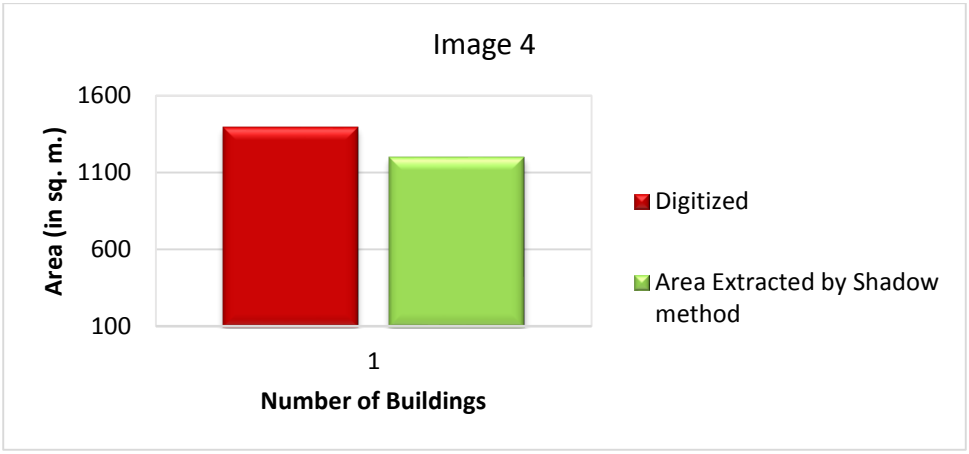

Figure 5.4 (d)

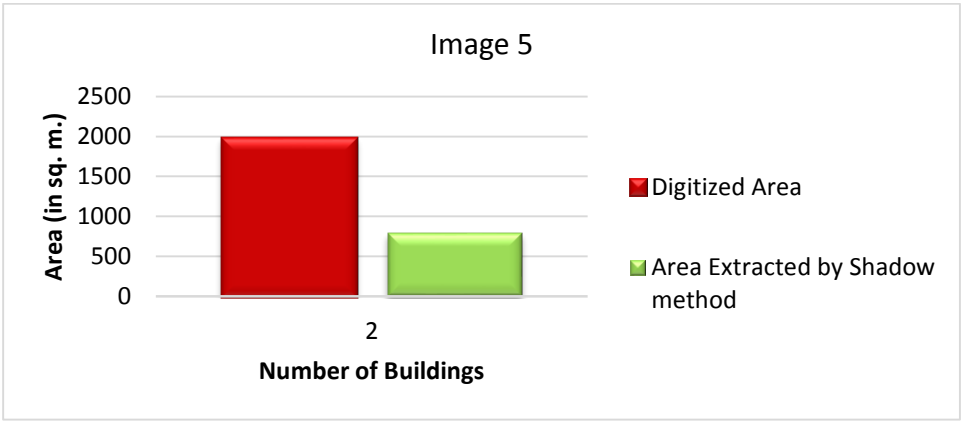

Figure 5.4 (e)

Figure 5.4 (f)

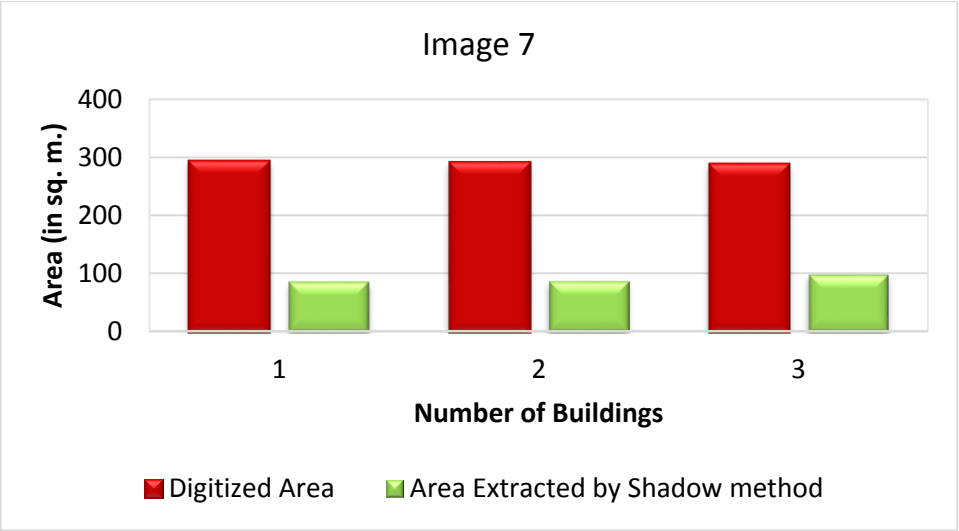

Figure 5.4 (g)

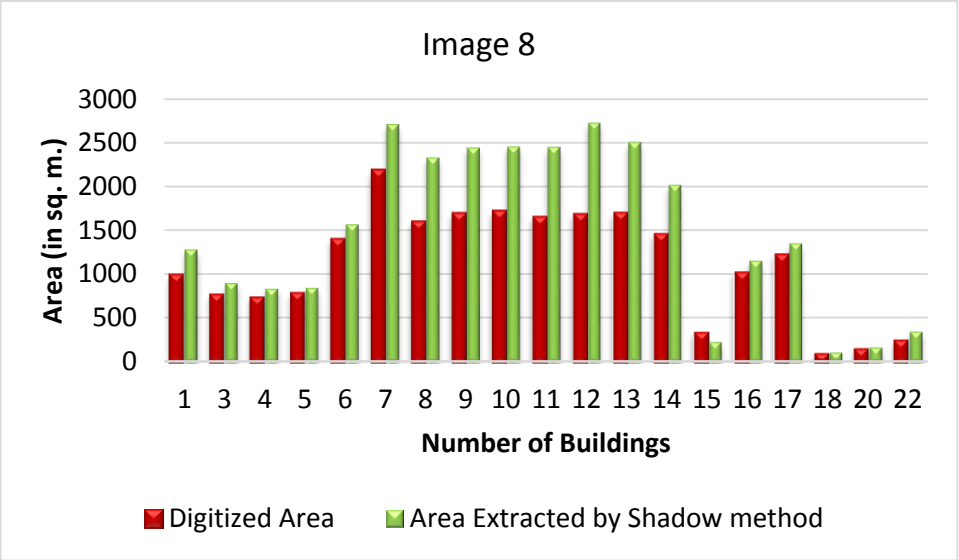

Figure 5.4 (h)

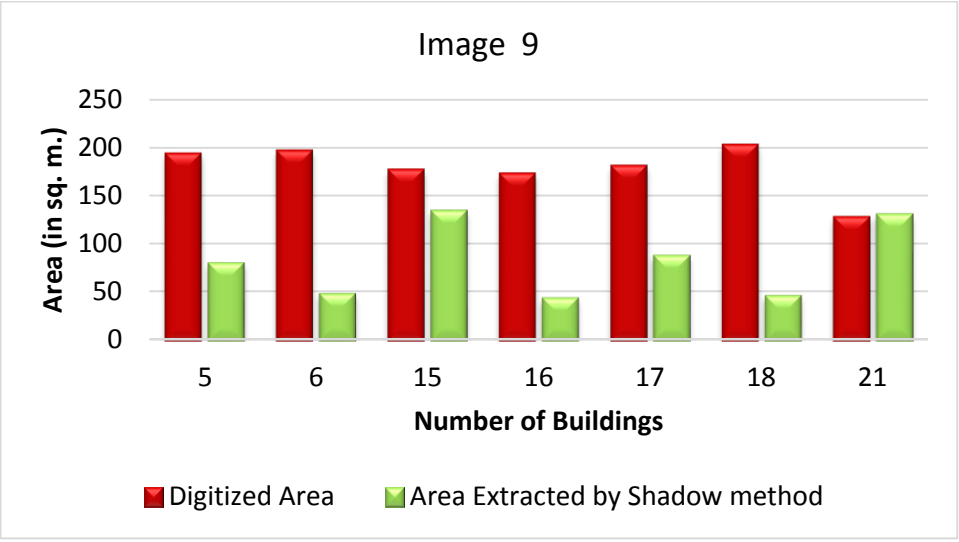

Figure 5.4 (i)

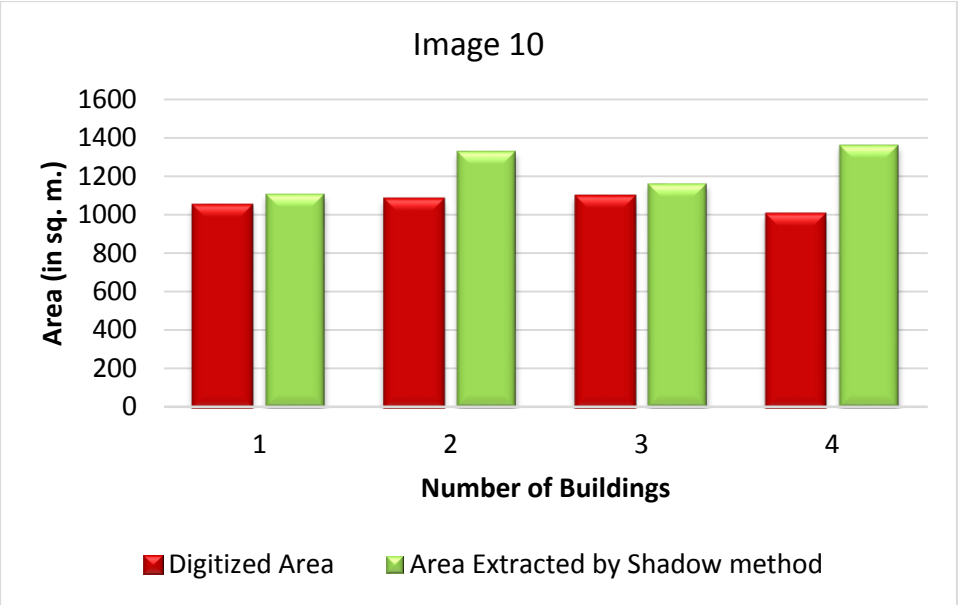

Figure 5.4 (j)

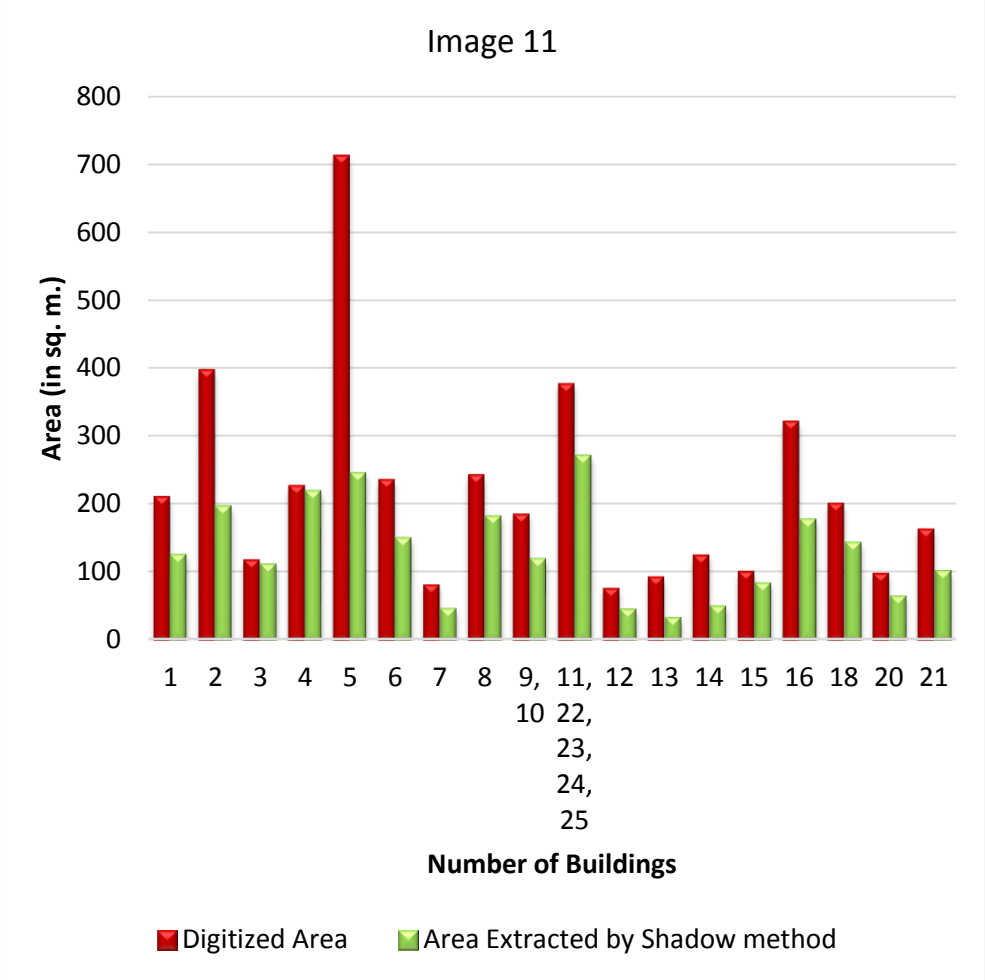

Figure 5.4 (k)

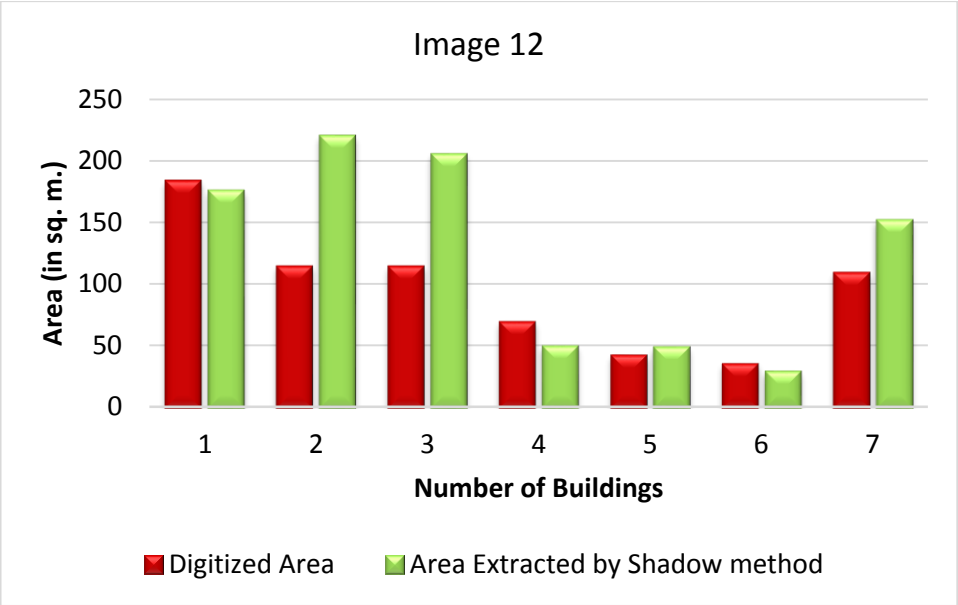

Figure 5.4 (k)

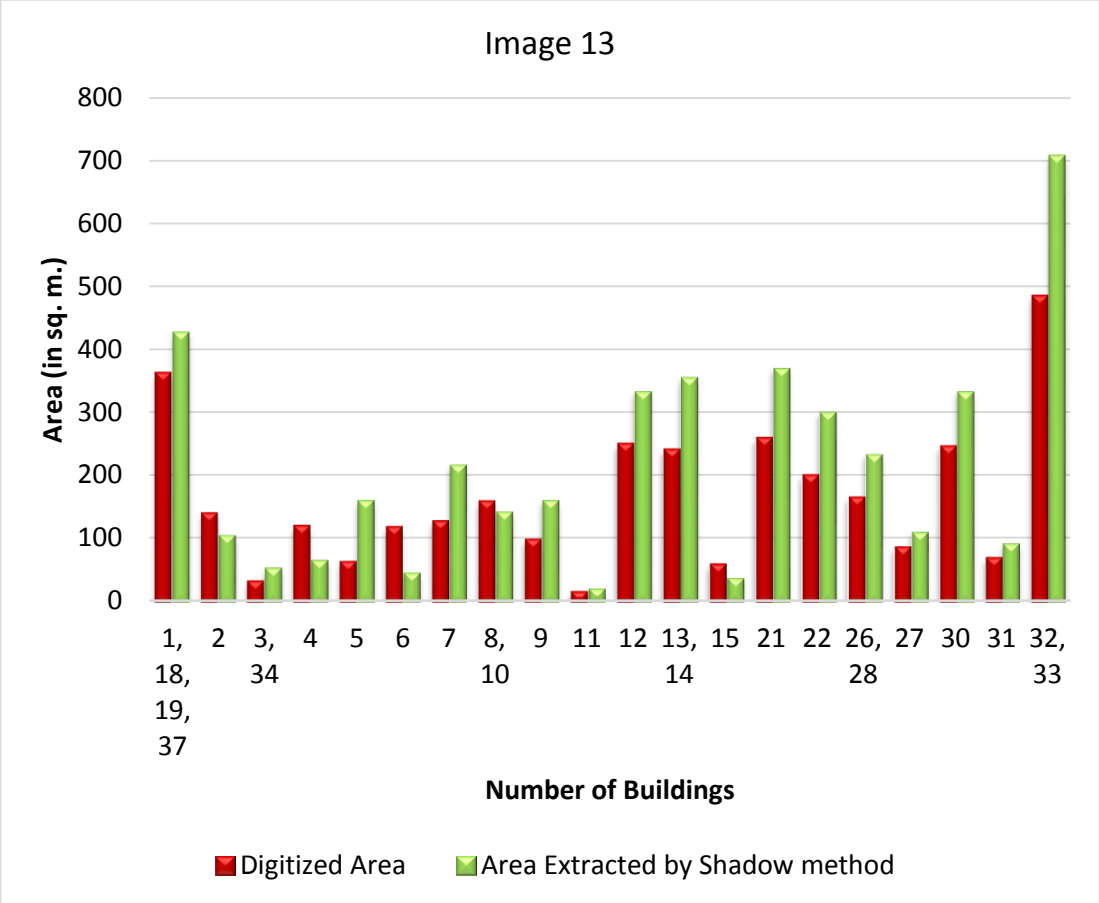

Figure 5.4 (l)

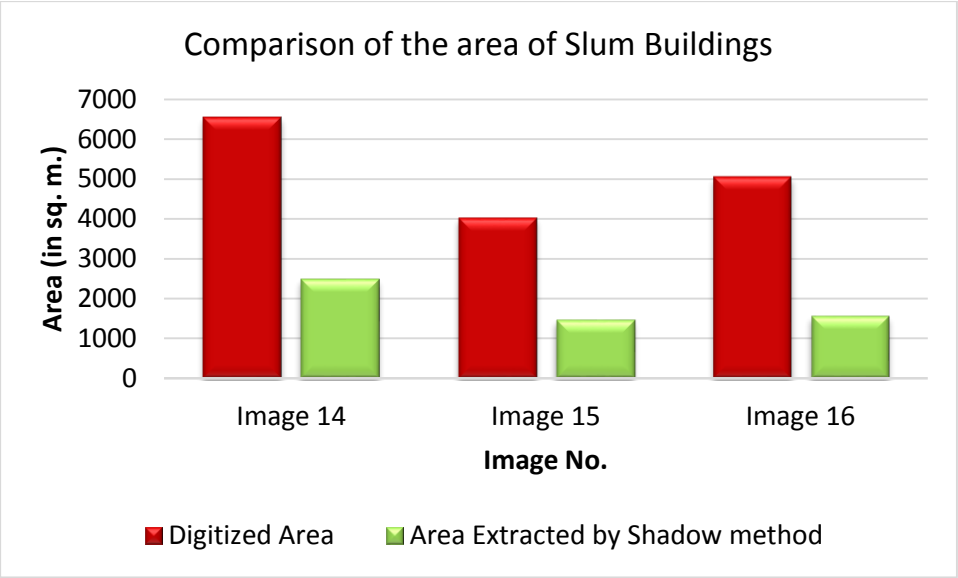

Figure 5.4 (m)

Figure 5.4: Results obtained after executing the developed method based on shadow and corner information on the QuickBird images of Jaipur.

The observations made from the plotted graphs are listed below:

i. The area of the buildings having regular shapes with associated shadow is almost equal to the area extracted by digitization method.

ii. For slum and complex shaped buildings, there is a huge variation in the area calculated by digitization method and the area extracted by the developed method. So this approach may not be suitable for extraction of slum buildings.

5.4 RESULTS OBTAINED AND ANALYSIS FOR BUILDING EXTRACTION METHOD BASED ON TEXTURE

This section presents the results obtained after running the developed code for the method based on texture have been presented. In addition, the results of both qualitative and quantitative analysis have been given, and accuracy assessment is carried out on the basis of analysis.

5.4.1. Results Obtained

Figure 5.5 (a): Image 1

Figure 5.5 (b) : Image 2

Figure 5.5 (c) : Image 3

Figure 5.5 (d) : Image 4

Figure 5.5 (e) : Image 5

Figure 5.5 (f) : Image 6

Figure 5.5 (g) : Image 7

Figure 5.5 (h) : Image 8

Figure 5.5 (i) : Image 9

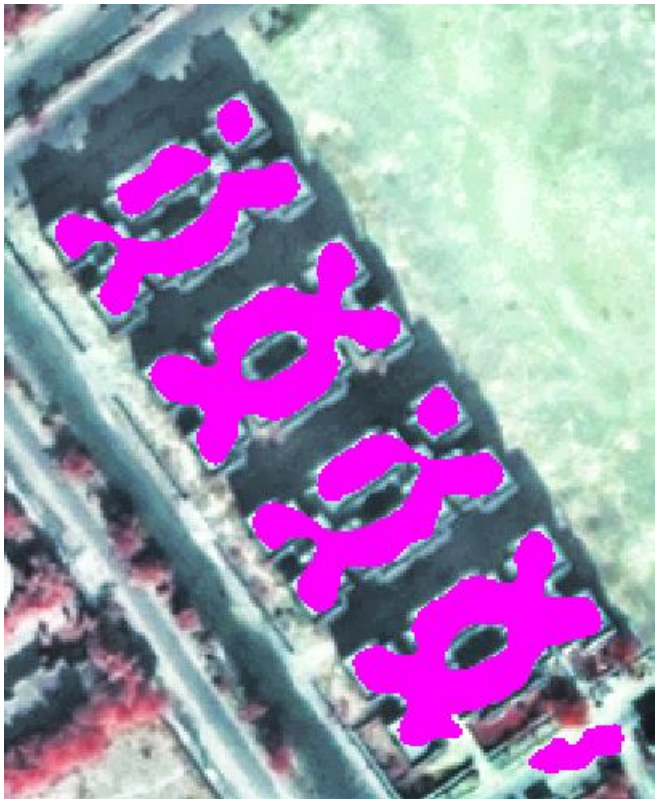

Figure 5.5 (j) : Image 10

Figure 5.5 (k) : Image 11

Figure 5.5 (l) : Image 12

Figure 5.5 (m) : Image 13

Figure 5.5 (n) : Image 14

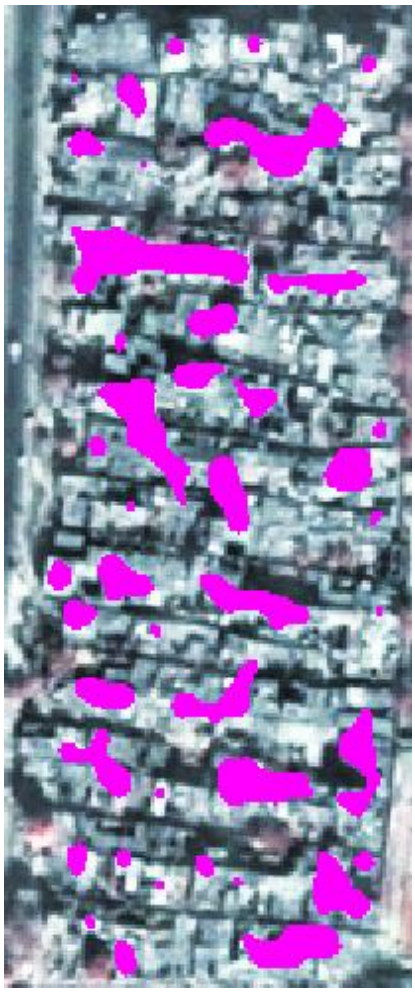

Figure 5.5 (o) : Image 15

Figure 5.5 (p) : Image 16

Figure 5.5: Results obtained after running the texture based method on the QuickBird satellite imageries of Jaipur.

5.4.2. Analysis of the Results

Qualitative Analysis:

Qualitative analysis of the results obtained has been done on the basis of visual interpretation. The findings of visual interpretation of the output images of all 20 combinations are listed below:

i. Except slums, most of the other buildings were extracted successfully. Although, there is a huge variation in the extracted area of buildings.

ii. While running the developed texture method, as the number of texture methods increased, the area of the extracted buildings also increased.

iii. The buildings either adjacent to each other, or having a small gap in between were extracted as one single building.

iv. The corners of extracted buildings were not very sharp and the edges were not smooth, because of this the boundary of the extracted buildings looked like free handed drawn shape.

v. In the areas, especially in case of slum and unplanned buildings, some areas of road and open/barren land were also extracted as buildings, as the texture of buildings resembles with the texture of road and open/barren land.

Object based accuracy assessment:

For object based accuracy assessment, Correct Extraction or TP, False Extraction or FP and Missed Extraction or FN have been calculated for all 20 combinations of texture methods and using these values SF, MF, BEP and OAP have been computed, as described in Chapter 4. The performance evaluation results are given in Table 5.5, Table 5.6, Table 5.7, Table 5.8, Table 5.9, and Table 5.10.

Except for images 10 and 11, low values for SF (0–0.14) were observed, which indicates that the rate of incorrectly extracted buildings is low. Due to the extraction of high FP having same texture as buildings, high values of SF have been observed for image 10(belonging to planned residential area) as 0.5 (for texture combinations 8 and 13) and 0.75 (for texture combinations 16 and 18). For image 11 (belonging to planned residential area) it comes between 0.28 – 0.76 for all combinations.

Low values of MF (0–0.1) for all twenty combinations for images 3, 4, 5, 7, 8, 9, 10, and 11 indicates that rate of missed buildings is very less. High values of MF has been observed for all combinations for images 2, 6, and 13due to the variation in the textures of the buildings present in these images.

However, except images6and 13, the BEP was observed between 75-100%.Very low values of BEP have been observed between 50-66.67% for image 6 belonging to industrial area, and between 61.11-86.11% for Image 13 belonging to unplanned residential area, because of the high FN attributed to the variation in texture of buildings.

Table 5.5: Performance Evaluation of the results obtained from the texture based method

Image No.	No. of Buildings	LAWS			LAWS, WAVELET			LAWS, GABOR			.LAWS, GLCM			.LAWS, TAMURA			LAWS, WAVELET, GLCM			LAWS, WAVELET, GABOR			LAWS, WAVELET, TAMURA			LAWS, WAVELET, GLCM, GABOR			LAWS, WAVELET, GLCM, TAMURA		
		TP	FN	FP	TP	FN	FP	TP	FN	FP	TP	FN	FP	TP	FN	FP	TP	FN	FP	TP	FN	FP	TP	FN	FP	TP	FN	FP	TP	FN	FP
Image 1	12	10	2	0	10	2	0	10	2	0	10	2	0	10	2	0	10	2	0	10	2	0	10	2	0	10	2	0	10	2	0
Image 2	7	5	2	0	5	2	0	5	2	0	7	0	0	7	0	0	7	0	0	5	2	0	5	2	0	7	0	0	7	0	0
Image 3	7	7	0	0	7	0	0	7	0	0	7	0	1	7	0	0	7	0	1	7	0	0	7	0	0	7	0	1	7	0	1
Image 4	1	1	0	0	1	0	0	1	0	0	1	0	0	1	0	0	1	0	0	1	0	0	1	0	0	1	0	0	1	0	0
Image 5	2	2	0	0	2	0	0	2	0	0	1	1	0	2	0	1	2	0	0	2	0	0	2	0	1	2	0	0	2	0	0
Image 6	36	21	15	0	19	17	0	18	18	0	24	12	0	22	14	0	24	12	0	23	13	0	20	16	0	24	12	0	24	12	0
Image 7	3	3	0	0	3	0	0	3	0	0	3	0	0	3	0	0	3	0	0	3	0	0	3	0	0	3	0	0	3	0	0
Image 8	22	21	1	0	20	2	0	21	1	0	20	1	1	20	1	1	20	1	1	20	2	0	20	2	0	20	1	1	20	1	1
Image 9	21	20	1	0	20	1	1	21	0	3	21	0	1	21	0	4	21	0	3	21	0	3	21	0	5	21	0	3	21	0	3
Image 10	4	4	0	1	4	0	1	4	0	1	4	0	1	4	0	1	4	0	1	4	0	1	4	0	2	4	0	1	4	0	1
Image 11	26	25	1	7	25	1	10	25	1	8	25	1	16	25	1	7	25	1	14	24	2	11	24	2	10	25	1	13	25	1	13
Image 12	8	6	2	0	6	2	0	6	2	0	7	1	0	7	1	1	7	1	1	6	2	0	6	2	0	7	1	1	7	1	1
Image 13	36	24	12	0	22	14	0	25	11	0	25	11	0	30	6	2	25	11	1	24	12	0	31	5	0	30	6	1	25	11	1

Table 5.6: Performance Evaluation of the results obtained from the texture based method

Image No.	No. of Buildings	LAWS, WAVELET, GABOR, TAMURA			LAWS, WAVELET, GLCM, GABOR, TAMURA			WAVELET			WAVELET, GLCM			WAVELET, GABOR			WAVELET, TAMURA			WAVELET, GLCM, GABOR			WAVELET, GLCM, TAMURA			WAVELET, GABOR, TAMURA			WAVELET, GLCM, GABOR, TAMURA		
		TP	FN	FP	TP	FN	FP	TP	FN	FP	TP	FN	FP	TP	FN	FP	TP	FN	FP	TP	FN	FP	TP	FN	FP	TP	FN	FP	TP	FN	FP
Image 1	12	10	2	0	10	2	0	10	2	0	10	2	0	10	2	0	10	2	0	10	2	0	10	2	0	10	2	0	10	2	0
Image 2	7	5	2	0	7	0	0	5	2	0	7	0	0	5	2	0	7	0	0	7	0	0	7	0	0	7	0	0	7	0	0
Image 3	7	7	0	0	7	0	0	7	0	0	7	0	1	7	0	0	7	0	1	7	0	1	7	0	1	7	0	0	7	0	1
Image 4	1	1	0	0	1	0	0	1	0	0	1	0	0	1	0	0	1	0	0	1	0	0	1	0	0	1	0	0	1	0	0
Image 5	2	2	0	1	2	0	0	2	0	0	2	0	0	2	0	0	2	0	0	2	0	0	1	0	0	1	0	0	2	0	0
Image 6	36	23	13	0	26	9	0	21	15	0	24	12	0	23	13	0	22	14	0	24	12	0	24	12	0	24	12	0	24	12	0
Image 7	3	3	0	0	3	0	0	3	0	0	3	0	0	3	0	0	3	0	0	3	0	0	3	0	0	3	0	0	3	0	0
Image 8	22	20	2	0	20	1	1	20	2	0	20	1	1	20	1	1	21	1	0	21	1	0	20	1	1	21	1	0	21	1	0
Image 9	21	21	0	4	21	0	3	20	1	1	21	0	4	21	0	4	21	0	4	21	0	4	21	0	3	21	0	4	21	0	3
Image 10	4	4	0	1	4	0	1	4	0	2	4	0	1	4	0	1	4	0	3	4	0	1	4	0	1	4	0	3	4	0	1
Image 11	26	25	1	11	25	1	11	24	2	16	25	1	16	24	2	18	24	2	18	25	1	13	25	1	13	25	1	19	25	1	12
Image 12	8	6	2	0	7	1	1	6	2	0	7	1	1	7	1	1	7	1	2	7	1	1	7	1	0	7	1	1	7	1	1
Image 13	36	26	10	1	30	6	0	27	9	1	29	7	2	26	10	1	30	6	3	30	6	1	30	6	2	27	9	1	29	7	1

Table 5.7: SF of Texture methods and their combinations

Image No.	LAWS	LAWS, WAVELET	LAWS, GABOR	LAWS, GLCM	LAWS, TAMURA	LAWS, WAVELET, GLCM	LAWS, WAVELET, GABOR	LAWS, WAVELET, TAMURA	LAWS, WAVELET, GLCM, GABOR	LAWS, WAVELET, GLCM, TAMURA	LAWS, WAVELET, GABOR, TAMURA	LAWS, WAVELET, GLCM, GABOR, TAMURA	WAVELET	WAVELET, GLCM	WAVELET, GABOR	WAVELET, TAMURA	WAVELET, GLCM, GABOR	WAVELET, GLCM, TAMURA	WAVELET, GABOR, TAMURA	WAVELET, GABOR, GLCM , TAMURA
Image 1	0	0	0	0	0	0	0	0	0	0	0	0	0	0	0	0	0	0	0	0
Image 2	0	0	0	0	0	0	0	0	0	0	0	0	0	0	0	0	0	0	0	0
Image 3	0	0	0	0.14	0	0.14	0	0	0.14	0.14	0	0	0	0.14	0	0.14	0.14	0.14	0	0.14
Image 4	0	0	0	0	0	0	0	0	0	0	0	0	0	0	0	0	0	0	0	0
Image 5	0	0	0	0	0.5	0	0	0.5	0	0	0.5	0	0	0	0	0	0	0	0	0
Image 6	0	0	0	0	0	0	0	0	0	0	0	0	0	0	0	0	0	0	0	0
Image 7	0	0	0	0	0	0	0	0	0	0	0	0	0	0	0	0	0	0	0	0
Image 8	0	0	0	0.05	0.05	0.05	0	0	0.05	0.05	0	0.05	0	0.05	0.05	0	0	0.05	0	0
Image 9	0	0.05	0.14	0.05	0.19	0.14	0.14	0.24	0.14	0.14	0.19	0.14	0.05	0.19	0.19	0.19	0.19	0.14	0.19	0.14
Image 10	0.25	0.25	0.25	0.25	0.25	0.25	0.25	0.5	0.25	0.25	0.25	0.25	0.5	0.25	0.25	0.75	0.25	0.25	0.75	0.25
Image 11	0.28	0.4	0.32	0.64	0.28	0.56	0.46	0.42	0.52	0.52	0.44	0.44	0.67	0.64	0.75	0.75	0.52	0.52	0.76	0.48
Image 12	0	0	0	0	0.14	0.14	0	0	0.14	0.14	0	0.14	0	0.14	0.14	0.29	0.14	0	0.14	0.14
Image 13	0	0	0	0	0.07	0.04	0	0	0.03	0.04	0.04	0	0.04	0.07	0.04	0.1	0.03	0.07	0.04	0.03

Table 5.8: MF of Texture methods and their combinations

Image No.	LAWS	LAWS, WAVELET	LAWS, GABOR	LAWS, GLCM	LAWS, TAMURA	LAWS, WAVELET, GLCM	LAWS, WAVELET, GABOR	LAWS, WAVELET, TAMURA	LAWS, WAVELET, GLCM, GABOR	LAWS, WAVELET, GLCM, TAMURA	LAWS, WAVELET, GABOR, TAMURA	LAWS, WAVELET, GLCM, GABOR, TAMURA	WAVELET	WAVELET, GLCM	WAVELET, GABOR	WAVELET, TAMURA	WAVELET, GLCM, GABOR	WAVELET, GLCM, TAMURA	WAVELET, GABOR, TAMURA	WAVELET, GABOR, GLCM TAMURA
Image 1	0.2	0.2	0.2	0.2	0.2	0.2	0.2	0.2	0.2	0.2	0.2	0.2	0.2	0.2	0.2	0.2	0.2	0.2	0.2	0.2
Image 2	0.4	0.4	0.4	0	0	0	0.4	0.4	0	0	0.4	0	0.4	0	0.4	0	0	0	0	0
Image 3	0	0	0	0	0	0	0	0	0	0	0	0	0	0	0	0	0	0	0	0
Image 4	0	0	0	0	0	0	0	0	0	0	0	0	0	0	0	0	0	0	0	0
Image 5	0	0	0	1	0	0	0	0	0	0	0	0	0	0	0	0	0	0	0	0
Image 6	0.71	0.89	1	0.5	0.64	0.5	0.57	0.8	0.5	0.5	0.57	0.57	0.71	0.5	0.57	0.64	0.5	0.5	0.5	0.5
Image 7	0	0	0	0	0	0	0	0	0	0	0	0	0	0	0	0	0	0	0	0
Image 8	0.05	0.1	0.05	0.05	0.05	0.05	0.1	0.1	0.05	0.05	0.1	0.05	0.1	0.05	0.05	0.05	0.05	0.05	0.05	0.05
Image 9	0.05	0.05	0	0	0	0	0	0	0	0	0	0	0.05	0	0	0	0	0	0	0
Image 10	0	0	0	0	0	0	0	0	0	0	0	0	0	0	0	0	0	0	0	0
Image 11	0.04	0.04	0.04	0.04	0.04	0.04	0.08	0.08	0.04	0.04	0.04	0.04	0.08	0.04	0.08	0.08	0.04	0.04	0.04	0.04
Image 12	0.33	0.33	0.33	0.14	0.14	0.14	0.33	0.33	0.14	0.14	0.33	0.14	0.33	0.14	0.14	0.14	0.14	0.14	0.14	0.14
Image 13	0.5	0.64	0.44	0.44	0.2	0.44	0.5	0.16	0.2	0.44	0.38	0.2	0.33	0.24	0.38	0.2	0.2	0.2	0.33	0.24

Table 5.9: BEP of Texture methods and their combinations

Image No.	LAWS	LAWS, WAVELET	LAWS, GABOR	LAWS, GLCM	LAWS, TAMURA	LAWS, WAVELET, GLCM	LAWS, WAVELET, GABOR	LAWS, WAVELET, TAMURA	LAWS, WAVELET, GLCM, GABOR	LAWS, WAVELET, GLCM, TAMURA	LAWS, WAVELET, GABOR, TAMURA	LAWS, WAVELET, GLCM, GABOR, TAMURA	WAVELET	WAVELET, GLCM	WAVELET, GABOR	WAVELET, TAMURA	WAVELET, GLCM, GABOR	WAVELET, GLCM, TAMURA	WAVELET, GABOR, TAMURA	WAVELET, GABOR, GLCM TAMURA
Image 1	83.33	83.33	83.33	83.33	83.33	83.33	83.33	83.33	83.33	83.33	83.33	83.33	83.33	83.33	83.33	83.33	83.33	83.33	83.33	83.33
Image 2	71.43	71.43	71.43	100	100	100	71.43	71.43	100	100	71.43	100	71.43	100	71.43	100	100	100	100	100
Image 3	100	100	100	100	100	100	100	100	100	100	100	100	100	100	100	100	100	100	100	100
Image 4	100	100	100	100	100	100	100	100	100	100	100	100	100	100	100	100	100	100	100	100
Image 5	100	100	100	50	100	100	100	100	100	100	100	100	100	100	100	100	100	100	100	100
Image 6	58.33	52.78	50	66.67	61.11	66.67	63.89	55.55	66.67	66.67	63.89	63.89	58.33	66.67	63.89	61.11	66.67	66.67	66.67	66.67
Image 7	100	100	100	100	100	100	100	100	100	100	100	100	100	100	100	100	100	100	100	100
Image 8	95.45	90.91	95.45	95.24	95.24	95.24	90.91	90.91	95.24	95.24	90.91	95.24	90.91	95.24	95.24	95.45	95.45	95.24	95.45	95.45
Image 9	95.45	95.45	100	100	100	100	100	100	100	100	100	100	95.45	100	100	100	100	100	100	100
Image 10	100	100	100	100	100	100	100	100	100	100	100	100	100	100	100	100	100	100	100	100
Image 11	96.15	96.15	96.15	96.15	96.15	96.15	92.31	92.31	96.15	96.15	96.15	96.15	92.31	92.31	92.31	92.31	96.15	96.15	96.15	96.15
Image 12	75	75	75	87.5	87.5	87.5	75	75	87.5	87.5	75	87.5	75	87.5	87.5	87.5	87.5	87.5	87.5	87.5
Image 13	66.67	61.11	69.44	69.44	83.33	69.44	66.67	86.11	83.33	69.44	72.22	83.33	75	80.56	72.22	83.33	83.33	83.33	75	80.56

Table 5.10: OAP of Texture methods and their combinations

Image No.	LAWS	LAWS, WAVELET	LAWS, GABOR	LAWS, GLCM	LAWS, TAMURA	LAWS, WAVELET, GLCM	LAWS, WAVELET, GABOR	LAWS, WAVELET, TAMURA	LAWS, WAVELET, GLCM, GABOR	LAWS, WAVELET, GLCM, TAMURA	LAWS, WAVELET, GABOR, TAMURA	LAWS, WAVELET, GLCM, GABOR, TAMURA	WAVELET	WAVELET, GLCM	WAVELET, GABOR	WAVELET, TAMURA	WAVELET, GLCM, GABOR	WAVELET, GLCM, TAMURA	WAVELET, GABOR, TAMURA	WAVELET, GABOR, GLCM TAMURA
Image 1	83.33	83.33	83.33	83.33	83.33	83.33	83.33	83.33	83.33	83.33	83.33	83.33	83.33	83.33	83.33	83.33	83.33	83.33	83.33	83.33
Image 2	71.43	71.43	71.43	100	100	100	71.43	71.43	100	100	71.43	100	71.43	100	71.43	100	100	100	100	100
Image 3	100	100	100	87.5	100	87.5	100	100	87.5	87.5	100	100	100	87.5	100	87.5	87.5	87.5	100	87.5
Image 4	100	100	100	100	100	100	100	100	100	100	100	100	100	100	100	100	100	100	100	100
Image 5	100	100	100	50	66.67	100	100	66.67	100	100	66.67	100	100	100	100	100	100	100	100	100
Image 6	58.33	52.78	50	66.67	61.11	66.67	63.89	55.56	66.67	66.67	63.89	63.89	58.33	66.67	63.89	61.11	66.67	66.67	66.67	66.67
Image 7	100	100	100	100	100	100	100	100	100	100	100	100	100	100	100	100	100	100	100	100
Image 8	95.45	90.91	95.45	90.91	90.91	90.91	90.91	90.91	90.91	90.91	90.91	90.91	90.91	90.91	90.91	95.45	95.45	90.91	95.45	95.45
Image 9	95.24	90.91	87.5	95.45	84	87.5	87.5	80.77	87.5	87.5	84	87.5	90.91	84	84	84	84	87.5	84	87.5
Image 10	80	80	80	80	80	80	80	66.67	80	80	80	80	66.67	80	80	57.14	80	80	57.14	80
Image 11	75.76	69.44	73.53	59.52	75.76	62.5	64.86	66.67	64.10	64.10	67.57	67.57	57.14	59.52	54.55	54.55	64.10	64.10	55.56	65.79
Image 12	75	75	75	87.5	77.78	77.78	75	75	77.78	77.78	75	77.78	75	77.78	77.78	70	77.78	87.5	77.78	77.78
Image 13	66.67	61.11	69.44	69.44	78.95	67.57	66.67	86.11	81.08	67.57	70.27	83.33	72.97	76.32	70.27	76.92	81.08	78.95	72.97	78.38

Table 5.11: Area (in sq. m.) Extracted by Different Combinations of Texture Methods

Image No.	Digitized Area	Area Extracted by																			
		LAWS	LAWS, WAVELET	LAWS, GABOR	LAWS, GLCM	LAWS, TAMURA	LAWS, WAVELET, GLCM	LAWS, WAVELET, GABOR	LAWS, WAVELET, TAMURA	LAWS, WAVELET, GLCM, GABOR	LAWS, WAVELET, GLCM, TAMURA	LAWS, WAVELET, GABOR, TAMURA	LAWS, WAVELET, GLCM, GABOR, TAMURA	WAVELET	WAVELET, GLCM	WAVELET, GABOR	WAVELET, TAMURA	WAVELET, GLCM, GABOR	WAVELET, GLCM, TAMURA	WAVELET, GABOR, TAMURA	WAVELET, GABOR, GLCM TAMURA
Image 1	3284	2034.36	2096.28	2486.16	2400.48	3160.08	2922.12	2312.28	2007.36	3012.48	2910.24	2198.88	3006.72	2144.16	2666.16	2539.8	3005.64	2791.8	2645.28	3157.92	2770.2
Image 2	6121	1959.48	2076.84	2884.68	5143.32	5270.04	5211.72	2243.88	2107.08	5252.4	5250.6	2273.04	5303.88	2149.92	4814.28	2568.6	4768.56	4879.44	4880.16	4805.64	4940.64
Image 3	5023	3277.8	3414.24	3458.16	4510.08	3259.08	4511.88	3485.16	3418.56	4574.88	4516.92	3487.32	4574.88	3466.44	4342.32	3694.32	4338.72	4441.32	4354.2	3731.4	4463.28
Image 4	1395	1017.36	1020.6	1405.8	1553.4	1585.8	1563.12	1377.72	875.16	1605.96	1560.24	1641.24	1605.96	1402.2	1527.12	1431.72	1542.24	1590.12	1519.56	1615.68	1432.8
Image 5	2071	1509.12	1471.32	1533.6	1081.5	1653.48	1424.88	1544.04	1675.44	1488.36	1425.96	1783.8	1488.96	1394.64	1027.44	1486.08	1520.28	1131.84	1040.4	1743.48	1157.76
Image 6	22788	8790.84	8907.84	8586	13598.64	9354.6	14012.28	10312.2	8681.4	14162.4	13683.96	9974.52	14162.4	8683.92	13409.28	11580.84	8854.92	13692.6	13465.08	14209.92	12714.12
Image 7	869	825.84	839.88	841.32	786.96	925.56	891.36	24.4842	829.44	896.4	885.96	836.64	896.4	853.2	862.92	878.4	939.6	875.88	855	950.04	859.68
Image 8	23822	13908.96	13280.4	16984.8	22577.4	22826.88	23187.96	13766.04	13518.36	23406.48	21265.2	14095.44	23458.32	12333.6	20323.8	14688.84	20180.88	22624.2	20476.44	22303.08	22235.76
Image 9	3366	1365.84	1276.2	2256.12	2992.68	2499.48	2738.16	1948.68	2638.8	2881.8	2758.68	2847.96	2900.52	1160.64	2647.08	2130.48	2234.52	2962.2	2661.12	2653.56	3038.04
Image 10	3938	2720.16	2720.52	2826.36	2908.08	3253.68	3180.96	2611.8	2751.84	3221.28	3193.2	2646	3237.48	2693.88	2944.08	3000.24	3164.76	3046.68	2966.4	3386.52	3062.16
Image 11	4112	4867.4	4631.4	4897.2	6541.8	4732.2	6394.8	4723.2	4662	7993.2	7927.2	4755	8182.8	4758	6960	4879.8	4833	7174.2	7056	5027.4	7215
Image 12	695	439.92	452.16	526.32	661.68	728.28	678.96	480.96	446.76	730.08	675	482.82	731.88	445.32	596.52	540	646.92	672.48	585	547.2	672.48
Image 13	3595	1493.28	1537.92	1994.76	2071.8	2732.04	2206.8	1598.64	1874.64	2379.6	2280.6	1915.2	2443.08	1455.84	1815	1781.52	2490.84	2448	2142.72	2281.224	2271.24
Image 14	6543	3667.8	3466.8	5736	4253.4	6330	3588.6	3622.8	3577.8	3577.8	3726.6	3621	3629.4	3147	5816.4	5226	5487.6	5199	5484	5727	5308.8
Image 15	5055	2946.6	2685	3123.6	5509.8	5181	5028	2555.4	2762.4	2762.4	5110.8	2624.4	5080.2	2466	4570.2	3883.2	4215	4492.2	4705.8	4053.6	4689.6
Image 16	4024	4333.8	4094.4	4266	6954	7012.8	6321	4027.8	4246.8	4246.8	6366	4219.2	6361.8	3609	5745	3804.6	5844	5814	5889.6	5917.8	5917.8

Table 5.12: Time Taken by Different Combinations of Texture Methods (in seconds)

Image	LAWS	LAWS, WAVELET	LAWS, GABOR	LAWS, GLCM	LAWS, TAMURA	LAWS, WAVELET, GLCM	LAWS, WAVELET, GABOR	LAWS, WAVELET, TAMURA	LAWS, WAVELET, GLCM, GABOR	LAWS, WAVELET, GLCM, TAMURA	LAWS, WAVELET, GABOR, TAMURA	LAWS, WAVELET, GLCM, GABOR, TAMURA	WAVELET	WAVELET, GLCM	WAVELET, GABOR	WAVELET, TAMURA	WAVELET, GLCM, GABOR	WAVELET, GLCM, TAMURA	WAVELET, GABOR, TAMURA	WAVELET, GABOR, GLCM TAMURA
Image 1	12.71	15.17	15.08	320.35	521.54	345.02	20.59	469.06	327.62	751.10	512.10	863.71	14.27	348.80	15.88	483.22	355.88	764.83	462.61	755.66
Image 2	9.13	13.23	12.77	54.89	86.79	59.91	16.20	74.84	62.87	122.54	79.53	121.21	12.79	63.53	13.90	68.87	58.92	113.00	71.79	128.92
Image 3	21.31	22.54	17.67	115.69	152.45	109.58	18.52	142.69	120.93	200.46	148.91	105.24	16.79	71.07	19.25	131.46	98.29	211.57	146.22	201.71
Image 4	11.92	13.43	16.73	195.06	206.27	200.19	15.23	251.55	185.75	334.42	244.32	172.16	9.25	160.26	11.74	261.16	193.62	436.25	260.76	283.25
Image 5	9.35	12.09	13.03	137.67	196.80	168.33	12.60	317.84	521.09	521.26	282.62	252.73	12.79	228.31	19.56	287.89	200.48	456.76	360.84	546.04
Image 6	20.76	28.42	39.95	111.22	180.05	115.89	40.81	182.50	150.28	295.16	195.86	132.49	22.30	207.52	35.93	209.32	130.80	282.78	202.65	208.00
Image 7	36.79	21.86	15.24	123.55	222.60	214.97	14.52	232.92	128.49	399.40	158.94	137.52	13.64	14.79	17.75	195.23	133.36	304.58	197.58	323.78
Image 8	40.51	35.67	34.65	109.58	116.23	96.94	35.80	128.55	108.37	211.01	151.45	228.64	19.39	91.83	61.83	135.59	219.00	221.09	141.49	211.64
Image 9	13.92	13.05	11.33	225.89	301.70	274.78	16.01	461.28	240.20	544.41	299.34	521.46	9.48	222.71	20.39	302.51	379.13	524.89	330.75	698.57
Image 10	12.68	55.39	12.31	228.43	402.87	294.89	30.92	324.47	256.12	506.35	305.45	511.68	8.70	260.80	17.21	318.25	239.47	546.95	337.08	544.25
Image 11	10.40	17.25	15.60	85.05	102.76	88.48	20.46	107.23	91.39	181.37	119.74	181.38	12.20	86.86	16.70	106.35	88.82	179.42	103.62	217.27
Image 12	7.44	8.44	8.58	62.35	90.08	61.76	9.67	78.63	63.90	133.81	82.63	138.07	6.82	61.68	7.39	78.95	62.21	136.31	82.43	138.35
Image 13	11.67	11.86	12.61	247.20	320.47	251.20	15.75	321.77	245.87	567.87	317.94	559.38	9.48	252.12	12.27	331.93	254.89	583.41	347.83	592.96
Image 14	15.45	13.07	13.74	46.28	54.29	49.38	14.74	64.30	43.62	89.60	64.70	105.63	9.35	49.98	9.69	62.77	49.50	102.03	61.64	92.34
Image 15	24.65	12.47	11.72	175.19	222.49	183.72	11.60	219.44	134.17	365.68	282.53	371.98	9.21	148.56	11.15	171.06	120.40	248.00	148.06	262.86
Image 16	27.21	13.58	11.89	255.30	379.50	256.91	12.93	292.85	231.39	505.17	296.24	485.81	9.87	266.54	14.53	322.26	219.23	558.65	337.94	612.59

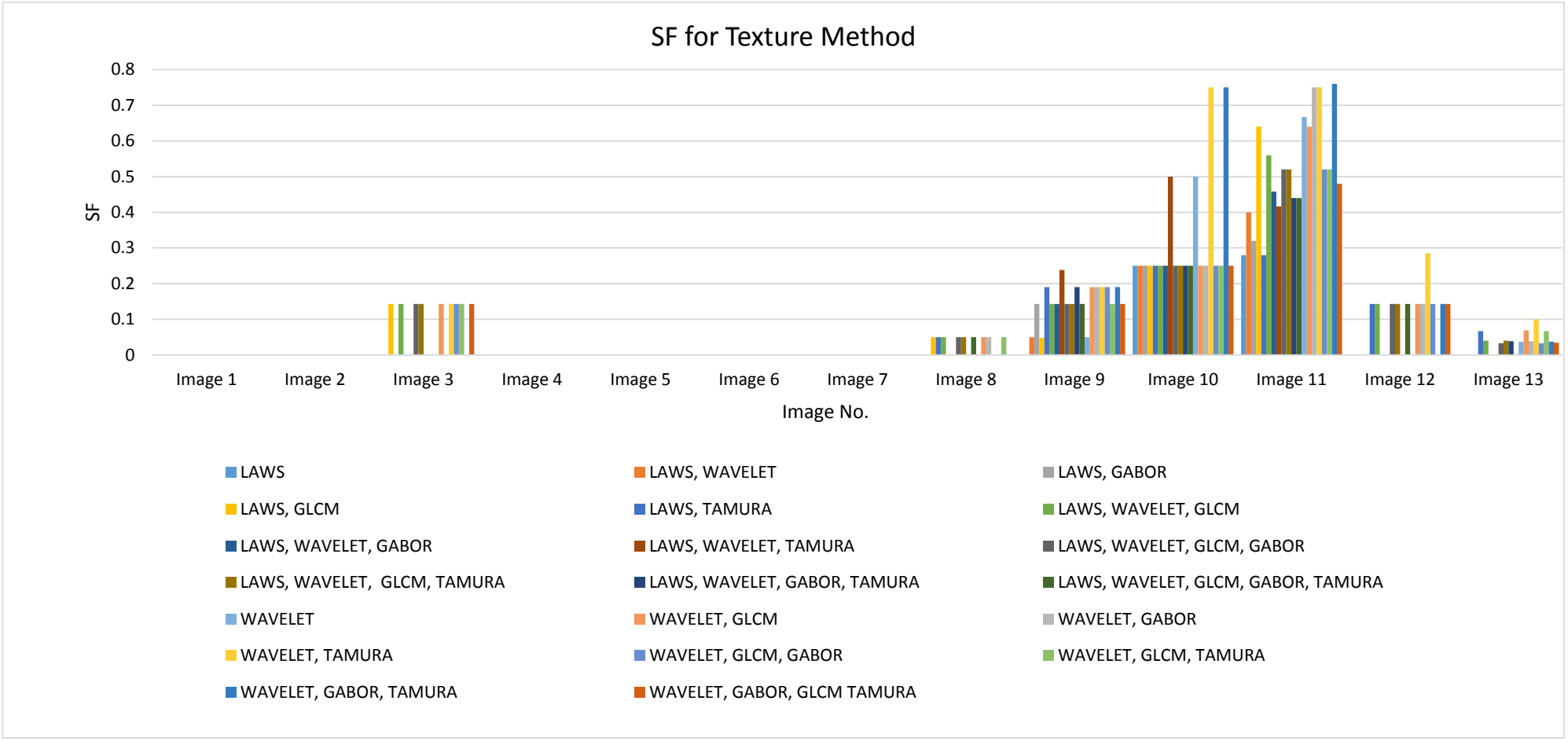

Figure 5.6: Graph between SF for the different texture methods and the combinations of texture methods

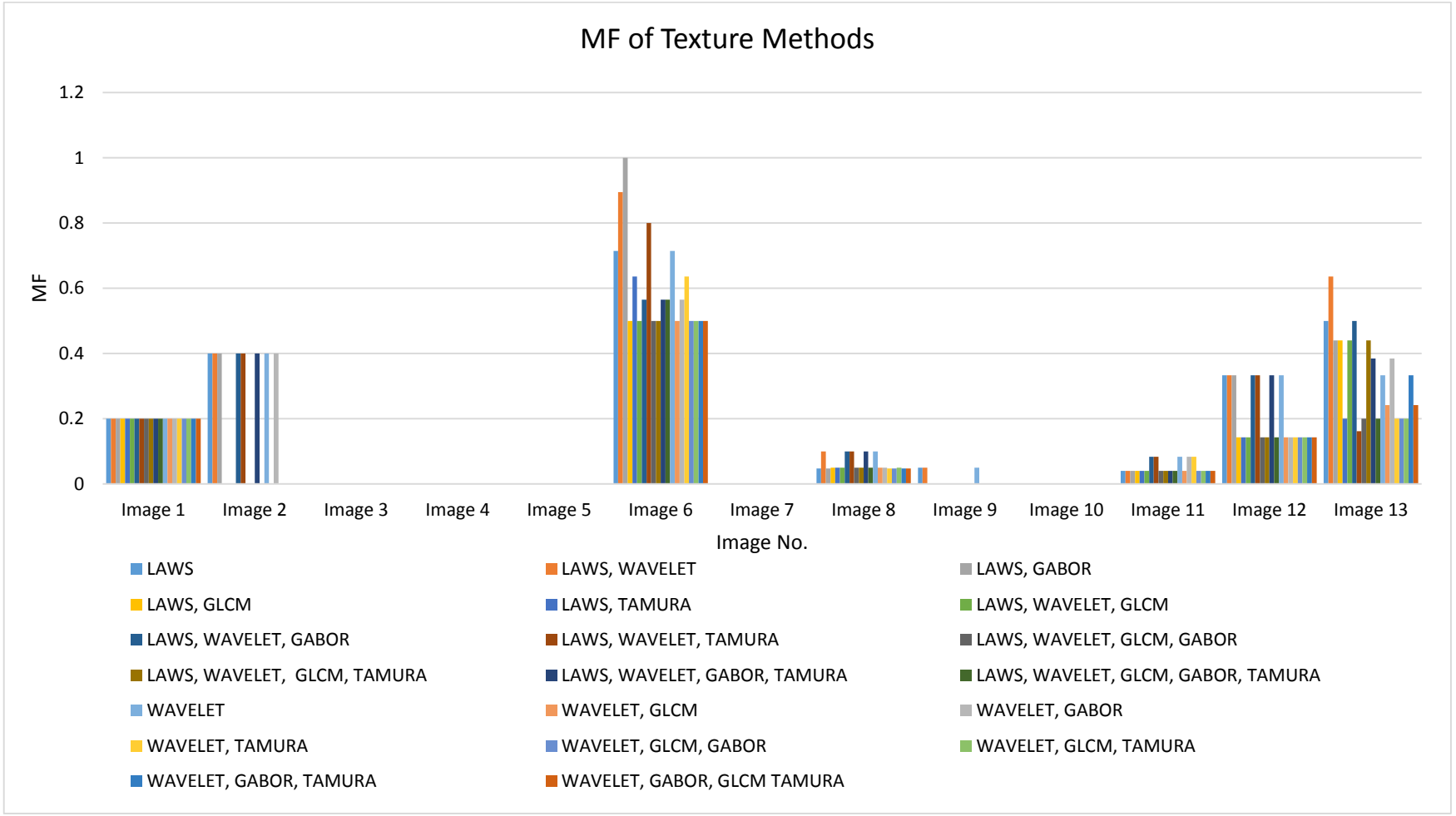

Figure 5.7: Graph between MF for the different texture methods and the combinations of texture methods

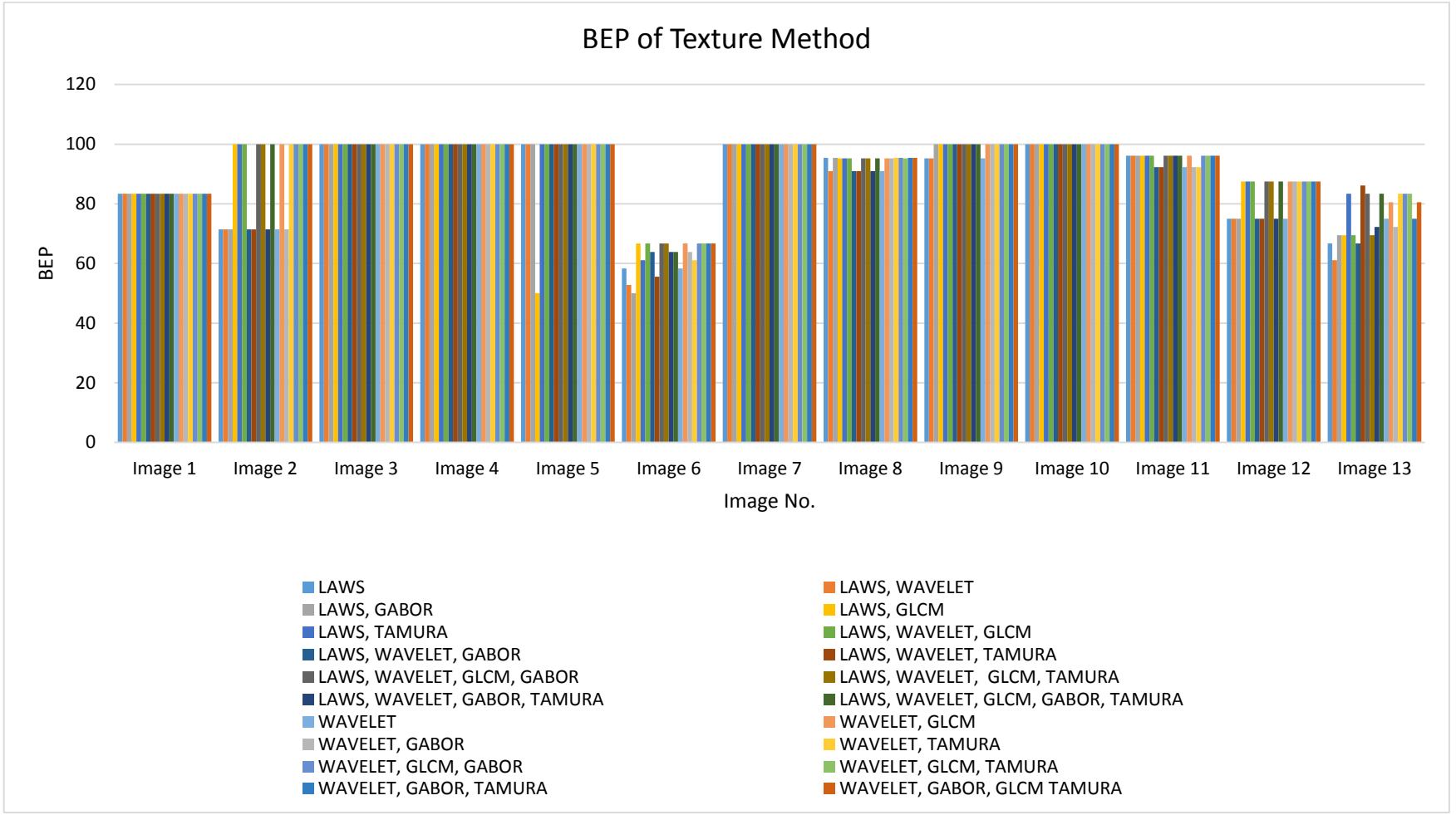

Figure 5.8: Graph between BEP of the different texture methods and the combinations of texture methods

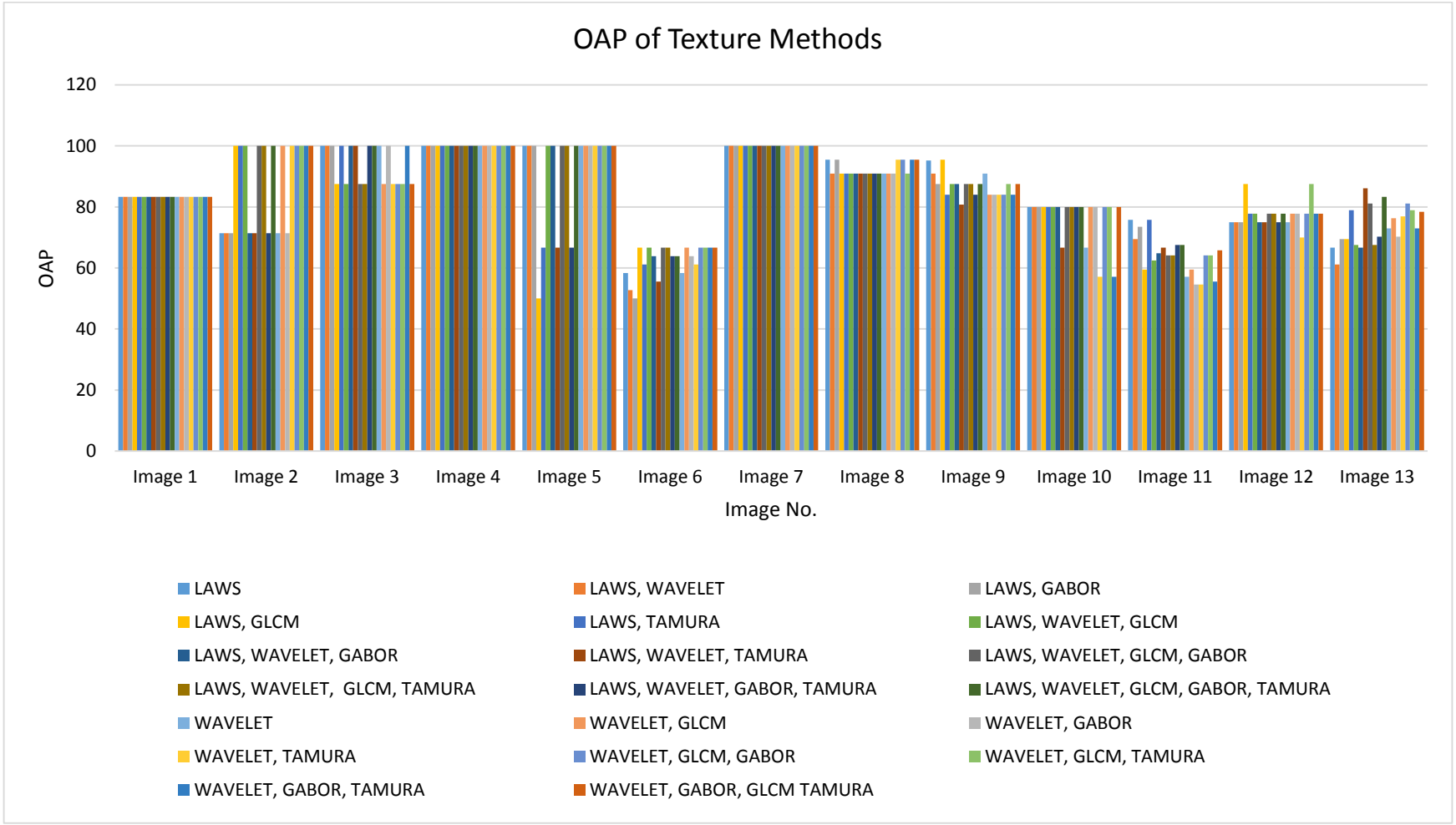

Figure 5.9: Graph between OAP of the different texture methods and the combinations of texture methods

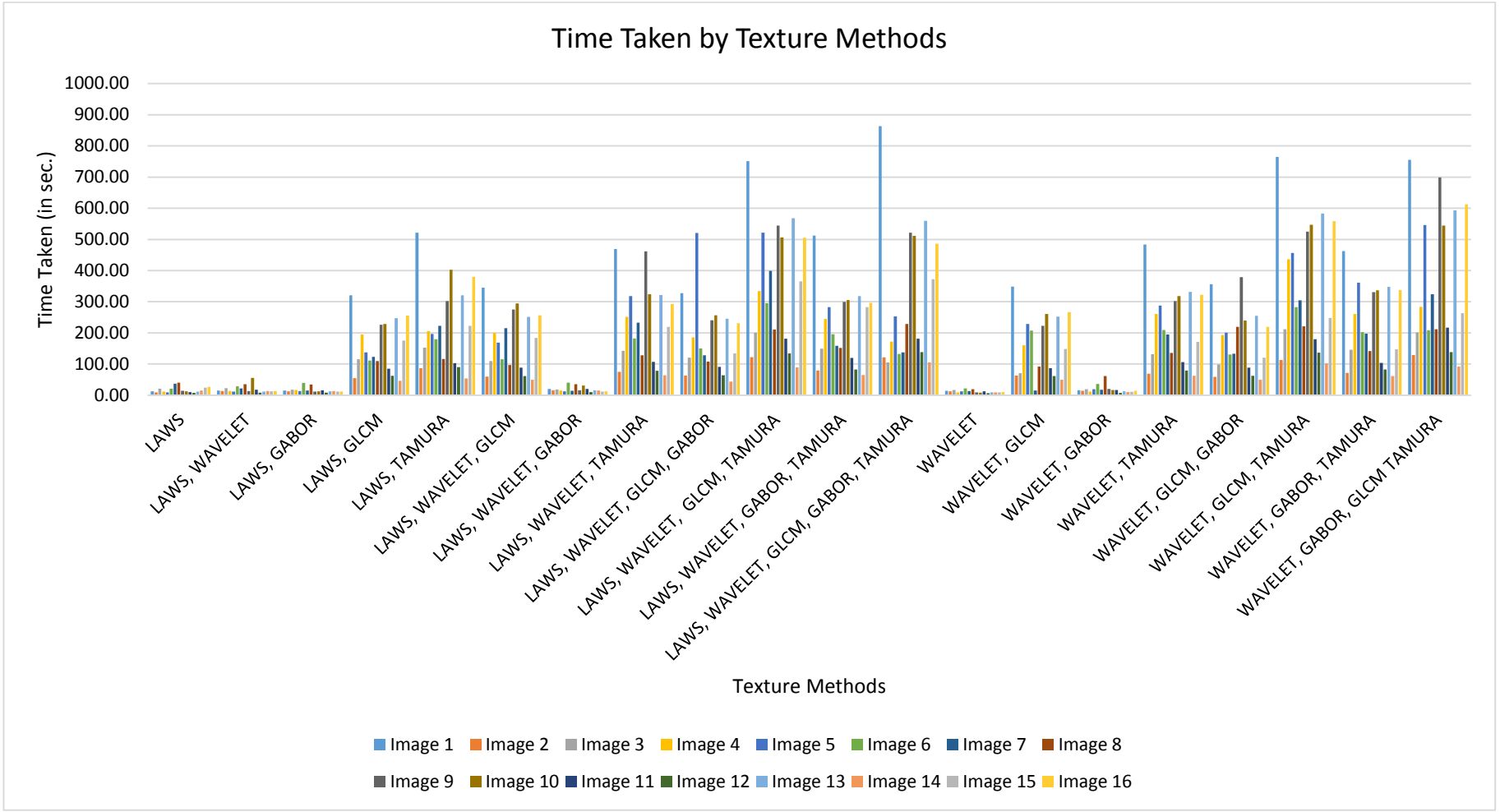

Figure 5.10: Graph between Time taken by different texture methods and the combinations of texture methods

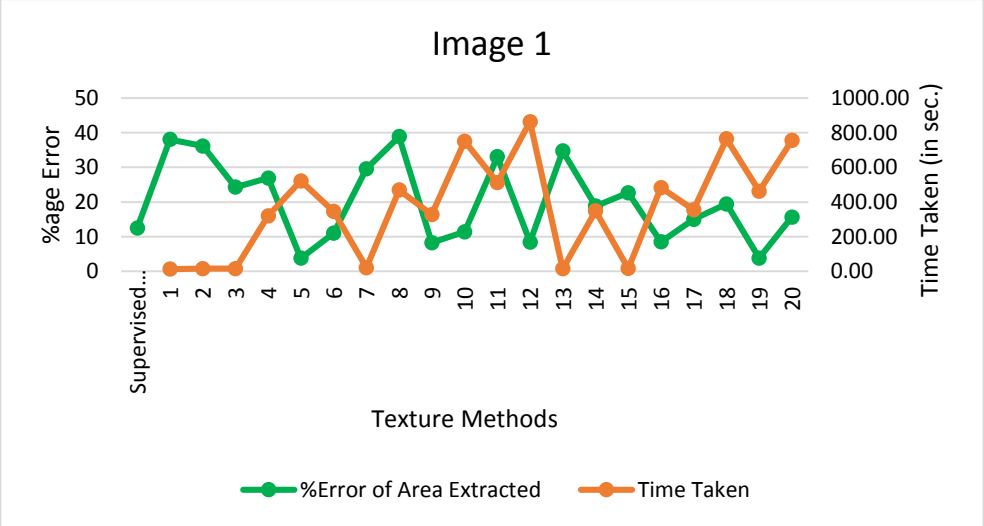

Figure 5.11 (a)

Figure 5.11 (b)

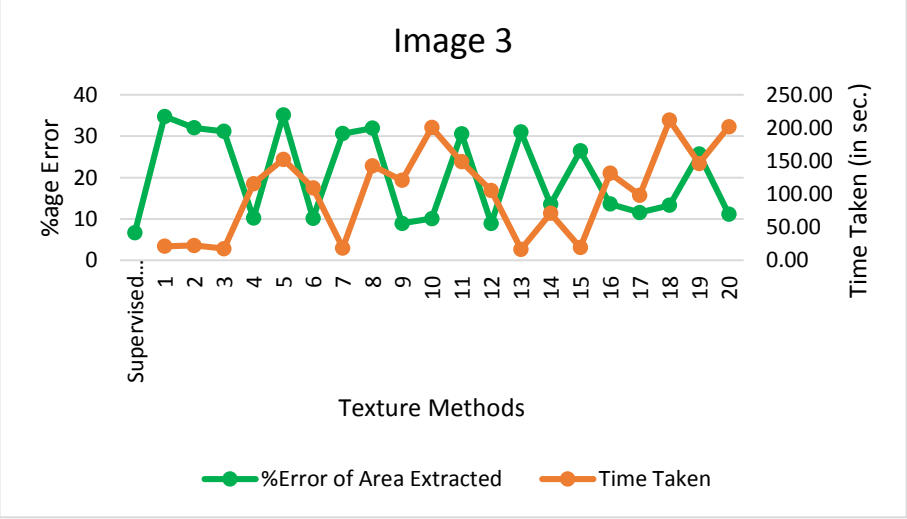

Figure 5.11 (c)

Figure 5.11 (d)

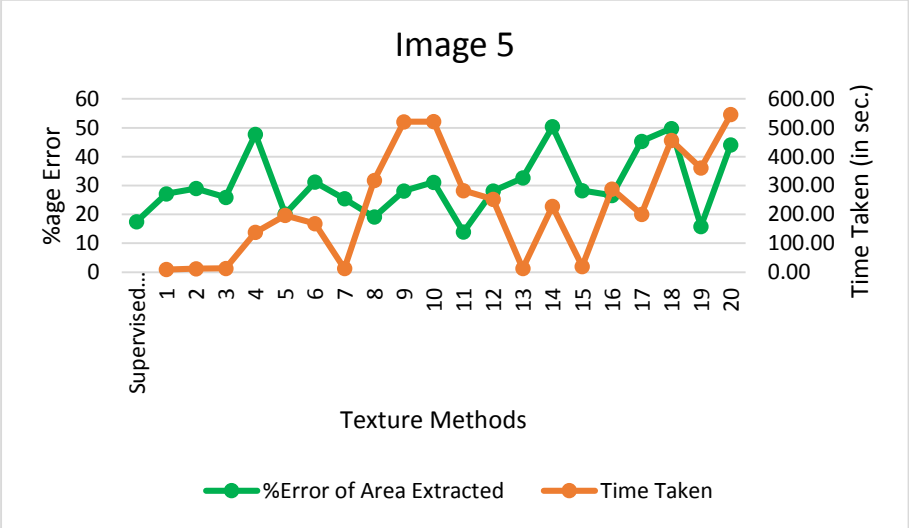

Figure 5.11 (e)

Figure 5.11 (f)

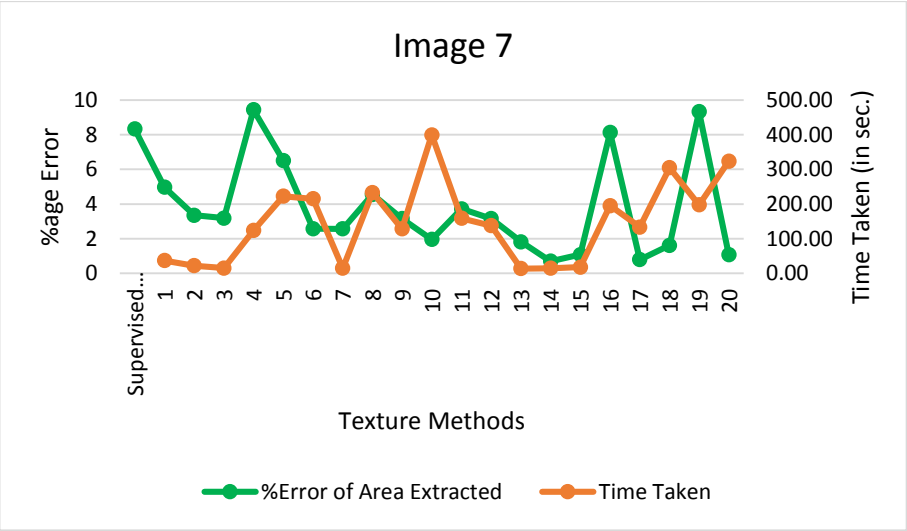

Figure 5.11 (g)

Figure 5.11 (h)

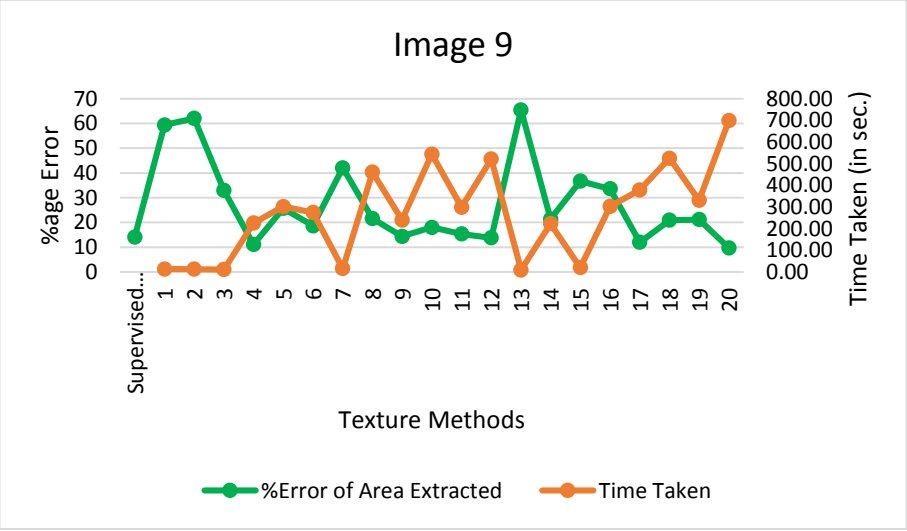

Figure 5.11 (i)

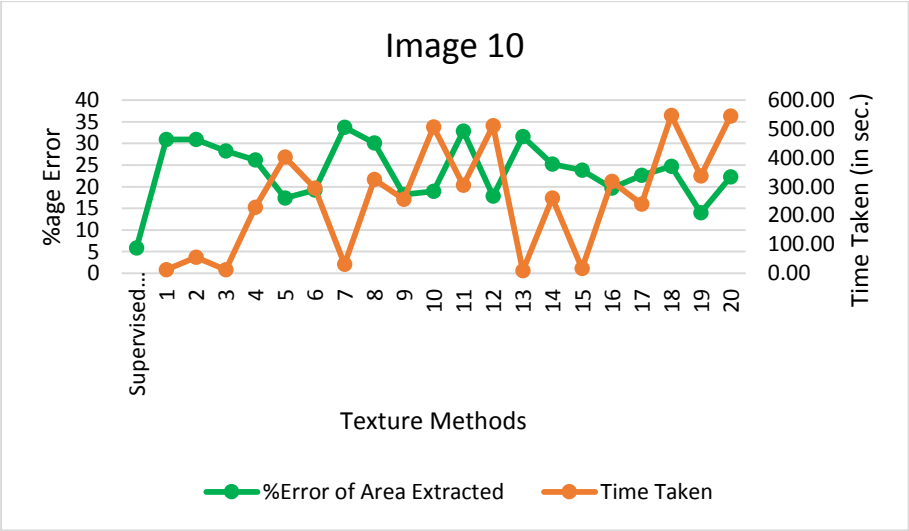

Figure 5.11 (j)

Figure 5.11 (k)

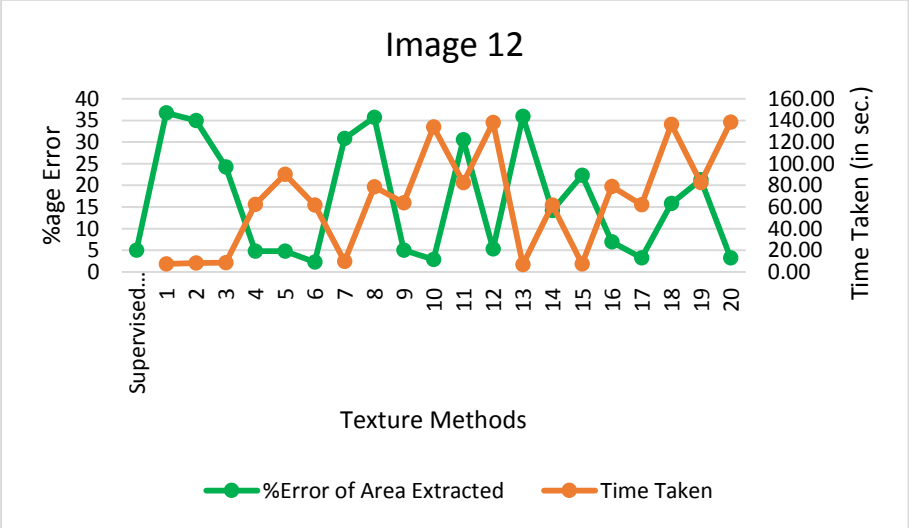

Figure 5.11 (l)

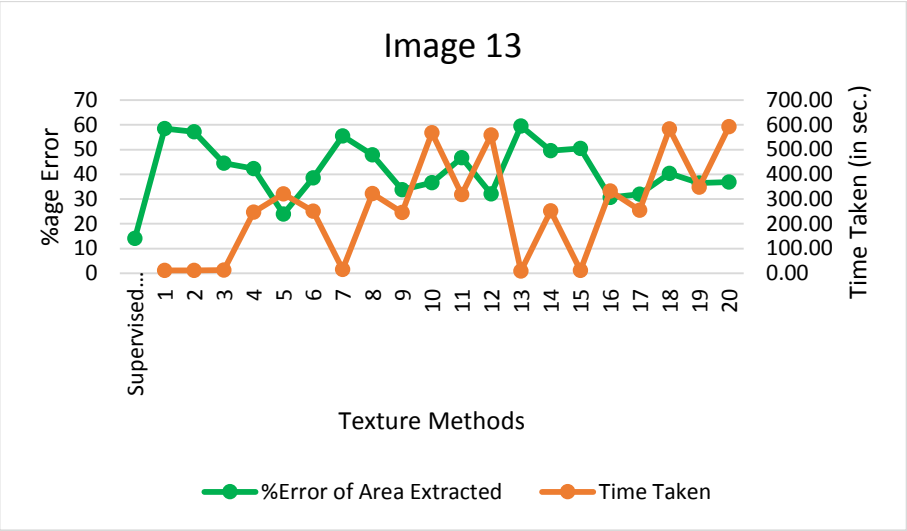

Figure 5.11 (m)

Figure 5.11 (n)

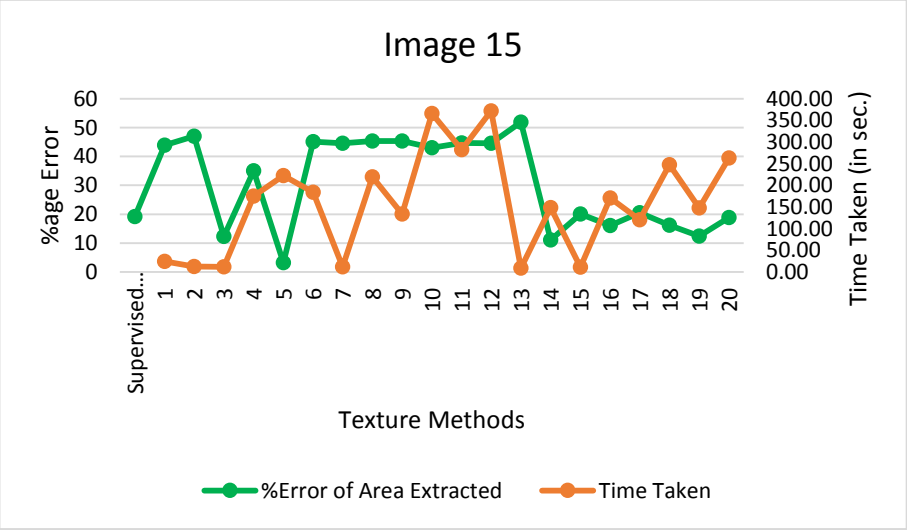

Figure 5.11 (o)

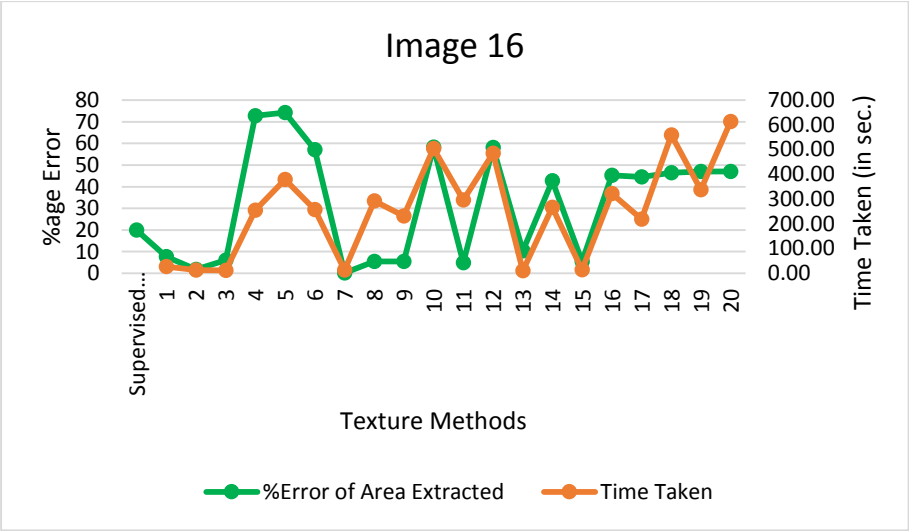

Figure 5.11 (p)

Figure 5.11: Graph between the combinations of the texture methods used while executing the developed method based on texture and the percentage error calculated for the extracted area

On the basis of Time Taken to complete the extraction process

The graph plotted between the execution time and the used texture methods w.r.t. the image number is shown in Figure 5.10. It has been observed that the combination no. 1, 2, 3, 7, 13 and 15 takes very few seconds to complete the extraction process, while the texture method having GLCM and/or Tamura takes maximum time to complete the extraction process (around 5 times more time in the presence of GLCM, around 10 times more time in the presence of Tamura and around 15 times more time in the presence of both).

Accuracy Assessment on the basis of Area extracted and time taken:

For each image, a graph plotted between the area extracted and the execution time is shown in Figure 5.11Figure 5.10. From the graph, it has been observed that if more than one texture methods are combined while running the developed texture method, the area extracted for the buildings also increases. But while assessing the accuracy of the texture methods, the time taken by the algorithm must also be considered. So, the graphs have been plotted between the time taken by the texture methods, % error of area extracted w.r.t. the digitized area verses the texture method combinations by taking three axis, one horizontal and two vertical. The horizontal axis represents texture methods used while running the developed code, the primary vertical axis represents an area extracted for the building and the secondary vertical axis represents time

taken by the developed code to extract the buildings. By analyzing the plotted graphs, it was observed that while running the code, as the number of texture methods increases, the % error of area of extracted buildings increases, but time taken by the code to finish the process also increases.

The % error of the area extracted by the texture methods has been compared with the % error calculated for supervised classified images, and it was found that for most of the images, combinations 1, 2, 3, 7, 8, 11, 13, 15 and 18 gave highest % error. The combinations 1, 2, 3, 7, 13 and 15 took very few seconds to complete the extraction process. The texture combination having GLCM and/or Tamura takes maximum time to complete the extraction process (around 5 times more time in the presence of GLCM, around 10 times more time in the presence of Tamura and around 15 times more time in the presence of both).

On the basis of % error and the time taken, from the twenty combinations, it was found that combination 6 (LAWS, Wavelet, GLCM) gives relatively less % error for extracted area than other combinations in relatively less time.

5.5 RESULTS OBTAINED FOR BUILDING EXTRACTION METHOD BASED ON THRESHOLD, TEXTURE AND SHADOW

This section presents the results obtained after running the developed code for the method based on threshold, texture and shadow. In addition, the results of both qualitative and quantitative analysis have been given, and accuracy assessment is carried out on the basis of analysis.

5.5.1 Results Obtained

Figure 5.12 (a): Image 1

Figure 5.12 (b): Image 2

Figure 5.12 (c): Image 3

Figure 5.12 (d): Image 4

Figure 5.12 (e): Image 5

Figure 5.12 (f): Image 6

Figure 5.12 (g): Image 7

Figure 5.12 (h): Image 8

Figure 5.12 (i): Image 9

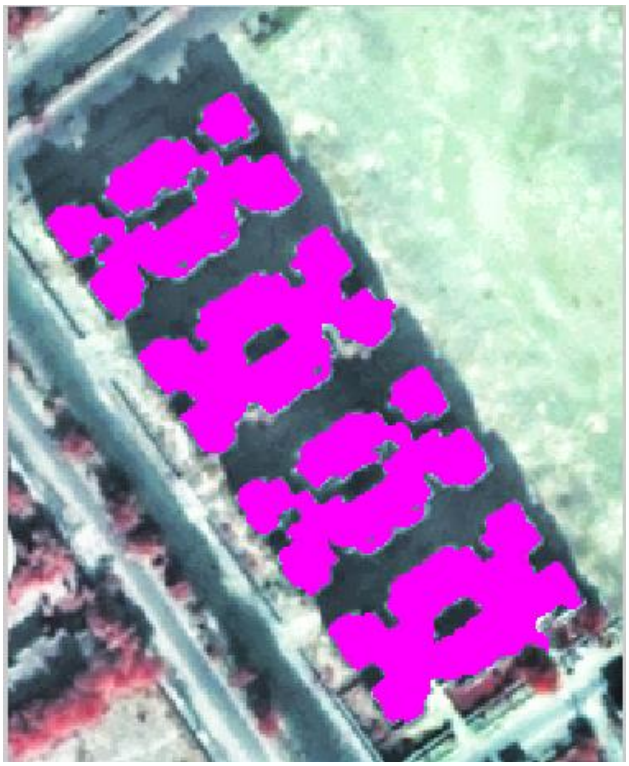

Figure 5.12 (j): Image 10

Figure 5.12 (k): Image 11

Figure 5.12 (l): Image 12

Figure 5.12 (m): Image 13

Figure 5.12 (n): Image 14

Figure 5.12 (o): Image 15

Figure 5.12 (p): Image 16

Figure 5.12: Results obtained after executing the method based on Threshold, Texture and Shadow using LAWS Texture method. On the basis of % error and the time taken, from the twenty combinations, it was found that combination 6 (LAWS, Wavelet, GLCM) gives relatively less % error for extracted area than other combinations in relatively less time.

5.5.2 Analysis of the Results

Qualitative Analysis:

Qualitative analysis of the results obtained has been done on the basis of visual interpretation. The findings of visual interpretation of the output images of all 20 combinations are listed below:

i. All types of buildings i.e., residential (planned, unplanned and slum), industrial, business and educational buildings were extracted successfully irrespective of their shape, size, orientation and density.
ii. All texture combinations gave almost similar results. There was no noticeable change between the results obtained from the twenty texture combinations.
iii. The buildings having a small gap in between were also extracted as separate buildings.
iv. The corners of extracted buildings were not sharp and the edges were not smooth, because of this the boundary of the extracted buildings looked like free handed drawn shape.

Object based accuracy assessment:

For object based accuracy assessment, Correct Extraction or TP, False Extraction or FP and Missed Extraction or FN have been calculated for all 20 combinations of texture methods and using these values SF, MF, BEP and OAP have been computed as described in Chapter 4. The performance evaluation results are given in Table 5.13 (a), Table 5.13 (b), Table 5.14, Table 5.15, Table 5.16 and Table 5.17.

For all twenty combinations, very low values for SF (0–0.12) and MF (0–0.16) have been observed, which indicates that the rate of incorrectly extracted buildings and rate of missed buildings is very less. Also, very high values for BEP (86.11–100%) and OAP (81.57–100%), means that the building extraction method successfully extracted all types of buildings.

On the basis of Time Taken to complete the extraction process

A graph has been plotted between the execution time and the texture methods used, along with threshold value and shadow information. It is shown in Figure 5.17. While analysing, it has been observed that the combinations 1, 2, 3, 7, 13 and 15 took very few seconds to complete the extraction process, while the texture method having GLCM and/or Tamura took maximum time to complete the extraction process (around 5 times more time in the presence of GLCM,

around 10 times more time in the presence of Tamura and around 15 times more time in the presence of both).

Accuracy Assessment on the basis of Area extracted and time taken:

For each input image, a graph has been plotted between the texture methods used while executing the developed methods, and the percentage error calculated for the extracted area is shown in Figure 5.18. While analysing the graphs, it has been observed that all twenty texture combinations when used with threshold value and shadow information gives same results without any significant difference in the output. But for assessing the accuracy of texture methods, % error in the output and the time taken by them must be considered. So, the graphs are plotted between the time taken by the texture methods, % error of area extracted w.r.t. the digitized area verses the texture methods combinations on three axis, one horizontal and two vertical. The horizontal axis represents texture methods used while running the developed code, the primary vertical axis represents area extracted for the building and the secondary vertical axis represents time taken by the developed code to extract the buildings. By analysing the plotted graphs, it was observed that as the number of texture methods increased, the time taken by the code to finish the process also increased.

Table 5.13 (a): Performance evaluation results for the texture combinations used while executing the Developed Method

Image No.	No. of Buildings	LAWS			LAWS, WAVELET			LAWS, GABOR			.LAWS, GLCM			.LAWS, TAMURA			LAWS, WAVELET, GLCM			LAWS, WAVELET, GABOR			LAWS, WAVELET, TAMURA			LAWS, WAVELET, GLCM, GABOR			LAWS, WAVELET, GLCM, TAMURA		
		TP	FN	FP	TP	FN	FP	TP	FN	FP	TP	FN	FP	TP	FN	FP	TP	FN	FP	TP	FN	FP	TP	FN	FP	TP	FN	FP	TP	FN	FP
Image 1	12	12	0	0	12	0	0	12	0	0	12	0	0	12	0	0	12	0	0	12	0	0	12	0	0	12	0	0	12	0	2
Image 2	7	7	0	0	7	0	0	7	0	0	7	0	0	7	0	0	7	0	0	7	0	0	7	0	0	7	0	0	7	0	0
Image 3	7	7	0	0	7	0	0	7	0	0	7	0	0	7	0	0	7	0	0	7	0	0	7	0	0	7	0	0	7	0	0
Image 4	1	1	0	0	1	0	0	1	0	0	1	0	0	1	0	0	1	0	0	1	0	0	1	0	0	1	0	0	1	0	0
Image 5	2	2	0	0	2	0	0	2	0	0	2	0	0	2	0	0	2	0	0	2	0	0	2	0	0	2	0	0	2	0	0
Image 6	36	32	4	0	32	4	0	32	4	0	32	4	0	32	4	0	32	4	0	32	4	0	32	4	0	32	4	0	32	4	0
Image 7	3	3	0	0	3	0	0	3	0	0	3	0	0	3	0	0	3	0	0	3	0	0	3	0	0	3	0	0	3	0	0
Image 8	22	21	1	1	21	1	1	21	1	1	21	1	1	21	1	1	21	1	1	21	1	1	21	1	1	21	1	1	21	1	1
Image 9	21	20	1	2	20	1	2	20	1	2	20	1	2	20	1	2	20	1	2	20	1	2	20	1	2	20	1	2	20	1	1
Image 10	4	4	0	0	4	0	0	4	0	0	4	0	0	4	0	0	4	0	0	4	0	0	4	0	0	4	0	0	4	0	0
Image 11	26	24	2	3	24	2	3	24	2	3	24	2	3	24	2	3	24	2	3	24	2	3	24	2	3	24	2	3	24	2	3
Image 12	8	7	1	0	7	1	0	7	1	0	7	1	0	7	1	0	7	1	0	7	1	0	7	1	0	7	1	0	7	1	0
Image 13	36	31	5	2	32	4	2	31	5	2	31	5	2	31	5	2	31	5	2	31	5	2	31	5	2	31	5	2	31	5	2

Table 5.13 (b): Performance evaluation results for the texture combinations used while executing the Developed Method based on Threshold, Texture and Shadow

Image No.	No. of Buildings	LAWS, WAVELET, GABOR, TAMURA			LAWS, WAVELET, GLCM, GABOR, TAMURA			WAVELET			WAVELET, GLCM			WAVELET, GABOR			WAVELET, TAMURA			WAVELET, GLCM, GABOR			WAVELET, GLCM, TAMURA			WAVELET, GABOR, TAMURA			WAVELET, GLCM, GABOR, TAMURA		
		TP	FN	FP	TP	FN	FP	TP	FN	FP	TP	FN	FP	TP	FN	FP	TP	FN	FP	TP	FN	FP	TP	FN	FP	TP	FN	FP	TP	FN	FP
Image 1	12	12	0	2	12	0	2	12	0	2	12	0	2	12	0	2	12	0	2	12	0	2	12	0	2	12	0	2	12	0	2
Image 2	7	7	0	0	7	0	0	7	0	0	7	0	1	7	0	0	7	0	0	7	0	0	7	0	0	7	0	0	7	0	0
Image 3	7	7	0	0	7	0	0	7	0	0	7	0	0	7	0	0	7	0	0	7	0	0	7	0	0	7	0	0	7	0	0
Image 4	1	1	0	0	1	0	0	1	0	0	1	0	0	1	0	0	1	0	0	1	0	0	1	0	0	1	0	0	1	0	0
Image 5	2	2	0	0	2	0	0	2	0	0	2	0	0	2	0	0	2	0	0	2	0	0	2	0	0	2	0	0	2	0	0
Image 6	36	32	4	0	32	4	0	32	4	0	32	4	0	32	4	0	32	4	0	32	4	0	32	4	0	32	4	0	32	4	0
Image 7	3	3	0	0	3	0	0	3	0	0	3	0	0	3	0	0	3	0	0	3	0	0	3	0	0	3	0	0	3	0	0
Image 8	22	21	1	1	21	1	1	21	1	1	21	1	1	21	1	1	21	1	1	21	1	1	21	1	1	21	1	1	21	1	1
Image 9	21	20	1	2	20	1	2	20	1	2	20	1	2	20	1	2	20	1	2	20	1	2	20	1	2	20	1	2	20	1	3
Image 10	4	4	0	0	4	0	0	4	0	0	4	0	0	4	0	0	4	0	0	4	0	0	4	0	0	4	0	0	4	0	0
Image 11	26	24	2	3	24	2	3	24	2	3	24	2	3	24	2	3	24	2	3	24	2	3	24	2	3	24	2	3	24	2	3
Image 12	8	7	1	0	7	1	0	7	1	0	7	1	0	7	1	0	7	1	0	7	1	0	7	1	0	7	1	0	7	1	0
Image 13	36	31	5	2	31	5	2	31	5	2	31	5	2	31	5	2	31	5	2	31	5	2	31	5	2	31	5	2	31	5	2

Table 5.14: SF of Texture combinations used while executing the Developed Method based on Threshold, Texture and Shadow

Image No.	LAWS	LAWS, WAVELET	LAWS, GABOR	LAWS, GLCM	LAWS, TAMURA	LAWS, WAVELET, GLCM	LAWS, WAVELET, GABOR	LAWS, WAVELET, TAMURA	LAWS, WAVELET, GLCM, GABOR	LAWS, WAVELET, GLCM, TAMURA	LAWS, WAVELET, GABOR, TAMURA	LAWS, WAVELET, GLCM, GABOR, TAMURA	WAVELET	WAVELET, GLCM	WAVELET, GABOR	WAVELET, TAMURA	WAVELET, GLCM, GABOR	WAVELET, GLCM, TAMURA	WAVELET, GABOR, TAMURA	WAVELET, GABOR, GLCM ,
Image 1	0	0	0	0	0	0	0	0	0.17	0.17	0.17	0.17	0.17	0.17	0.17	0.17	0.17	0.17	0.17	0.17
Image 2	0	0	0	0	0	0	0	0	0	0	0	0	0	0.14	0	0	0	0	0	0
Image 3	0	0	0	0	0	0	0	0	0	0	0	0	0	0	0	0	0	0	0	0
Image 4	0	0	0	0	0	0	0	0	0	0	0	0	0	0	0	0	0	0	0	0
Image 5	0	0	0	0	0	0	0	0	0	0	0	0	0	0	0	0	0	0	0	0
Image 6	0	0	0	0	0	0	0	0	0	0	0	0	0	0	0	0	0	0	0	0
Image 7	0	0	0	0	0	0	0	0	0	0	0	0	0	0	0	0	0	0	0	0
Image 8	0.04	0.04	0.04	0.04	0.04	0.04	0.04	0.04	0.04	0.04	0.04	0.04	0.04	0.04	0.04	0.04	0.04	0.04	0.04	0.04
Image 9	0.1	0.1	0.1	0.1	0.1	0.1	0.1	0.1	0.1	0.05	0.1	0.1	0.1	0.1	0.1	0.1	0.1	0.1	0.1	0.15
Image 10	0	0	0	0	0	0	0	0	0	0	0	0	0	0	0	0	0	0	0	0
Image 11	0.12	0.12	0.12	0.12	0.12	0.12	0.12	0.12	0.12	0.12	0.12	0.12	0.12	0.12	0.12	0.12	0.12	0.12	0.12	0.12
Image 12	0	0	0	0	0	0	0	0	0	0	0	0	0	0	0	0	0	0	0	0
Image 13	0.06	0.06	0.06	0.06	0.06	0.06	0.06	0.06	0.06	0.06	0.06	0.06	0.06	0.06	0.06	0.06	0.06	0.06	0.06	0.06

Table 5.15: MF of Texture combinations used while executing the Developed Method based on Threshold, Texture and Shadow

Image No.	LAWS	LAWS, WAVELET	LAWS, GABOR	LAWS, GLCM	LAWS, TAMURA	LAWS, WAVELET, GLCM	LAWS, WAVELET, GABOR	LAWS, WAVELET, TAMURA	LAWS, WAVELET, GLCM, GABOR	LAWS, WAVELET, GLCM, TAMURA	LAWS, WAVELET, GABOR, TAMURA	LAWS, WAVELET, GLCM, GABOR, TAMURA	WAVELET	WAVELET, GLCM	WAVELET, GABOR	WAVELET, TAMURA	WAVELET, GLCM, GABOR	WAVELET, GLCM, TAMURA	WAVELET, GABOR, TAMURA	WAVELET, GABOR, GLCM TAMURA
Image 1	0	0	0	0	0	0	0	0	0	0	0	0	0	0	0	0	0	0	0	0
Image 2	0	0	0	0	0	0	0	0	0	0	0	0	0	0	0	0	0	0	0	0
Image 3	0	0	0	0	0	0	0	0	0	0	0	0	0	0	0	0	0	0	0	0
Image 4	0	0	0	0	0	0	0	0	0	0	0	0	0	0	0	0	0	0	0	0
Image 5	0	0	0	0	0	0	0	0	0	0	0	0	0	0	0	0	0	0	0	0
Image 6	0.12	0.12	0.12	0.12	0.12	0.12	0.12	0.12	0.12	0.12	0.12	0.12	0.12	0.12	0.12	0.12	0.12	0.12	0.12	0.12
Image 7	0	0	0	0	0	0	0	0	0	0	0	0	0	0	0	0	0	0	0	0
Image 8	0.04	0.04	0.04	0.04	0.04	0.04	0.04	0.04	0.04	0.04	0.04	0.04	0.04	0.04	0.04	0.04	0.04	0.04	0.04	0.04
Image 9	0.05	0.05	0.05	0.05	0.05	0.05	0.05	0.05	0.05	0.05	0.05	0.05	0.05	0.05	0.05	0.05	0.05	0.05	0.05	0.05
Image 10	0	0	0	0	0	0	0	0	0	0	0	0	0	0	0	0	0	0	0	0
Image 11	0.08	0.08	0.08	0.08	0.08	0.08	0.08	0.08	0.08	0.08	0.08	0.08	0.08	0.08	0.08	0.08	0.08	0.08	0.08	0.08
Image 12	0.14	0.14	0.1	0.1	0.14	0.14	0.14	0.14	0.14	0.14	0.14	0.14	0.14	0.14	0.14	0.14	0.14	0.14	0.14	0.14
Image 13	0.16	0.12	0.16	0.16	0.16	0.16	0.16	0.16	0.16	0.16	0.16	0.16	0.16	0.16	0.16	0.16	0.16	0.16	0.16	0.16

Table 5.16: BEP of Texture combinations used while executing the Developed Method based on Threshold, Texture and Shadow

Image No.	LAWS	LAWS, WAVELET	LAWS, GABOR	LAWS, GLCM	LAWS, TAMURA	LAWS, WAVELET, GLCM	LAWS, WAVELET, GABOR	LAWS, WAVELET, TAMURA	LAWS, WAVELET, GLCM, GABOR	LAWS, WAVELET, GLCM, TAMURA	LAWS, WAVELET, GABOR, TAMURA	LAWS, WAVELET, GLCM, GABOR, TAMURA	WAVELET	WAVELET, GLCM	WAVELET, GABOR	WAVELET, TAMURA	WAVELET, GLCM, GABOR	WAVELET, GLCM, TAMURA	WAVELET, GABOR, TAMURA	WAVELET, GABOR, GLCM TAMURA
Image 1	100	100	100	100	100	100	100	100	100	100	100	100	100	100	100	100	100	100	100	100
Image 2	100	100	100	100	100	100	100	100	100	100	100	100	100	100	100	100	100	100	100	100
Image 3	100	100	100	100	100	100	100	100	100	100	100	100	100	100	100	100	100	100	100	100
Image 4	100	100	100	100	100	100	100	100	100	100	100	100	100	100	100	100	100	100	100	100
Image 5	100	100	100	100	100	100	100	100	100	100	100	100	100	100	100	100	100	100	100	100
Image 6	88.89	88.89	88.89	88.89	88.89	88.89	88.89	88.89	88.89	88.89	88.89	88.89	88.89	88.89	88.89	88.89	88.89	88.89	88.89	88.89
Image 7	100	100	100	100	100	100	100	100	100	100	100	100	100	100	100	100	100	100	100	100
Image 8	95.45	95.45	95.45	95.45	95.45	95.45	95.45	95.45	95.45	95.45	95.45	95.45	95.45	95.45	95.45	95.45	95.45	95.45	95.45	95.45
Image 9	95.24	95.24	95.24	95.24	95.24	95.24	95.24	95.24	95.24	95.24	95.24	95.24	95.24	95.24	95.24	95.24	95.24	95.24	95.24	95.24
Image 10	100	100	100	100	100	100	100	100	100	100	100	100	100	100	100	100	100	100	100	100
Image 11	92.31	92.31	92.31	92.31	92.31	92.31	92.31	92.31	92.31	92.31	92.31	92.31	92.31	92.31	92.31	92.31	92.31	92.31	92.31	92.31
Image 12	87.5	87.5	87.5	87.5	87.5	87.5	87.5	87.5	87.5	87.5	87.5	87.5	87.5	87.5	87.5	87.5	87.5	87.5	87.5	87.5
Image 13	86.11	88.89	86.11	86.11	86.11	86.11	86.11	86.11	86.11	86.11	86.11	86.111	86.11	86.11	86.11	86.11	86.11	86.11	86.11	86.11

Table 5.17: OAP of Texture combinations used while executing the Developed Method based on Threshold, Texture and Shadow

Image No.	LAWS	LAWS, WAVELET	LAWS, GABOR	LAWS, GLCM	LAWS, TAMURA	LAWS, WAVELET, GLCM	LAWS, WAVELET, GABOR	LAWS, WAVELET, TAMURA	LAWS, WAVELET, GLCM, GABOR	LAWS, WAVELET, GLCM, TAMURA	LAWS, WAVELET, GABOR, TAMURA	LAWS, WAVELET, GLCM, GABOR, TAMURA	WAVELET	WAVELET, GLCM	WAVELET, GABOR	WAVELET, TAMURA	WAVELET, GLCM, GABOR	WAVELET, GLCM, TAMURA	WAVELET, GABOR, TAMURA	WAVELET, GABOR, GLCM TAMURA
Image 1	100	100	100	100	100	100	100	100	85.71	85.71	85.71	85.71	85.71	85.71	85.71	85.71	85.71	85.71	85.71	85.71
Image 2	100	100	100	100	100	100	100	100	100	100	100	100	100	87.5	100	100	100	100	100	100
Image 3	100	100	100	100	100	100	100	100	100	100	100	100	100	100	100	100	100	100	100	100
Image 4	100	100	100	100	100	100	100	100	100	100	100	100	100	100	100	100	100	100	100	100
Image 5	100	100	100	100	100	100	100	100	100	100	100	100	100	100	100	100	100	100	100	100
Image 6	88.89	88.89	88.89	88.89	88.89	88.89	88.89	88.89	88.89	88.89	88.89	88.89	88.89	88.89	88.89	88.89	88.89	88.89	88.89	88.89
Image 7	100	100	100	100	100	100	100	100	100	100	100	100	100	100	100	100	100	100	100	100
Image 8	91.30	91.30	91.30	91.30	91.30	91.30	91.30	91.30	91.30	91.30	91.30	91.30	91.30	91.30	91.30	91.30	91.30	91.30	91.30	91.30
Image 9	86.95	86.95	86.95	86.95	86.95	86.95	86.95	86.95	86.95	90.91	86.95	86.95	86.95	86.95	86.95	86.95	86.95	86.95	86.95	83.33
Image 10	100	100	100	100	100	100	100	100	100	100	100	100	100	100	100	100	100	100	100	100
Image 11	82.75	82.75	82.75	82.75	82.75	82.75	82.75	82.75	82.75	82.75	82.75	82.75	82.75	82.75	82.75	82.75	82.75	82.75	82.75	82.75
Image 12	87.5	87.5	87.5	87.5	87.5	87.5	87.5	87.5	87.5	87.5	87.5	87.5	87.5	87.5	87.5	87.5	87.5	87.5	87.5	87.5
Image 13	81.57	84.21	81.57	81.57	81.57	81.57	81.57	81.57	81.57	81.57	81.57	81.57	81.57	81.57	81.57	81.57	81.57	81.57	81.57	81.57

Table 5.18: Area (in sq. m.) Extracted by Different Combinations of Texture Methods while executing the Developed Method based on Threshold, Texture and Shadow

Image No.	Digitized Area	Area Extracted by																		
		LAWS	LAWS, WAVELET	LAWS, GABOR	LAWS, GLCM	LAWS, TAMURA	LAWS, WAVELET, GLCM	LAWS, WAVELET, GABOR	LAWS, WAVELET, TAMURA	LAWS, WAVELET, GLCM, GABOR	LAWS, WAVELET, GLCM, TAMURA	LAWS, WAVELET, GABOR, TAMURA	LAWS, WAVELET, GLCM, GABOR, TAMURA	WAVELET	WAVELET, GLCM	WAVELET, GABOR	WAVELET, TAMURA	WAVELET, GLCM, GABOR	WAVELET, GLCM, TAMURA	WAVELET, GABOR, TAMURA	WAVELET, GABOR, GLCM TAMURA
Image 1	3284	3007.68	3013.2	2994.5	3004.2	3067.5	3038.8	3014.2	3045.4	3203.3	3195.2	3172.1	3201.7	3178.9	3188.3	3186.7	3201.1	3199.8	3186.4	3213.9	3199.8
Image 2	6121	5689.1	5698.4	5701.3	5752.8	5744.1	5784.2	5696.6	5697.3	5751.3	5744.1	5697	5748.1	5703.4	5749.5	5715.7	5740.2	5757.8	5756.7	5718.6	5756.7
Image 3	5023	4851	4833.4	4842.7	4906.8	4907.8	4885.2	4835.1	4831.9	4886.6	4888.4	4832.6	4890.9	4841.6	4879.3	4848.1	4881.6	4880.8	4883.1	4853.1	4884.1
Image 4	1395	1440.12	1439.7	1438.4	1438.5	1439.1	1437.8	1443.4	1440.7	1439.4	1443.4	1439.4	1442.7	1441.7	1443.4	1443.4	1443.4	1443.7	1444.7	1444.1	1443.7
Image 5	2071	1932.12	1918.8	1931.0	1928.5	1935	1923.4	1927.1	1926	1928.1	1922.1	1937.8	1928.5	1921.3	1920.9	1923.1	1920.6	1924.2	1920.9	1941.8	1925.6
Image 6	22788	18163.48	18151	18138.9	18122.8	18162	18124.3	18148.1	18149.5	18126.5	18126.5	18149.2	18128.7	18147.3	18149.2	18139.3	18147.3	18148.4	18151.7	18138.5	18156.2
Image 7	869	825.84	839.8	841.32	786.9	925.5	891.3	846.72	829.4	896.4	885.96	836.6	896.4	853.2	862.9	878.4	939.6	875.8	855	950.1	859.6
Image 8	23822	23435.64	23423	23465.8	23533.2	23552.6	23565.6	23422.6	23422.6	23574.2	23576.7	23426.2	23574.2	23457.6	23567.7	23492.5	23568.8	23576.1	23568.8	23633.6	23582.1
Image 9	3366	2582.64	2588	2592	2654.6	2571.1	2590.5	2559.6	2583.3	2592	2590.5	2647.8	2592	2589.8	2591.2	2566.4	2572.5	2640.6	2592.3	2617.5	2636.2
Image 10	3938	3910.56	3916.8	3909.6	3915.8	3925.4	3942.7	3917.2	3921.6	3940.8	3941.2	3918.7	3942.2	3941.7	3953.7	3956.1	3958.1	3956.1	3953.7	3973.4	3957.1
Image 11	4112	4867.4	4631.4	4897.2	4654.8	4732.2	4639.8	4723.2	4662	4799.2	4792.2	4755	4818.8	4758	4960	4879.8	4833	4717.2	4705.6	4502.4	4721.5
Image 12	695	822.24	822.24	824.4	829.1	828.7	827.64	824.1	822.2	828.7	827.28	822.2	827.6	826.5	826.2	825.1	826.2	827.2	826.2	824.4	826.9
Image 13	3595	3745.44	3746.1	3753.7	3760.9	3781.8	3744.7	3745.4	3673.4	3755.1	3744	3747.6	3759.1	3754.4	3758.76	3754.8	3767.4	3777.1	3760.5	3794.1	3776.4
Image 14	6543	7718.2	7717.1	7725.2	7716.1	7730.6	7717.1	7719.3	7717.6	7719.3	7717.6	7719.3	7719.3	7726.8	7766.2	7770.1	7761.9	7767.3	7764.1	7766.2	7765.7
Image 15	5055	5723.8	5726.0	5906.4	5801.9	5763.4	5773.3	5726.6	5726.1	5781.6	5772.2	5726.6	5776.6	5729.9	5782.1	5756.3	5756.3	5836.6	5778.3	5763.4	5833.8
Image 16	4024	4656.3	4657.2	4661.1	4678.5	4676.4	4670.7	4659.9	4658.7	4676.4	4670.1	4659.9	4675.2	4665.6	4689	4666.5	4680	4690.5	4689.9	4680.6	4691.7

Table 5.19: Time Taken by Different Combinations of Texture Methods (in seconds) while executing the Developed Method based on Threshold, Texture and Shadow

Image No.	LAWS	LAWS, WAVELET	LAWS, GABOR	LAWS, GLCM	LAWS, TAMURA	LAWS, WAVELET, GLCM	LAWS, WAVELET, GABOR	LAWS, WAVELET, TAMURA	LAWS, WAVELET, GLCM, GABOR	LAWS, WAVELET, GLCM, TAMURA	LAWS, WAVELET, GABOR, TAMURA	LAWS, WAVELET, GLCM, GABOR, TAMURA	WAVELET	WAVELET, GLCM	WAVELET, GABOR	WAVELET, TAMURA	WAVELET, GLCM, GABOR	WAVELET, GLCM, TAMURA	WAVELET, GABOR, TAMURA	WAVELET, GABOR, GLCM TAMURA
Image 1	15.731	29.521	18.934	378.03	556.47	491.94	31.838	682.97	488.93	1144.2	660.4	1212.6	12.095	498.98	16.504	687.37	510.59	1134.3	546.95	1016.5
Image 2	13.48	14.887	16.296	183.463	115.54	87.311	21.995	118.96	90.965	254.32	254.68	420.86	25.376	80.423	17.195	122.83	147.04	186.18	110	173.75
Image 3	13.34	16.297	17.512	109.4	138.09	126.4	18.516	124.18	95.25	230.06	199.99	264.75	16.252	115.09	19.586	124.52	105.07	229.84	165.73	207.54
Image 4	10.76	20.937	14.731	158.84	248.68	143.15	16.603	363.84	126.8	298.43	216.41	556.33	12.008	120.33	12.331	323.58	272.22	607.27	330.6	539.19
Image 5	15.154	14.522	12.56	202.33	264.28	191.48	15.805	277.11	208.36	452.25	266.66	450.91	10.573	195.58	16.965	261.08	206.94	441.45	397.47	606.06
Image 6	14.233	13.93	32.868	146.71	169.85	127.7	41.689	180.48	139.08	293.19	195.11	273.57	25.272	119.98	30.505	155.17	143.55	244.19	179.96	255.92
Image 7	9.9316	12.999	10.925	169.13	246.25	144.8	14.892	225.84	139.37	324.83	214.25	368.43	10.583	192.89	11.445	257.12	175.43	426.34	327.2	374.12
Image 8	22.627	24.174	63.143	127.08	158.23	137.32	57.163	166.73	143.97	268.1	219.37	149.48	39.065	120.85	86.87	214.93	159.82	270.89	197.39	323.46
Image 9	20.57	36.239	15.875	263.33	414.73	302.78	20.005	440.41	279.67	606.87	387.2	276.14	33.415	266.83	18.07	402.39	307.63	676.23	407.57	741.34
Image 10	9.4123	28.321	12.997	376.29	506.61	339.77	27.12	608.69	343.07	647.12	456.33	883.31	14.046	252.34	14.138	335.93	306.3	665.47	455.56	774.92
Image 11	15.537	23.554	22.276	82.745	115.98	124.15	23.382	119.17	101.22	201.36	120.72	198.64	19.439	73.361	24.078	153.61	110.24	235.96	172.7	239.88
Image 12	14.013	16.758	10.628	99.874	104.62	61.851	14.419	79.348	93.28	204.2	117.82	198.94	9.3184	100.89	10.193	121.56	130.39	182.3	116.07	186.89
Image 13	17.418	43.31	21.865	331.15	564.48	389.57	127.31	620.48	642.76	1028.9	552.88	847.01	11.991	625.82	17.168	532.9	409.24	924.81	525.03	880.7
Image 14	10.049	13.354	11.892	191.53	248.62	164.11	12.839	216.24	247.02	390.53	273.94	324.06	42.054	198.32	14.922	229.57	159.18	341.77	195.77	327.4
Image 15	15.495	17.61	17.182	40.857	52.22	40.681	18.22	54.639	41.129	76.779	52.218	78.097	12.981	39.926	13.654	44.232	44.162	74.079	47.75	83.834
Image 16	14.233	17.715	13.478	213.19	273.98	212.64	16.038	308.65	219.04	468.85	285.52	224.87	11.218	195.85	29.461	307.85	254.9	562.49	328.82	554.85

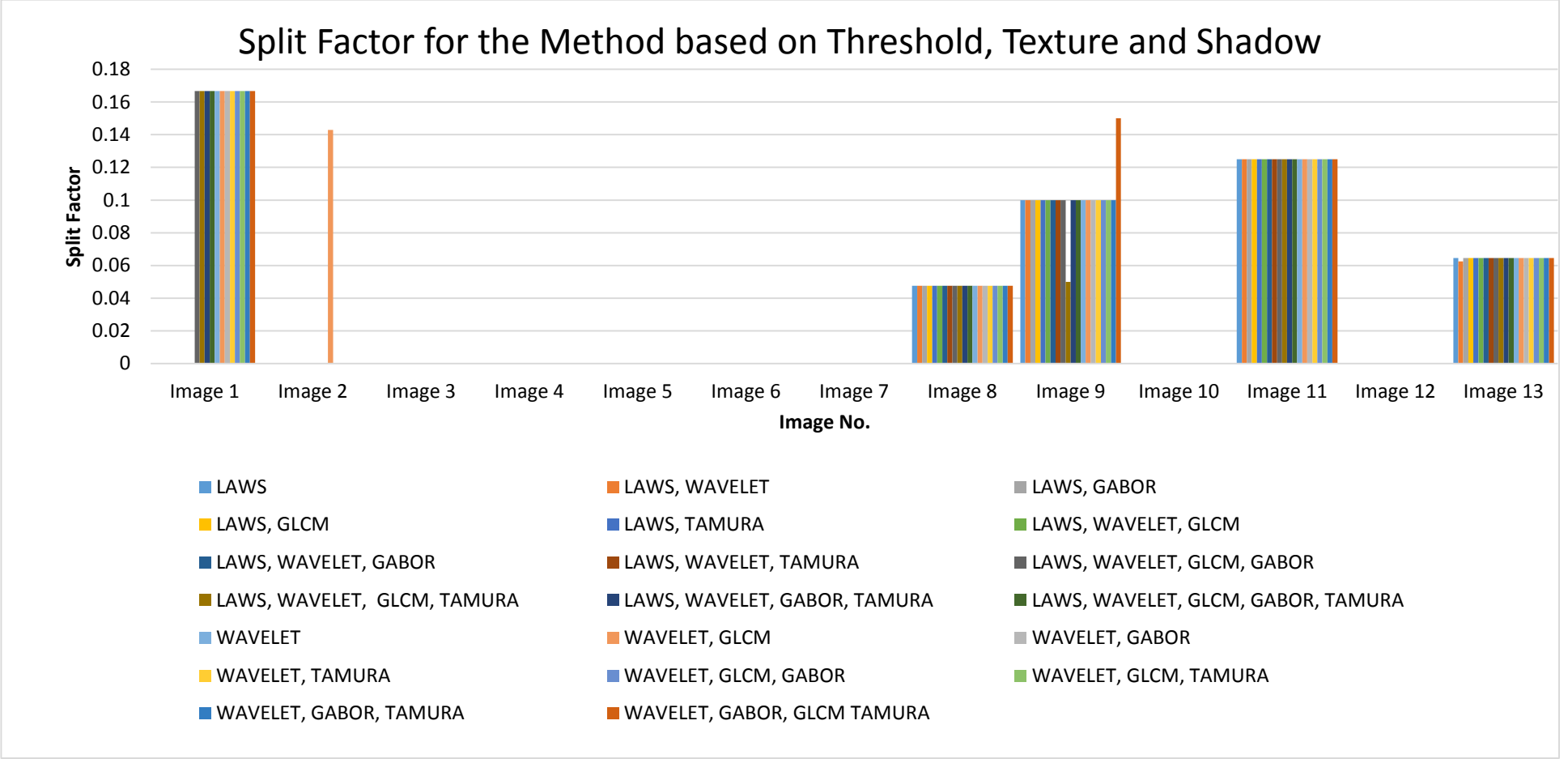

Figure 5.13: Graph between SF and the texture combination used while executing the Developed Method based on Threshold, Texture and Shadow

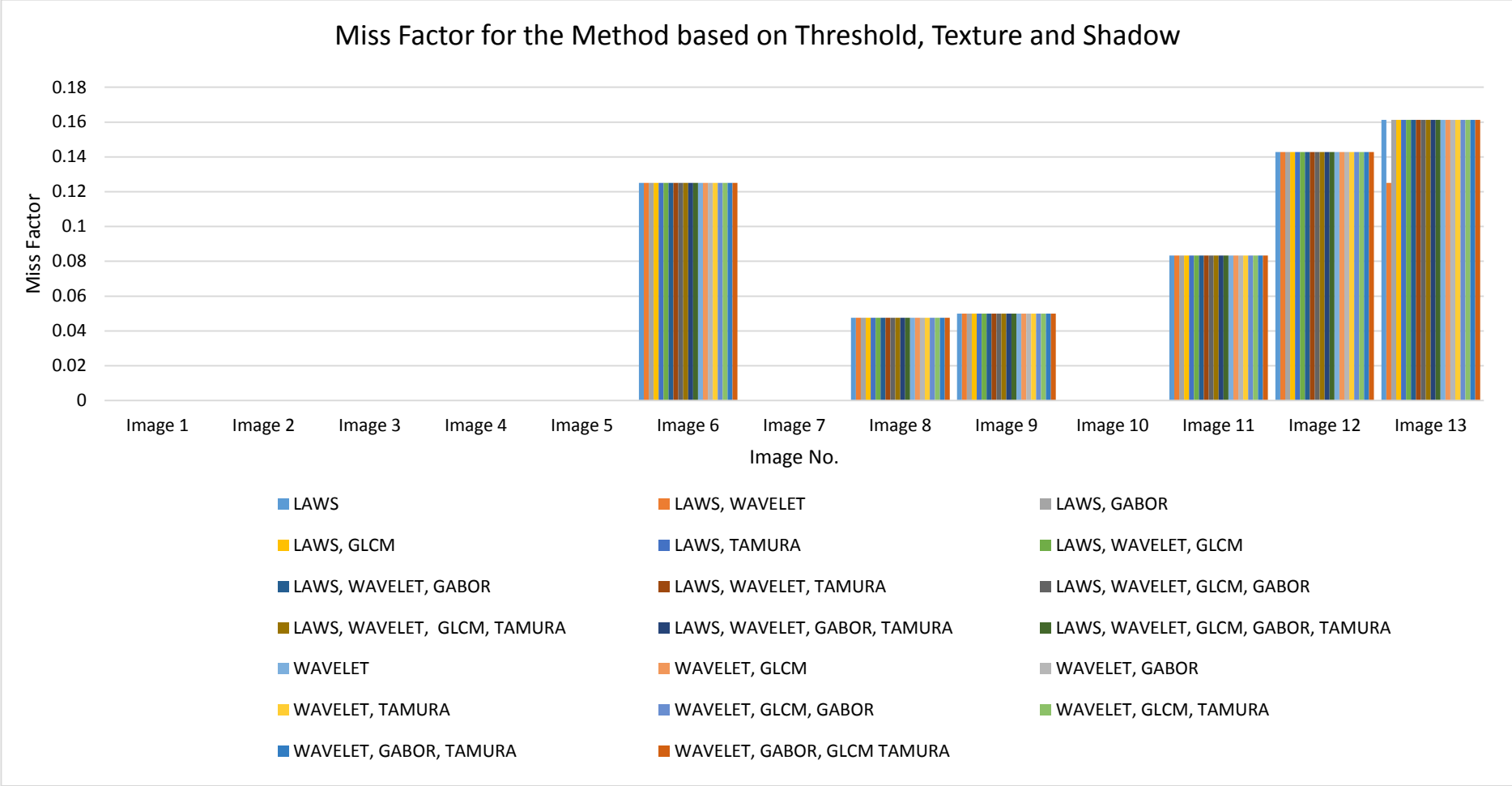

Figure 5.14: Graph between MF and the texture combination used while executing the Developed Method based on Threshold, Texture and Shadow

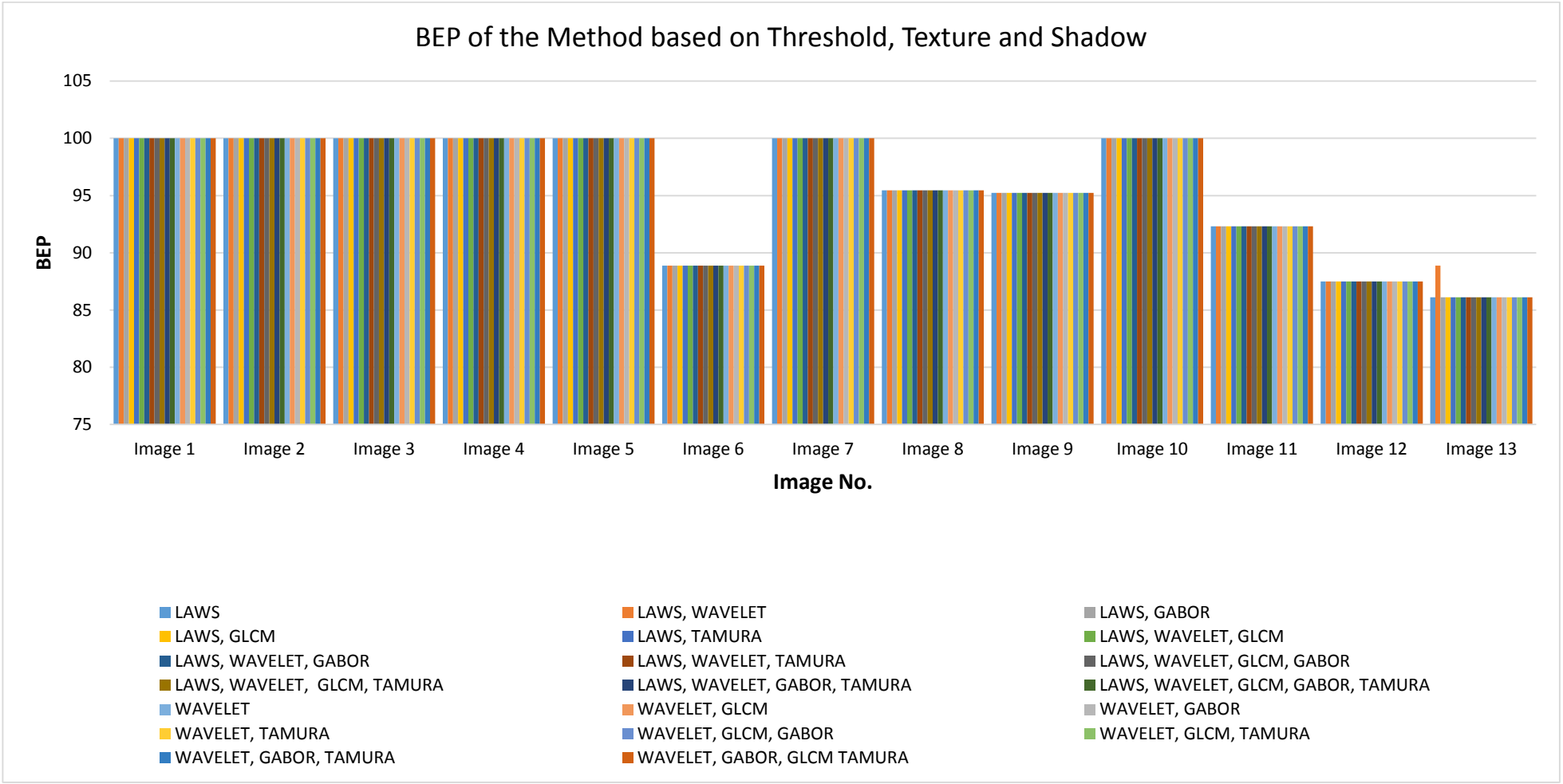

Figure 5.15: Graph between BEP and the texture combination used while executing the Developed Method based on Threshold, Texture and Shadow

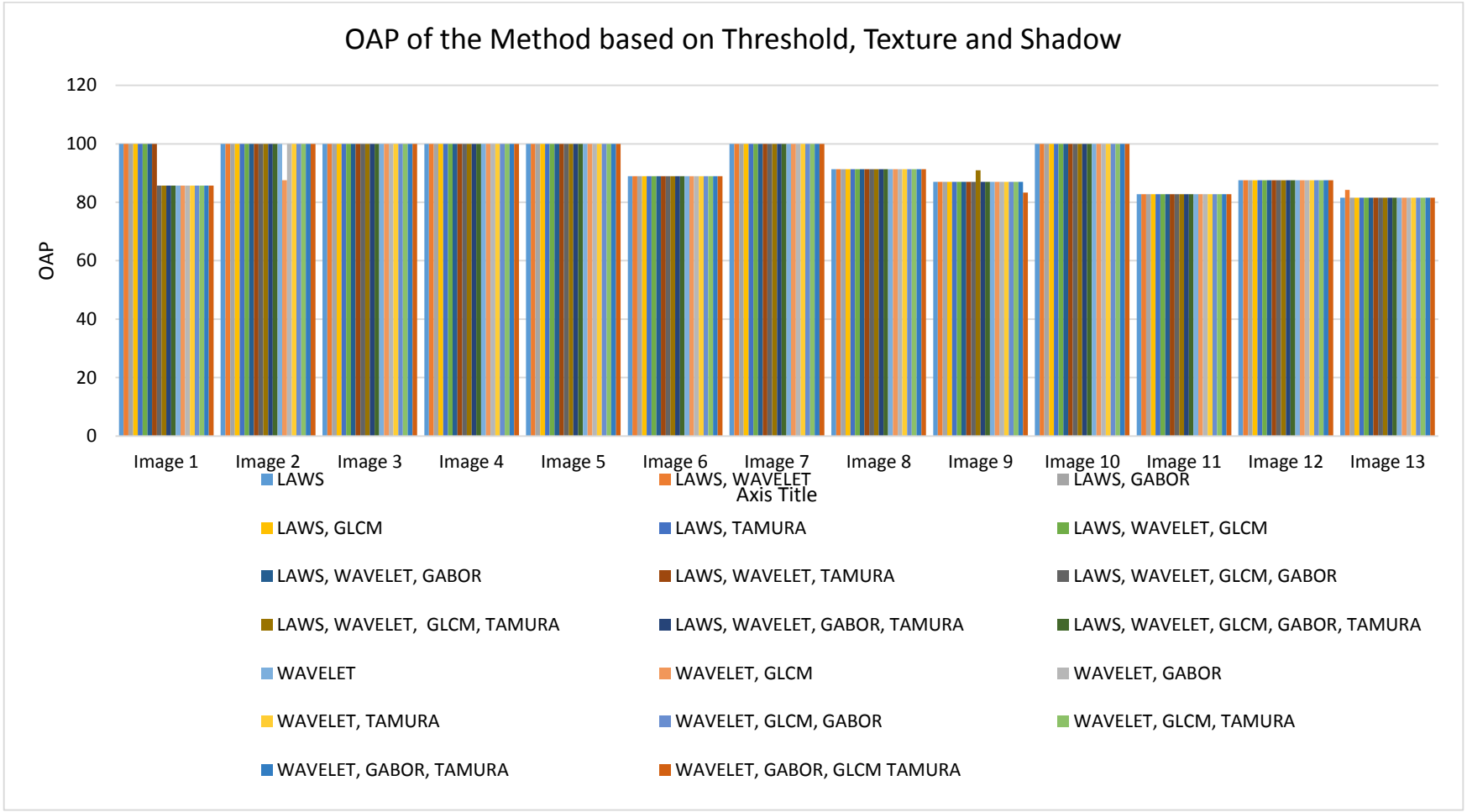

Figure 5.16: Graph between OAP and the texture combination used while executing the Developed Method based on Threshold, Texture and Shadow

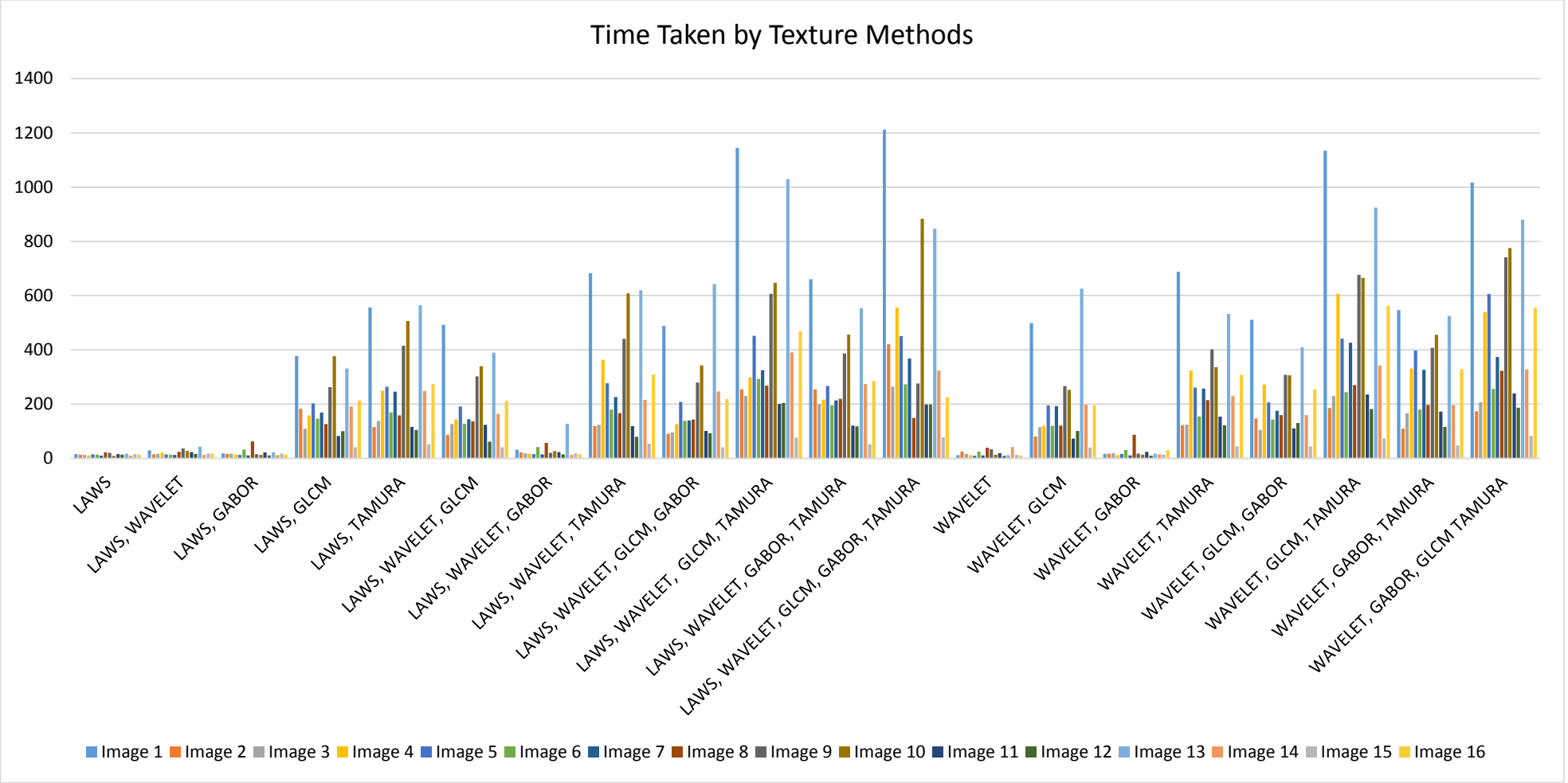

Figure 5.17: Graph between the Execution Time and the Texture Combination used while executing the Developed Method based on Threshold, Texture and Shadow

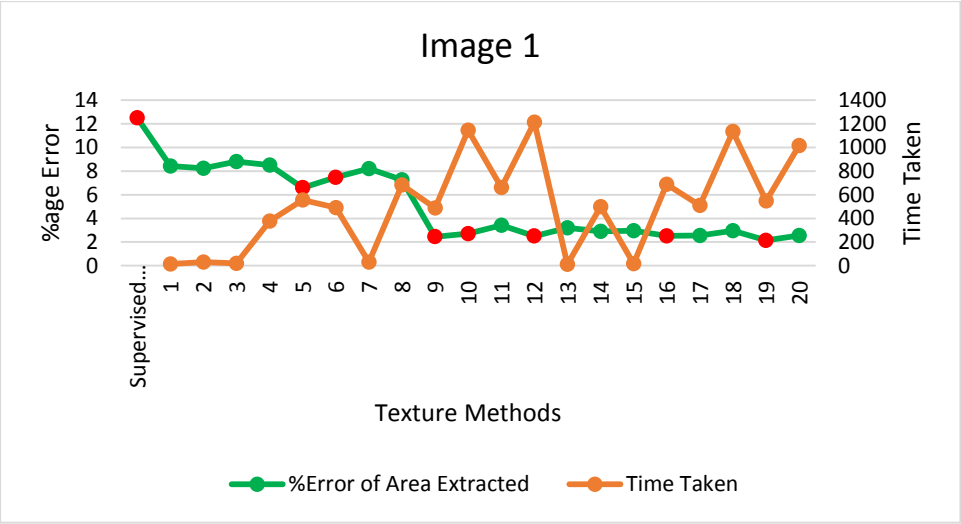

Figure 5.18 (a)

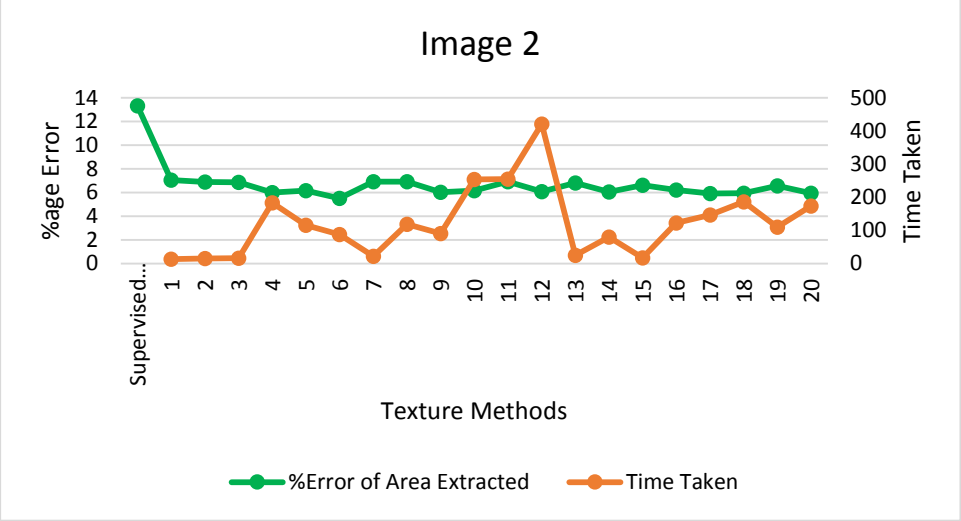

Figure 5.18 (b)

Figure 5.18 (c)

Figure 5.18 (d)

Figure 5.18 (e)

Figure 5.18 (f)

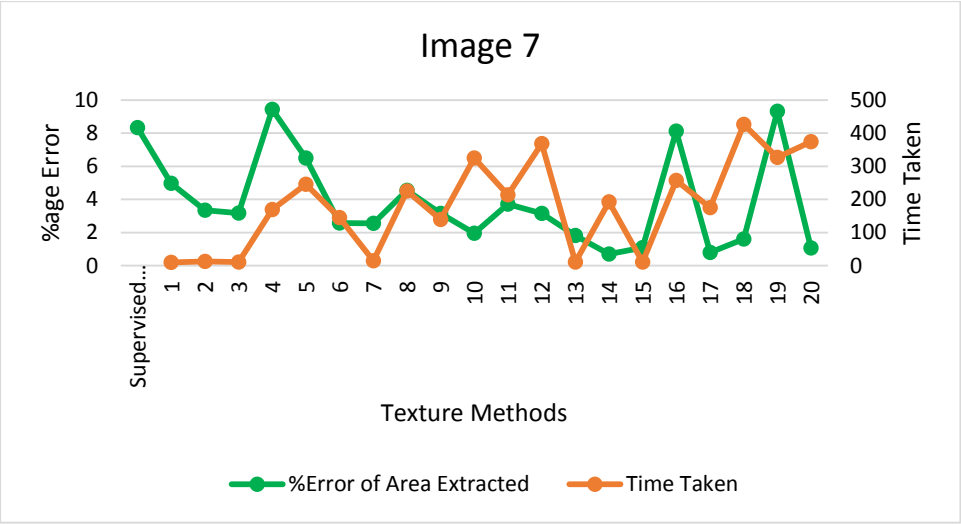

Figure 5.18 (g)

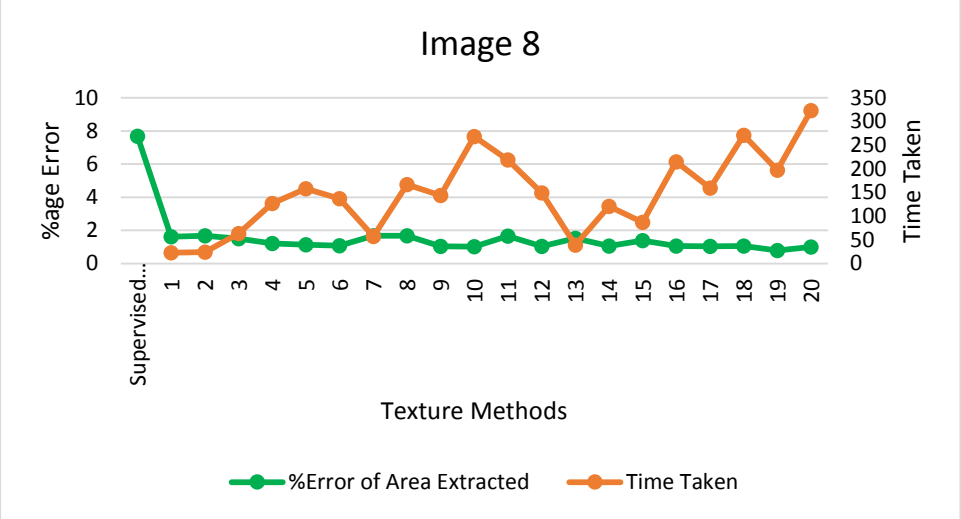

Figure 5.18 (h)

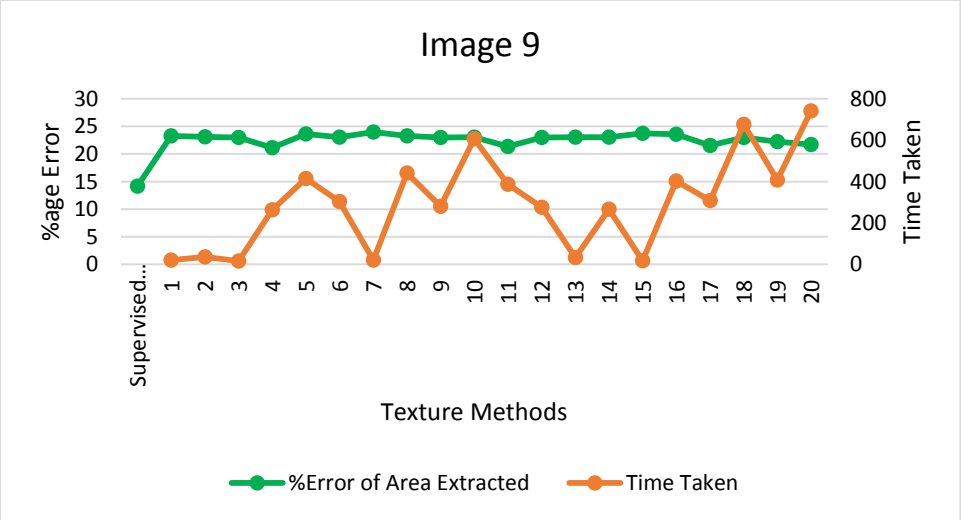

Figure 5.18 (i)

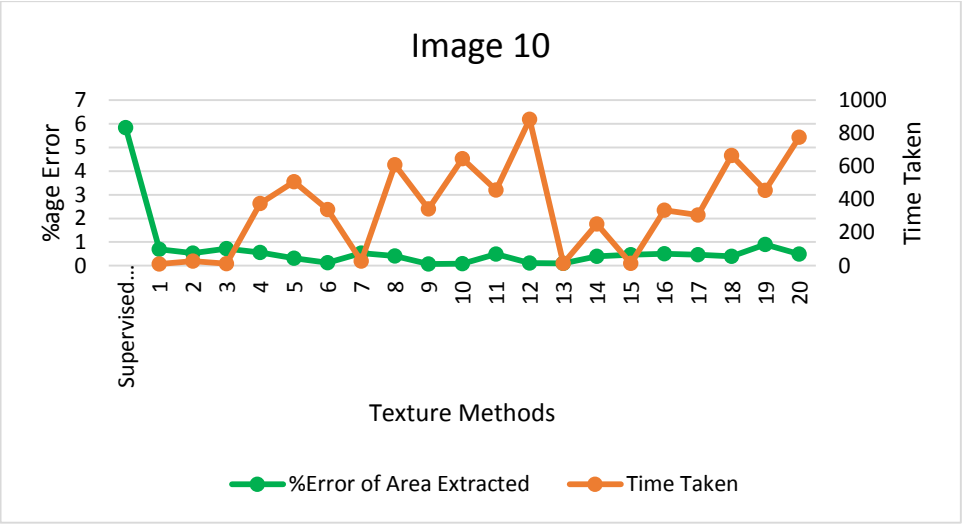

Figure 5.18 (j)

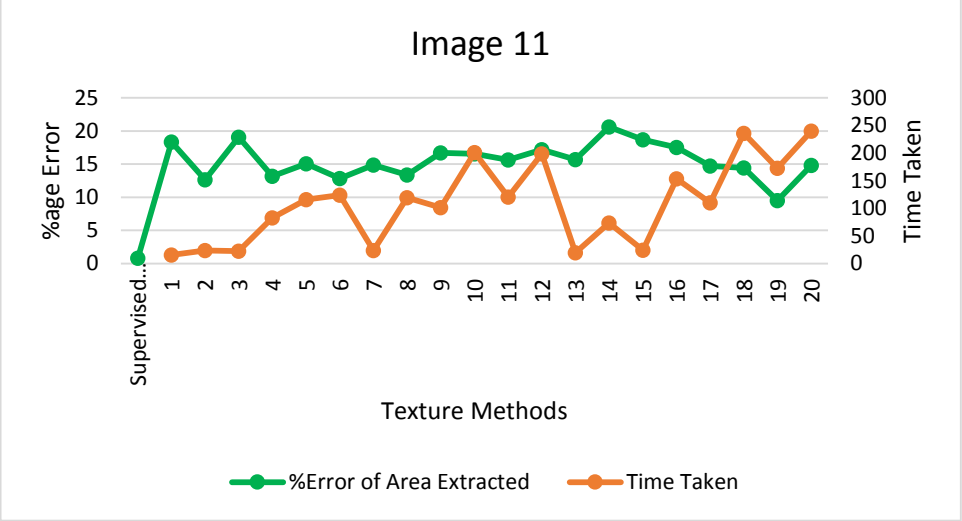

Figure 5.18 (k)

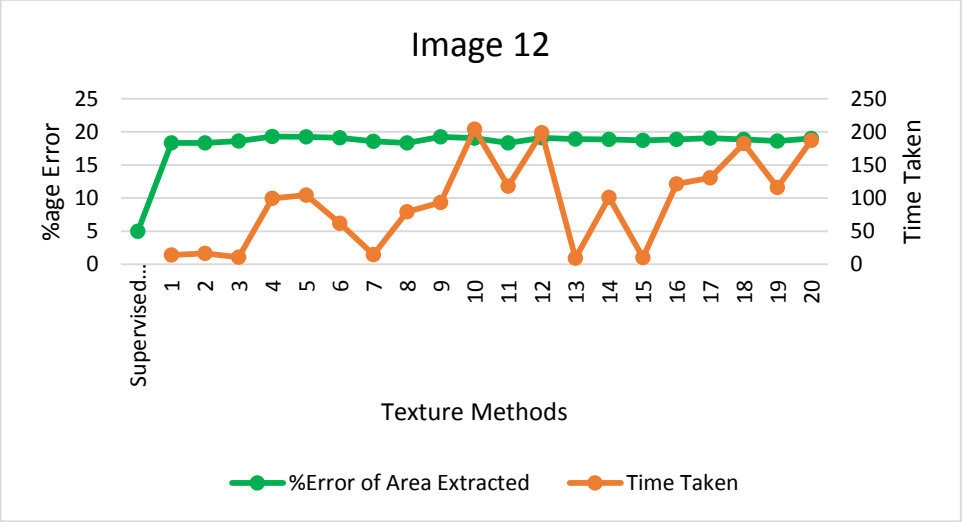

Figure 5.18 (l)

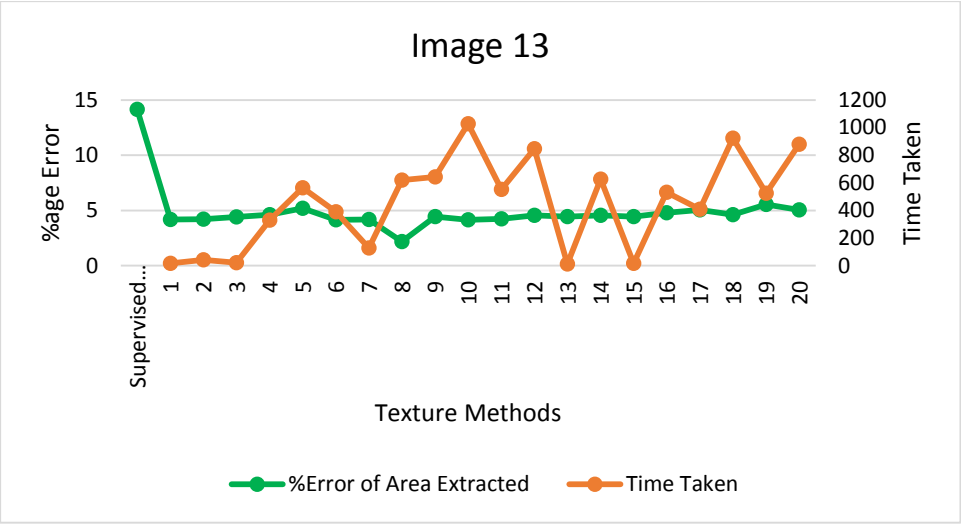

Figure 5.18 (m)

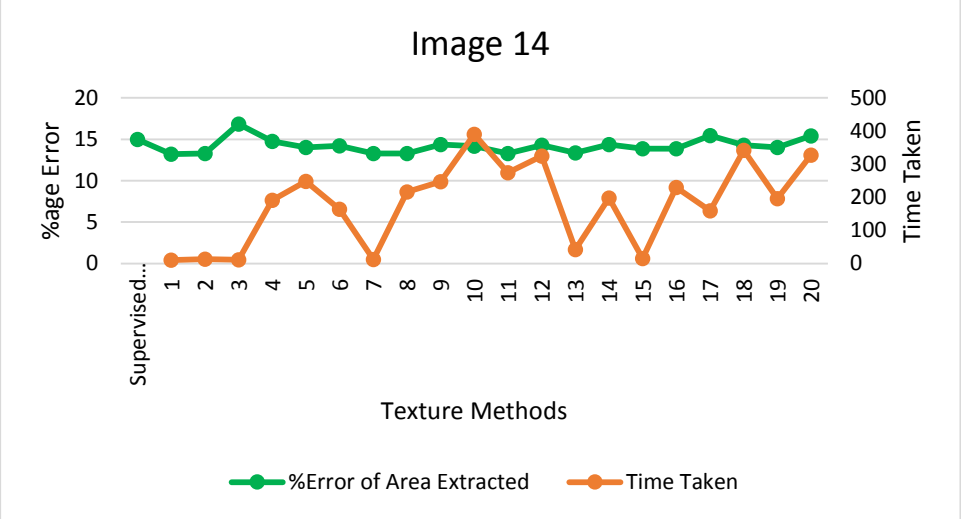

Figure 5.18 (n)

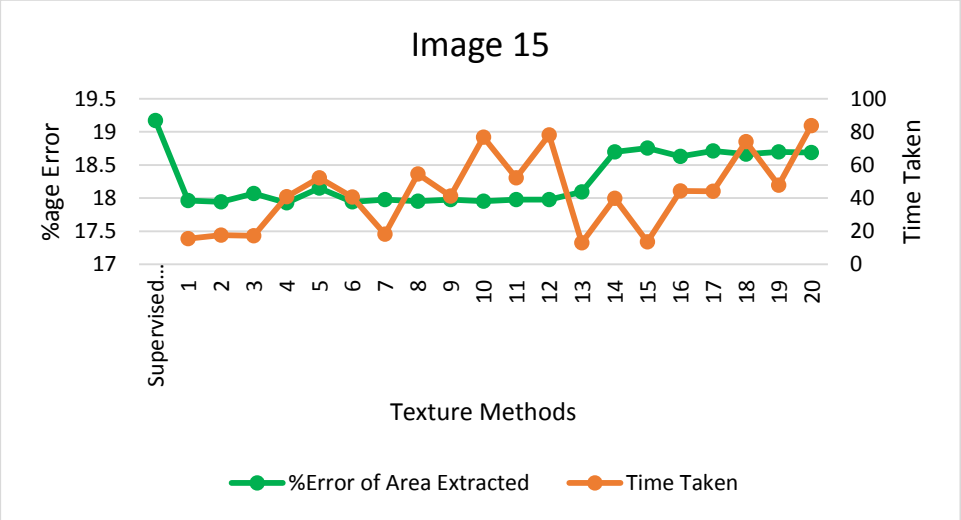

Figure 5.18 (o)

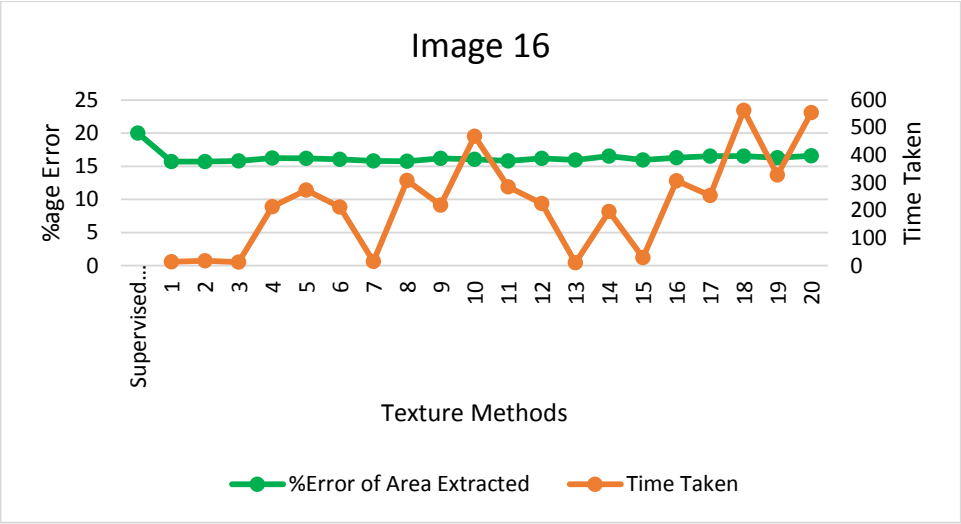

Figure 5.18 (p)

Figure 5.18: Graph between the texture methods used while executing the developed method based on Threshold, Texture and Shadow and the percentage error calculated for the extracted area.

The % error of area extracted by the texture methods has been compared with the % error calculated for supervised classified images, and it was found that for most of the images, % error is less than the % error obtained from the supervised classification method.

On the basis of % error and the time taken, from the twenty combinations, it was found that LAWS texture method gave less % error for extracted area and at the same time it takes relatively less time to complete the extraction process.

5.6 OVERALL ACCURACY ASSESSMENT OF THE DEVELOPED METHODS

The overall accuracy assessment of the four developed methods has been done by comparing the percentage error of area obtained from the developed methods and for supervised classification method. For developed methods, percentage error of the area has been calculated from the area extracted by the developed methods and the area extracted by manual digitization. The calculated percentage error has been given in Table 5.20 and the graph plotted between the percentage error and developed methods has been given in Figure 5.19.

Table 5.20: Percentage Error on the basis of Area

Image	%age Error By Threshold	%age Error By Shadow and Corner Information	%age Error By Texture	%age Error By Threshold, Texture and Shadow	%age Error By Supervised Classification
Image 1	5.37	34.09	11.01	8.41	12.5
Image 2	13.42	3.08	14.85	7.05	13.33
Image 3	4.05	14.50	10.17	3.42	6.67
Image 4	6.37	14.11	12.05	3.23	13
Image 5	12.23	62.19	31.19	6.70	17.5
Image 6	25.66	28.69	38.51	20.29	11.67
Image 7	68.99	68.99	2.57	4.96	8.33
Image 8	7.805	13.74	2.66	1.62	7.69
Image 9	21.90	83.20	18.65	23.27	14.17
Image 10	5.76	25.98	19.22	0.69	5.83
Image 11	20.69	43.03	55.51	18.37	0.83
Image 12	2.50	26.21	2.30	18.30	5
Image 13	9.60	18.16	38.61	4.18	14.17
Image 14	51.98	84.16	53.41	13.23	15
Image 15	15.75	75.44	45.15	17.96	19.17
Image 16	3.46	69.79	57.08	15.71	20

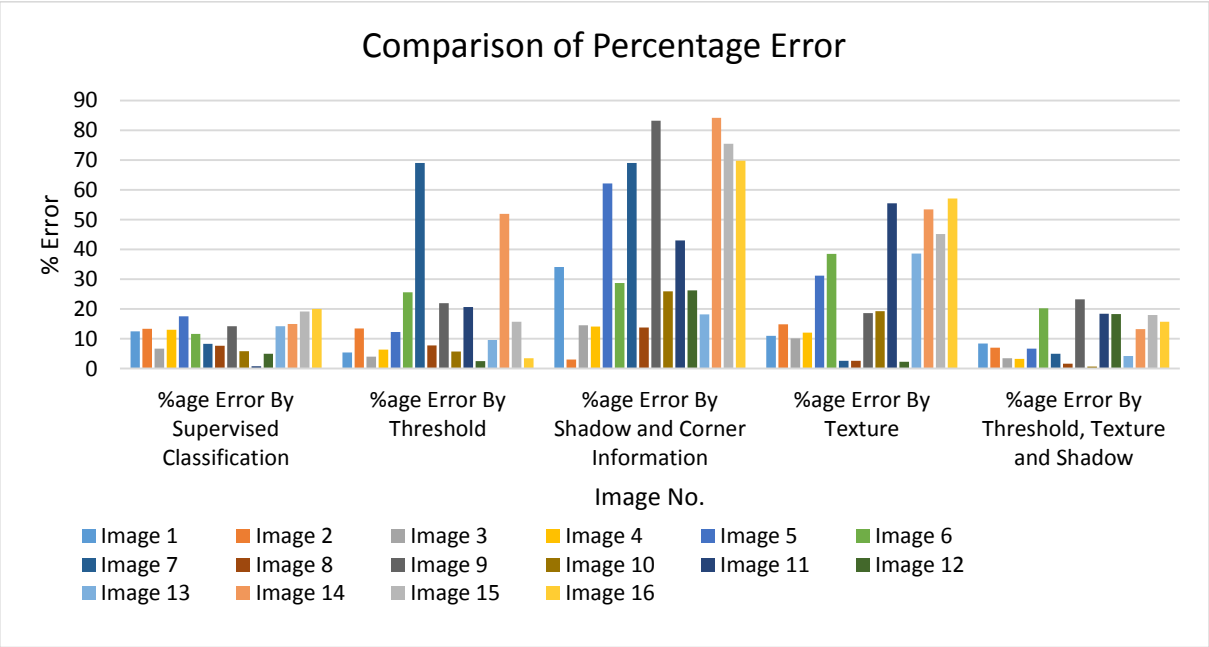

Figure 5.19: Graph between Percentage Error and Developed Methods

5.7 SUMMARY

In this chapter, the results obtained after executing the developed methods have been provided, analyzed and discussed. These results shows that BEP and OAP depend on the complexity and texture of the region. Also, the performance of the developed methods changes w.r.t. surface materials and spectral reflectance similarity of the test regions. Although, all four methods are able to extract the building successfully, but the method based on threshold, texture and shadow successfully gives best results for all types of buildings irrespective of their shape, size, orientation and density.

CHAPTER 6 CONCLUSIONS

6.1. INTRODUCTION

Extraction of buildings from high resolution remote sensing images is an important GIS application. The precise knowledge of buildings not only serves as a reference for physical planning and development, but also provides a more realistic scenario of complexities associated with any settlement. Extracting information about individual buildings from high resolution remote sensing images had always been a challenging task for research community. The reasons attribute to the high spectral variation within the building boundaries, and similarity in spectral characteristics among different land cover types, such as buildings, roads, parking lots etc. The spectral variation is due to the diversity in the materials and construction technology applied in buildings, while spectral similarity is due to the use of similar materials used in buildings, and several objects on land identified other than buildings.

India being a vast country with a large population residing in various climatic zones and topography has a complex and diversified built environment. The diversity in quality, combination, application of the combination of materials in the range of buildings makes it difficult to come up with a standard data of the typology of buildings. In absence of the standard typology of buildings with reference to applied materials, there is an enormous scope of research in the field of remote sensing and GIS applications for Indian context. The recent and only (2013) categorisation of visible building typologies provided by the NDMA, India for seismic assessment has been analysed. The analysis of the same has been discussed in chapter 1 to arrive at the conclusion that India has a huge range of building typologies contributing to its diversified built environment. This formed the rationale to take up this research for Indian context, where the researcher couldn't find any fully automatic building extraction method developed for an Indian case.

The present research was undertaken with an intension to contribute to the efficiency of different applications used in urban planning, management and development. The present research incorporates the development of four methods for building extraction using high resolution satellite images. Keeping in view, the rationale for an Indian case, QuickBird satellite images of the Jaipur city, India were chosen to test and analyse the workability and the suitability of the developed methods.

6.2. CONCLUSIONS

From the results of this research, it has been found that out of the four developed methods, method developed by using threshold value, texture and shadow was able to extract all types of buildings. The major conclusions drawn from the research can be summarized as follows:

i. In this research, review of literature in chapter 2 formed the basis to understand the process of identification and usage of various parameters in established researches. After analysing the strength and weaknesses of each parameter for different cases, the parameters selected for the present research to extract buildings from high resolution satellite images were threshold value (pixel value), colour, texture, shadow, corner information and size. Concluding the major strengths of the parameters, which became the basis for their uses in present research, were that they can be calculated from the pixel values of the image itself. Other information, like date of image acquisition, time of image acquisition, and the sun angle at the time of acquiring the image etc., are not required to compute these parameters. The identification and analysis of parameters required for automatic extraction of buildings from high resolution satellite images meet the first objective of this research.

ii. By using the selected parameters, four fully automatic methods have been developed for extracting buildings from high resolution satellite images. The first building extraction method has been developed on the basis of threshold values (pixel values) of buildings areas. The second building extraction method has been developed on the basis of shadow and corner information. The third building extraction method has been developed on the basis of texture. The fourth building extraction method has been developed on the basis of threshold, texture and shadow. The strength of the developed methods is that these do not require any significant human intervention. The user has to just select the satellite images from which buildings have been extracted, and feed the threshold value for area to eliminate the small artifacts extracted as buildings. Thus, second objective of the study has been achieved.

iii. The developed building extraction methods have been tested on 16 test images of different places of Jaipur city, India. All test images contained buildings belonging to any one of urban infrastructure/buildings/built structures i.e., planned, unplanned, slum, industrial, business and educational buildings having different shapes, sizes and orientations. On the basis of the analysis of the obtained results, it has been concluded that

a. The building extraction method based on threshold value successfully extracts all types of buildings, irrespective of their shapes, sizes and orientation. The shapes of the buildings have not been retained by this method. This method has not been able to extract individual slum buildings successfully, as such buildings exist close to each other with a wide range of spectral reflectance values. This method results in high FP and FN for those areas, where there is a difference between the spectral reflectance values of the buildings and objects other than building having same reflectance values as that of buildings. The high values of FP and FN results in low values for BEP and OAP. As compared to the area extracted by the digitization, the area extracted by this method has been found more for those buildings which are merged by the program and extracted as one single building (Image 6) or the buildings belonging to unplanned areas (Images 11 and 12). The area extracted by this method has been found less for those buildings having a difference between the spectral reflectance values within the boundary of the buildings (Image 16).

b. The building extraction method based on shadow and corner information successfully extracts the buildings having regular shapes. This method was not able to extract the buildings having complex shapes, and also the buildings not having the shadow associated with them. Because of this limitation, this method resulted in high FN for those areas either having complex shaped buildings or buildings without shadow information or both. The high values of FN resulted in low values for BEP and OAP. Also, for slum buildings (Images 14, 15 and 16), this method extracted only few buildings resulting in a huge difference between the area extracted and the area calculated by digitization (84%, 75%, 69% respectively).

c. The building extraction method based on texture successfully extracted all types of buildings but resulted in the high % error rate of area especially in case of slum buildings (within a range of 40-50% as compared to area extracted from digitization). Also, as the number of texture methods increased in the combination, the % error rate of area decreased but the time taken for completing the extraction process increased (around 5-15 times more depending on the texture methods used in the combination). However, using the combination of Laws, Wavelet and GLCM texture methods gave comparatively less % error rate of area and took less time to complete the extraction process.

d. The method based on threshold, texture and shadow successfully extracted all types of buildings present in the images, including slum buildings. All texture combinations used in this method gave very low value for SF (0–0.12) and MF (0–0.16) and high values for BEP (86.11–100%) and OAP (81.57–100%). Except image 6 and 9, the OAP obtained by this method is less than overall accuracy obtained from supervised classification. Also, the % error rate of area extracted was very less for all texture combinations (0.69-23.27%), but the time taken for completing the extraction process increased, as the number of texture methods increased in combination. After comparing the time taken by the extraction method and the % error obtained, it may be concluded that the laws texture method is best for extracting buildings using this method.

For the comparative accuracy assessment of the developed methods, % error of the total area extracted has been calculated and compared with the % error obtained for the supervised classification method. The % error obtained for the supervised classification method is 0.83-17.5, for the first developed method is 2.50-68.99, for the second developed method is 3.08-84.16, for the third developed method is 2.57-55.51, and for the fourth developed method is 0.69-23.27%. On comparison of four developed methods, it has been found that the fourth method based on threshold, texture and shadow gave the best results for extraction of all types of buildings, irrespective of their shape, size, orientation and typology. This method also gave the best result for slum buildings over other methods, and extracted most of the slum buildings. Thus, by developing the fourth method for automatic building extraction, the third objective has been achieved.

Other key points of the developed methods are:

1. The proposed methodology gave better results than the buildings classified by supervised classification approach, except for buildings having a slanting roof.
2. The proposed methodology is faster to extract the buildings.
3. No earlier knowledge is required for running the program for extracting buildings which otherwise is required in supervised classification method.
4. The proposed methodology accepts raw image and no pre-processing is required to be done before using an image in the developed program.
5. The proposed methodology is cost effective as only three bands of multispectral images (NIR, Red, and Green) are required for the extraction of buildings.

6.3. LIMITATIONS

The limitations of developed methods are as follows:

(i) The developed method has not been able to extract buildings having either very bright or very dark appearances.

(ii) The developed method also extracts some non-building objects, barren or open land as building, as their spectral reflectance values are same as that of buildings.

(iii) The exact shape of the buildings, especially in case of unplanned and slum buildings, has not been retained.

(iv) The developed method can work only for a limited size of image as the Matlab programming environment provides limited space for storing the values of variables while executing the program.

6.4. SCOPE FOR FUTURE WORK

Since it is an initial attempt to develop a fully automatic building extraction method in Indian context, future researches are suggested:

1. To test its application of this program in various geographical locations, with various shapes and types of buildings. Developed methods can also be tested for other high resolution satellite images. For increasing the accuracy of the buildings extracted, the height of the buildings can be considered as a factor for the multi-storey buildings in which shadow of the upper storey falls on the rooftop of the lower one.
2. In India where population growth rate and rapid urbanisation is phenomenal, urban sprawls/slums pose major challenge to the existing urban infrastructure, since these are unplanned developments non concurrent with planning process of the country. In absence of reliable data for such development, building extraction process needs extensive improvement. The database preparation of roof construction materials verified through field surveys of slum areas and identification of more parameters to decrease the % error rate of area leaves a further scope of research.

REFERENCES

1. Aboulmagd H., El-Gayar N., and Onsi H., 2009. A new approach in content-based image retrieval using fuzzy. Telecommunication System, Springer, 55-66.
2. Aigrain P., Zhang H., and Petkovic D., 1996. Content-based representation and retrieval of visual media: A review of the state-of-the-art. Multimedia Tools and Applications, 3, 179-202.
3. Ahmadi, S., Zoej, M. J. V., Ebadi, H., Moghaddam, H. A., and Mohammadzadeh, A., 2010. Automatic urban building boundary extraction from high resolution aerial images using an innovative model of active contours. International Journal of Applied Earth Observation and Geoinformation, 12(3), 150-157.
4. Amini, J., Lucas, C., Saradjian, M., Azizi, A. and Sadeghian, S., 2002. Fuzzy logic system for road identification using IKONOS images. Photogrammetric Record, 17, 493–503.
5. Aminipouri, M. et al., 2009. Object-oriented analysis of very high resolution orthophotos for estimating the population of slum areas, case of Dar-Es-Salaam, Tanzania. In Proceedings of ISPRS XXXVIII Conference, 1-51.
6. Katartzis A. and Sahli H., 2008. A Stochastic Framework for the Identification of Building Rooftops Using a Single Remote Sensing Image. Transactions on Geoscience and Remote Sensing, IEEE, 46 (1), 259-271.
7. Aytekin, O. and Erener, A., 2009. Automatic and Unsupervised Building Extraction in Complex Urban Environments from Multi Spectral Satellite Imagery. IEEE, 287-291.
8. Baillard, C. and Maitre, H., 1999. 3-D reconstruction of urban scenes from aerial stereo imagery: a focusing strategy. Computer Vision and Image Understanding. 76 (3), 244-258.
9. Baillard, C., Dissard, O., Jamet, O., and Maître, H., 1998. Extraction and textural characterization of above-ground areas from aerial stereo pairs: a quality assessment. ISPRS Journal of Photogrammetry and Remote Sensing, 53 (2), 130-141.
10. Baltsavias, E., Pateraki, M. and Zhang, L., 2001, Radiometric and geometric evaluation of IKONOS geo images and their use for 3D building modelling. Proceeding of Joint ISPRS Workshop on High Resolution Mapping from Space, 19–21 September 2001, Hannover, Germany.
11. Bariar A., Gupta R. D., and Prasad S. C., 2006. Geospatial Database Development for Urban Planning using Satellite Data under GIS Environment, The International Archives

of the Photogrammetry, Remote Sensing & Spatial Information Science, ISPRS, 36(4), 455-459.

12. Barzohar, M. and Cooper, D.B., 1996. Automatic finding of main roads in aerial images by using geometric-stochastic models and estimation. IEEE Transactions on Pattern Analysis and Machine Intelligence, 18, 707–721.
13. Beauchemin, M. and Thomson, K. P. B., 1997. The evaluation of segmentation results and the overlapping area matrix. International Journal of Remote Sensing, 18, 3895–3899.
14. Benedek C., Descombes X. and Zerubia J., 2010. Building Detection in a Single Remotely Sensed Image with a Point Process of Rectangles. International conference on Pattern Recognition, IEEE, 1417-1420.
15. Benediktsson, A., Arnason, K., and Pesaresi, M., 2001. The use of morphological profiles in classification of data from urban areas. In IEEE/ISPRS Joint Workshop on Remote Sensing and Data Fusion over Urban Areas 8–9 November 2001, Rome, Italy (Piscataway: IEEE), 30–34.
16. Benediktsson, J. A., Pesaresi, M., and Amason, K., 2003. Classification and feature extraction for remote sensing images from urban areas based on morphological transformations. IEEE Transactions on Geoscience and Remote Sensing, 41(9), 1940-1949.
17. Bhatti, S. S. and Tripathi N. K., 2014. Built-up area extraction using Landsat 8 OLI imagery. GIScience & Remote Sensing, 51(4), 445-467.
18. Bicego, M., Dalfini, S., Vernazza, G. and Murino, V., 2003. Automatic road extraction from aerial images by probabilistic contour tracking. In IEEE International Conference on Image Processing, ICIP'03, 14–17 September, 3, Barcelona, Spain, 585–588.
19. Bing X., Introduction to Remote Sensing and Applications, Department of Geography, The University of Utah.
20. Boloorani, A. D., Erasmi S., and Kappas, M., 2006. Urban land cover mapping using object/pixel-based data fusion and IKONOS images. Pan, 450, 900.
21. Census, 2011. District Census 2011: Office of the Registrar General & Census Commissioner, India.
22. Champion, N., Boldo, D., Pierrot-Deseilligny, M., and Stamon, G., 2010. 2D building change detection from high resolution satellite imagery: A two-step hierarchical method based on 3D invariant primitives. Pattern Recognition Letters, 31(10), 1138-1147.

23. Collins, R. T., Jaynes, C.O., Cheng, Y.-Q., Wang, X., Stolle, F., Riseman, E.M., and Hanson, A.R., 1998. The ascender system: automated site modeling from multiple aerial images. Computer Vision and Image Understanding, 72 (2), 143-162.
24. Cord, M. and Declercq, D., 2001. Three-dimensional building detection and modeling using a statistical approach. IEEE Transactions on Image Processing, 10 (5), 715-723.
25. Cord, M., Jordan, M. and Cocquerez, J.-P., 2001. Accurate building structure recovery from high resolution aerial imagery. Computer Vision and Image Understanding, 82 (2), 138-173.
26. Croitoru, A. and Doytsher, Y., 2003. Monocular right-angle building hypothesis generation in regularized urban areas by pose clustering. Photogrammetric Engineering and Remote Sensing, 69 (2), 151-169.
27. Cui, S. Y., Yam, Q., Liu, Z. J., and Li, M., 2008. Building detection and recognition from high resolution remotely sensed imagery. Paper presented at the Proceedings of the XXIst ISPRS Congress.
28. Cui, S., Yan, Q. and Reinartz, P., 2011. Graph search and its application in building extraction from high resolution remote sensing imagery, Search Algorithms and Applications. Nashat Mansour (Ed.), InTech.
29. Dadhwal V. K., 1999. Remote sensing applications for agriculture: retrospective and perspective. Proceedings of ISRS, 11-22.
30. Datcu M. et al., 2003. Information Mining in Remote Sensing Image Archives - Part A: System Concepts, IEEE Transactions on geosciences and Remote Sensing, 2923-2936.
31. Digital Globe Data Sheet: QuickBird. (12 Feb. 2014). www.digitalglobe.com.
32. Dikshit, O. and Behl V., 2009. Segmentation-assisted classification for IKONOS imagery. Journal of the Indian Society of Remote Sensing, 37(4), 551-564.
33. Erasmi S., Cyffka B. and Kappas M., 2005. Remote Sensing & GIS for Environmental Studies: Applications in Geography, Edition: Göttinger geographische Abhandlungen, 113, Publisher: Goltze.
34. Ferro, C. J. and Warner, T. A., 2002. Scale and texture in digital image classification. Photogrammetric Engineering and Remote Sensing, 68(1), 51-63.
35. Fischer, A., Kolbe, T. H., Lang, F., Cremers, A. B., Förstner, W., Plümer, L., and Steinhage, V., 1998. Extracting buildings from aerial images using hierarchical aggregation in 2D and 3D. Computer Vision and Image Understanding 72 (2), 185-203.

36. Forlani, G., Nardinocchi, C., Scaioni, M., and Zingaretti, P., 2006. Complete classification of raw LIDAR data and 3D reconstruction of buildings. Pattern Analysis and Applications, 8(4), 357-374.
37. Fradkin, M., Maitre, H., and Roux, M., 2001. Building detection from multiple aerial images in dense urban areas. Computer Vision and Image Understanding, 82 (3), 181–207.
38. Gamba, P., Houshmand, B., and Saccani, M., 2000. Detection and extraction of buildings from interferometric SAR data. IEEE Transactions on Geoscience and Remote Sensing, 38(1 II), 611- 618.
39. Gereke, M., Straub, B.-M., and Koch, A., 2001. Automatic detection of buildings and trees from aerial imagery, using different levels of abstraction. In Publications of the German Society for Photogrammetry and Remote Sensing, X. E. Seyfert (Ed.), 273-280.
40. Guo, X. et al., 2012. Effects of classification approaches on CRHM model performance. Remote Sensing Letters, 3(1), 39-47.
41. Gupta R. D., Srivastava R. K., Prakash D. V. S. S., 2002. Remote Sensing Based Resource Mapping using Digital Satellite Data, Indian Geotechnical Conference 2002 on Geotechnical Engineering: Environmental Challenges, 20-22 December, Allahabad, India.
42. Harris, C. and Stephens, M., 1988. A combined corner and edge detector. Paper presented at the Alvey vision conference.
43. Haralick, R. M., Shanmugam, K., and Dinstein. 1973. Texture features for image classification. IEEE Transactions on Systems, Man. and Cibernetics, SMC-3, 610-622.
44. Haverkamp, D., 2004. Automatic building extraction from IKONOS imagery. In Proceedings of ASPRS 2004 Conference, 23-28 May 2004, Denver, CO (Denver: ASPRS).
45. Herman, M. and Kanade, T., 1986, Incremental reconstruction of 3D scenes from multiple, complex images. Artificial Intelligence, 30, 289-341.
46. Hoover, A., et al., 1996. An experimental comparison of range image segmentation algorithms. IEEE Transactions on Pattern Analysis and Machine Intelligence, 18, 673-689.
47. Huang, X., Zhang, L., and Li, P., 2007. An adaptive multiscale information fusion approach for feature extraction and classification of IKONOS multispectral imagery over urban areas. IEEE Geoscience and Remote Sensing Letters, 4, 654–658.
48. http://jaipur.rajasthan.gov.in/content/raj/jaipur/en/about-jaipur/history.html.

49. http://www.ballaerospace.com/page.jsp?page=77, Retrieved 29 January, 2015
50. http://www.imd.gov.in/.
51. http://www.mapsofindia.com/maps/rajasthan/districts/jaipur.htm.
52. Huertas, A. and Nevatia, R., 1988. Detecting buildings in aerial images. Computing Vision, Graphics Image Processing, 41, 131–152.
53. Huy, M. Q. and Kappas, M., 2010, Developing Multi Objective Linear Programming (Molp) To Improve The Decision Making Of Land Use Planning." In Proceeding of ACRS 2010.
54. Inglada, J., 2007. Automatic recognition of man-made objects in high resolution optical remote sensing images by SVM classification of geometric image features. ISPRS Journal of Photogrammetry and Remote Sensing, 62(3), 236-248.
55. Irvin, R. B. and Mckeown, D. M., 1989, Method for exploiting the relationship between buildings and their shadows in aerial imagery. IEEE Transactions on Systems, Man and Cybernetics, 19, 1564-1575.
56. Izadi, M., Saeedi, P., 2012. Three-dimensional polygonal building model estimation from single satellite images. IEEE Transactions on Geoscience and Remote Sensing, 50(6), 2254-2272.
57. Jaynes, C., Riseman, E., Hanson, A., 2003. Recognition and reconstruction of buildings from multiple aerial images. Computer Vision and Image Understanding, 90(1), 68-98.
58. Jin, X., and Davis, C. H., 2005. Automated building extraction from high-resolution satellite imagery in urban areas using structural, contextual, and spectral information. EURASIP Journal on Applied Signal Processing, 2005, 2196-2206.
59. Karantzalos, K., and Paragios, N., 2009. Recognition-Driven Two-Dimensional Competing Priors Toward Automatic and Accurate Building Detection. IEEE Transactions on Geoscience and Remote Sensing, 47(1), 133-144.
60. Katartzis, A. and Sahli, H., 2008. A Stochastic Framework for the Identification of Building Rooftops Using a Single Remote Sensing Image. IEEE Transactions on Geoscience and Remote Sensing, 46(1), 259-271.
61. Kim, T. and Muller, J.-P., 1998. A technique for 3D building reconstruction. Photogrammetric Engineering and Remote Sensing, 64 (9), 923-930.
62. Kim, T. and Muller, J.-P., 1999. Development of a graph-based approach for building detection. Image and Vision Computing, 17(1), 3-14.
63. Kim, W.Z. and Nevatia, R., 1999, Uncertain reasoning and learning for fearum grouping. Computer Vision and Image Understranding, 76, 278-288.

64. Kim, Z. and Nevatia, R., 2004. Automatic description of complex buildings from multiple images. Computer Vision and Image Understanding, 96 (1), 60–95.
65. Kit, O., Ludeke, M., and Reckien, D, 2012. Texture-based identification of urban slums in Hyderabad, India using remote sensing data. Applied Geography, 32(2), 660-667.
66. Koc-San, D. and Turker, M., 2012. A model-based approach for automatic building database updating from high-resolution space imagery. International Journal of Remote Sensing 33 (13), 4193-4218.
67. Krishnamachari, S. and Chellappa, R., 1996. Delineating buildings by grouping lines with MRFs. IEEE Transactions on Image Processing, 5(1), 164-168.
68. Kumar Anil, Ghosh S. K., and Dadhwal V. K., 2006. Sub-pixel land cover mapping: SMIC system, ISPRS International Symposium on Geospatial Databases for Sustainable Development, 27 September, Goa, India.
69. Kumar Anil, Ghosh S. K., and Dadhwal V. K., 2010. ALCM: Automatic land cover mapping, Journal of the Indian Society of Remote Sensing, 38(2), 239-245.
70. Kumar Anil, Ghosh S. K., Dadhwal V. K., 2006. A comparison of the performance of fuzzy algorithm versus statistical algorithm based sub-pixel classifier for remote sensing data. In Proceedings of mid-term symposium ISPRS, 8-11.
71. Lafarge F., Descombes X., Zerubia J., and Marc P.-D., 2006. An Automatic Building Reconstruction Method: A Structural Approach Using High Resolution Satellite Images, ICIP, IEEE, 205-208.
72. Lafarge, F., Descombes, X., Zerubia, J., and Pierrot-Deseilligny, M., 2008. Automatic building extraction from DEMs using an object approach and application to the 3D-city modeling. ISPRS Journal of Photogrammetry and Remote Sensing, 63 (3), 365-381.
73. Lari, Z. and Ebadi, H., 2007. Automated building extraction from high-resolution satellite imagery using spectral and structural information based on artificial neural networks. Paper presented at the ISPRS Hannover Workshop.
74. Laws, K., 1980. Textured image segmentation. University of Southern California.
75. Lee, D. S., Shan, J., and Bethel, J. S., 2003. Class-guided building extraction from Ikonos imagery. Photogrammetric engineering and remote sensing, 69(2), 143-150.
76. Lefevre, S., Weber, J., and Sheeren, D., 2007. Automatic building extraction in VHR images using advanced morphological operators. Paper presented at the Urban Remote Sensing Joint Event, 2007.
77. Lin, C., Nevatia, R., 1998. Building detection and description from a single intensity image. Computer Vision and Image Understanding, 72 (2), 101-121.

78. Liu, W., and Prinet, V., 2005. Building detection from high-resolution satellite image using probability model. Paper presented at the International Geoscience and Remote Sensing Symposium.
79. Liu, Z., Cui, S., and Yan, Q., 2008. Building extraction from high resolution satellite imagery based on multi-scale image segmentation and model matching. Paper presented at the International Workshop on Earth Observation and Remote Sensing Applications, 2008. EORSA 2008.
80. Liu, Z. J., Wang, J., and Liu, W. P., 2005. Building Extraction from High Resolution Imagery based on Multi-scale Object Oriented Classification and Probabilistic Hough Transform.
81. Mallat, S. G., 1989. A theory of multi resolution signal decomposition: The wavelet representation. IEEE Transactions on Pattern Analysis and Machine Intelligence, 11(7), 674-693.
82. Matsuyama, T. and Hwang, V. S. S., 1990, SIGMA: A Knowledge Based Aerial Image Understanding System (New York: Plenum).
83. Mayer, H., 1999. Automatic object extraction from aerial imagery-a survey focusing on buildings. Computer Vision and Image Understanding, 74 (2), 138-149.
84. McGlone, J. C. and Shufelt, J. A., 1994. Projective and object space geometry for monocular building extraction. In: Proc. of Computer Vision and Pattern Recognition, 54-61.
85. Michaelsen, E., Stilla, U., Soergel, U., and Doktorski, L., 2010. Extraction of building polygons from SAR images: Grouping and decision-level in the GESTALT system. Pattern Recognition Letters, 31(10), 1071-1076.
86. Mohan, R. and Nevatia, R., 1989. Using perceptual organization to extract 3D structures. IEEE Transactions on Pattern Analysis and Machine Intelligence, 11(11), 1121-1139.
87. Mozumder, C. and N. K. Tripathi, 2012. Use of Multiple Satellite Images in Multiple Scales for Feature Extraction and Image Classification: A Case Study of Ramsar Wetland in North East India, 33rd Asian conference on remote sensing: Aiming Smart Space Sensing.
88. Muller, J. P., Ourzik, C., Kim, T. and Dowman, I. J., 1997. Assessment of the effects of resolution on automated DEM and building extraction. In Automatic Extraction of Man-Made Objects from Aerial and Space Images (II), A. Gruen, O. Kuebler and P. Agouris (Eds.), 245-256 (Basel: Birkhauser Verlag).

89. Muttitanon, W. and Tripathi N. K., 2005. Land use/land cover changes in the coastal zone of Ban Don Bay, Thailand using Landsat 5 TM data. International journal of remote sensing, 26(11), 2311-2323.
90. National Building Code of India, 2005. Bureau of Indian Standards.
91. Navalgund Ranganath R., Jayaraman V., and Roy P. S., 2007. Remote sensing applications: An overview, Current Science, 93(12).
92. Newsam Shawn D. and Kamath Chandrika, 2004. Retrieval Using Texture Features in High Resolution Multi-spectral Satellite Imagery, submitted to Data Mining and Knowledge Discovery: Theory, Tools and Technology, VI SPIE Defense and Security Symposium, Orlando, Florida, April 12-16.
93. Nikolakopoulos, K. G., 2004. Pansharp vs. wavelet vs. PCA fusion technique for use with Landsat ETM panchromatic and multispectral data. In Image and Signal Processing for Remote Sensing, Proceedings of the SPIE, 5573, 30–40.
94. Noronha, S. and Nevatia, R., 2001. Detection and modeling of buildings from multiple aerial images. IEEE Transactions on Pattern Analysis and Machine Intelligence 23(5), 501–518.
95. Ok, A. O., 2013. Automated detection of buildings from single VHR multispectral images using shadow information and graph cuts. ISPRS Journal of Photogrammetry and Remote Sensing, 86, 21-40.
96. Otsu, N., 1979. A Threshold Selection Method From Graylevel Histograms. IEEE Transactions on Systems, Man and Cybernetics, 9(1), 62-66.
97. Paparoditis, N., Cord, M., Jordan, M., Cocquerez, J.P., 1998. Building detection and reconstruction from mid- and high-resolution aerial imagery. Computer Vision and Image Understanding, 72 (2), 122-142.
98. Peng, J. and Jin, Y.Q., 2007. An unbiased algorithm for detection of curvilinear structures in urban remote sensing images. International Journal of Remote Sensing, 28, 5377–5395.
99. Peng, J. and Liu, Y. C., 2005. Model and context-driven building extraction in dense urban aerial images. International journal of Remote Sensing, 26(7), 1289-1307.
100. Persson, M., Sandvall, M., and Duckett, T., 2005, Automatic building detection from aerial images for mobile robot mapping proceedings. 2005 IEEE International Symposium on Computational Intelligence in Robotics and Automation, 27-30 June 2005, Espoo, Finland.
101. Pesaresi, M., 2000. Texture analysis for urban pattern recognition using fine-resolution panchromatic satellite imagery. Geographical and Environmental Modelling, 4, 43–63.

102. Pesaresi, M. and Benediktsson, J. A., 2001. A new approach for the morphological segmentation of high-resolution satellite imagery. IEEE Transactions on Geoscience and Remote Sensing, 39(2), 309-320.
103. Pu, S. and Vosselman, G., 2009. Knowledge based reconstruction of building models from terrestrial laser scanning data. ISPRS Journal of Photogrammetry and Remote Sensing, 64(6), 575-584.
104. Ramasamy, Singh B and Brig. Kumar R. S., 2006. Landslide triggered Tsunami in Norway. Geomatics (Ed) SM. Ramasamy et al, Special Volume on Geomatics in Tsunami, New India Publishers, New Delhi, 221-225.
105. Ramasamy, S. M., Palanivel, K., Md. Sartaj Basha, S. K., Muthukumar, M., Reddy L. K., K., Kumanan, C.J. and Singh B., 2010. Geological Complexities, Landslide Vulnerabilities and Possible Mitigation, Tirumala Hills, India. Journal in Indian Institute of Technology, Mumbai (Ed) T. P. Singh, Allied Publishers, 166-181.
106. Ramasamy, S. M., Kumanan, C. J., Palanivel, K. and Gunasekaran, S. Geospatial Technology Based SDSS for District Planning: Pudukottai, Tamil Nadu. SM. Ramasamy, C.J. Kumanan, K. Palanivel and Bhoop Singh (ed.), 2005. Geospatial Technology for Developmental Planning, Allied Publisher, 359-367.
107. Randen, T. and Husoy, J. H., 1999. Filtering for texture classification: A comparative study. IEEE Transactions on Pattern Analysis and Machine Intelligence, 21(4), 291-310.
108. Roychowdhury, K., Jones, S., Arrowsmith, C., Reinke, K., 2011. Indian census using satellite images: Can DMSP-OLS data be used for small administrative regions? Urban Remote Sensing Event (JURSE), 2011 Joint, IEEE, 153-156.
109. Roychowdhury, K., Jones, S., Arrowsmith, C., Reinke, K., Bedford, A., 2010. The role of satellite data in census: Case study of an Indian State, Proceedings of the Asia-Pacific Advanced Network, August, 30, 207-218.
110. Rüther, H., Martine, H.M., Mtalo, E.G., 2002. Application of snakes and dynamic programming optimisation technique in modeling of buildings in informal settlement areas. ISPRS Journal of Photogrammetry and Remote Sensing, 56 (4), 269-282.
111. Sahin, H., et al., 2004. Comparison of object oriented image analysis and manual digitizing for feature extraction. Paper presented at the Proceedings of the ISPRS 2004 annual conference, Istanbul, Turkey.
112. San A, D. K., 2007. Automatic Building Extraction from High Resolution Stereo Satellite Images.

113. San, D. K. and Turker, M., 2010. Building extraction from high resolution satellite images using Hough transform. International Archives of the Photogrammetry, Remote Sensing and Spatial Information Science, 38(Part 8), 1063-1068.
114. Schindler, K., 2012. An overview and comparison of smooth labeling methods for land-cover classification. IEEE Transactions on Geoscience and Remote Sensing, 50(11), 4534-4545.
115. Seismic Vulnerability Assessment of Building Types in India, 2013. National Disaster Management Authority, 1-34.
116. Senaras, C., Ozay, M., and Yarman Vural, F. T., 2013. Building Detection with Decision Fusion. Selected Topics in Applied Earth Observations and Remote Sensing, IEEE, 6(3), 1295-1304.
117. Seresht M. S. and Ali A., 2000. Automatic Building Recognition from Digital Aerial Images. International Archives of Photogrammetry and Remote Sensing, 33(B3). Amsterdam, 792-798.
118. Sengar, S. S., Kumar A., et al., 2013. Earthquake-induced built-up damage identification using fuzzy approach. Geomatics, Natural Hazards and Risk, 4(4), 320-338.
119. Shaban, M. A. and Dikshit O., 1998. Textural classification of high resolution digital satellite imagery. Geoscience and Remote Sensing Symposium Proceedings, IGARSS'98. 1998 IEEE International, IEEE.
120. Shaban, M. A. and Dikshit O., 1999. Land use classification for urban areas using spatial properties. IEEE 1999 International Geoscience and Remote Sensing Symposium, IGARSS'99, Proceedings, IEEE.
121. Shaban, M. A., and Dikshit, O., 2001. Improvement of classification in urban areas by the use of textural features: the case study of Lucknow city, Uttar Pradesh. International Journal of Remote Sensing, 22, 565-593.
122. Shaban, M. A., and Dikshit, O., 2002. Evaluation of the merging of SPOT multispectral and panchromatic data for classification of an urban environment. International Journal of Remote Sensing. 23, 249-262.
123. Shackelford, A. K. and Davis, C. H., 2003. A combined fuzzy pixel-based and object-based approach for classification of high-resolution multispectral data over urban areas. IEEE Transactions on Geoscience and Remote Sensing, 41(10 PART I), 2354-2363.
124. Shackelford, A.K., Davis, C.H., 2003. A combined fuzzy pixel-based and object-based approach for classification of high-resolution multispectral data over urban areas. IEEE Transactions on Geoscience and Remote Sensing, 41(10), 2354-2363.

125. Shackelford, A. K., C. H. Davis, and X. Wang., 2004. Automated 2-D building footprint extraction from high-resolution satellite multispectral imagery. IEEE.
126. Shen, L. and Guo X., 2014. Spatial quantification and pattern analysis of urban sustainability based on a subjectively weighted indicator model: A case study in the city of Saskatoon, SK, Canada. Applied Geography, 53, 117-127.
127. Shufelt, J. A. and Mckeown. 1993. Fusion Of Molocular Cues To Detect Man-Made Structures In Aerial Imagery. Cvgip: Image Understanding, 57(3), 307-330.
128. Shufelt, J. A., 1996. Exploiting photogrammetric methods for building extraction in aerial images. International Archives of Photogrammetry and Remote Sensing 31 (Part B6), 74–79.
129. Shufelt, J. A., 1999. Performance evaluation and analysis of monocular building extraction from aerial imagery. IEEE Transactions on Pattern Analysis and Machine Intelligence, 21(4), 311-326.
130. Simonetto, E., Oriot, H., and Garello, R. (2005). Rectangular building extraction from stereoscopic airborne radar images. IEEE Transactions on Geoscience and Remote Sensing, 43(10), 2386-2395.
131. Sirmacek, B., Unsalan, C., 2009. Urban-area and building detection using SIFT keypoints and graph theory. IEEE Transactions on Geoscience and Remote Sensing 47 (4), 1156-1167.
132. Sirmacek, B., & Unsalan, C., 2009. Urban-Area and Building Detection Using SIFT Keypoints and Graph Theory. IEEE Transactions on Geoscience and Remote Sensing, 47(4), 1156-1167.
133. Sirmacek, B., & Unsalan, C., 2011. A probabilistic framework to detect buildings in aerial and satellite images. IEEE Transactions on Geoscience and Remote Sensing, 49(1), 211-221.
134. Sohn, G. and Dowman, I. J., 2001, Extraction of buildings from high-resolution satellite data. In Automatic Extraction of Man-Made Objects from Aerial and Space Images (III), A. Gruen, O. Kuebler and P. Agouris (Eds.), 345–355.
135. Sohn, G. and Dowman, I., 2007. Data fusion of high-resolution satellite imagery and LiDAR data for automatic building extraction. ISPRS Journal of Photogrammetry and Remote Sensing, 62(1), 43-63.
136. Song, Z., Pan, C., and Yang, Q., 2006. A region-based approach to building detection in densely build-up high resolution satellite image. Paper presented at the IEEE International Conference on Image Processing.

137. Srivastava S. K. and Gupta R. D., 2003. Monitoring of Changes in Land Use/ Land Cover using Multi-sensor Satellite Data, 6th International Conference on GIS/GPS/RS: Map India, New Delhi.
138. Sumer, E. and Turker, M., 2013. An adaptive fuzzy-genetic algorithm approach for building detection using high-resolution satellite images. Computers, Environment and Urban Systems, 39, 48-62.
139. Suveg, I. and Vosselman, G., 2004. Reconstruction of 3D building models from aerial images and maps. ISPRS Journal of Photogrammetry and Remote Sensing 58 (3-4), 202-224.
140. Tatem, A. J., Lewis, H. G., Atkinson, P. M. and Nixon, M. S., 2001. Super-resolution mapping of urban scenes from IKONOS imagery using a hopfield neural network. In Proceedings of IGARSS, 2001, Southampton, UK (Sydney: IEEE Conference Proceedings), 3203-3205.
141. Thach, N. N. and Canh, P. X., 2012. Simulation of flash–muddy flash and inundation of western Tamdao mountain region, Vinhphuc Province, Vietnam by using integrated concept of hydrology and geomorphology, VNU Journal of Science, Earth Sciences, 28, 44-56.
142. Thach, N. N., Hien, N. T. T., and Canh, P. X., 2011. Sensitivity and vulnerability assessment of socio-ecosystem to oil spill and sea level rising impact at hai phong coastal zone, Vietnam, 32nd Asian Conference on Remote Sensing, 1, 1152-1162.
143. Thach, N. N., Truc, N. N., and Hau, L. P., 2007. Studying shoreline change by using LITPACK mathematical model (case study in Cat Hai Island, HaiPhong City, Vietnam). VNU J. Sci., Earth Sci., 23:244-252.Tom, V.T., 1987. System for and method of enhancing images using multiband information. USA Patent, 4, 496.
144. Theng, L. B., 2006. Automatic building extraction from satellite imagery. Engineering Letters, 13(3), 255-259.
145. Torres Ricardo da Silva, Falcão Alexandre Xavier, 2006. Content-Based Image Retrieval: Theory and Applications", RITA, 8(2).
146. Tournaire, O., Brédif, M., Boldo, D., and Durupt, M., 2010. An efficient stochastic approach for building footprint extraction from digital elevation models. ISPRS Journal of Photogrammetry and Remote Sensing 65 (4), 317–327.
147. Tripathi, N. K. and Tripathi A., 1993. Feature extraction from multispectral digital images using artificial neural networks and Bayesian classifier. Geoscience and Remote Sensing

Symposium, 1993. IGARSS'93. Better Understanding of Earth Environment. International, IEEE, 18-21 Aug, 905-906.

148. Tsai, V. J. D., 2006. A comparative study on shadow compensation of color aerial images in invariant color models. *IEEE Transactions on Geoscience and Remote Sensing*, 44, 1661-1671.
149. Tupin, F. and Roux, M., 2003. Detection of building outlines based on the fusion of SAR and optical features. ISPRS Journal of Photogrammetry and Remote Sensing, 58(1-2), 71-82.
150. Turlapaty, A., Gokaraju, B., Du, Q., Younan, N.H., and Aanstoos, J.V., 2012. A hybrid approach for building extraction from spaceborne multi-angular optical imagery. IEEE Journal of Selected Topics in Applied Earth Observations and Remote Sensing, 5(1), 89-100.
151. UN, 2007. UN Habitat Twenty First Session of Governing Council.
152. Unsalan, C. and Boyer, K. L., 2005. A system to detect houses and residential street networks in multispectral satellite images. Computer vision and image understanding, 98(3), 423-461.
153. Van de Vower, G., Scheunders, P., Van Dyck, D., 1999. Statistical Texture Characterization from Discrete Wavelet Representations. IEEE Transactions on Image Processing, 8(4), 592-598.
154. Venkateswar, V. and Chellappa, R., 1991, A hierarchical approach to detection of buildings in aerial images, Technical Report No. CAR-TR 567, University of Maryland, College Park, MD.
155. Vestri, C., 2006. Using range data in automatic modeling of buildings. Image and Vision Computing 24 (7), 709–719.
156. Wang, J., Yang, X., Qin, X., Ye, X., and Qin, Q., 2015. An Efficient Approach for Automatic Rectangular Building Extraction from Very High Resolution Optical Satellite Imagery. Geoscience and Remote Sensing Letters, IEEE, 12(3), 487-491.
157. Wald, L., Ranchin, T. and Mangolini, M., 1997. Fusion of satellite images of different spatial resolutions: assessing the quality of resulting images. Photogrammetric Engineering and Remote Sensing, 63, 691-699.
158. Wang, K., Franklin S. E., Guo X., and Cattet M., 2010. Remote sensing of ecology, biodiversity and conservation: a review from the perspective of remote sensing specialists, Sensors, 10(11), 9647-9667.

159. Wei Li, Weihong Wang, Feng Lu, 2009. Research on Remote Sensing Image Retrieval Based on Geographical and Semantic Features, IEEE.

160. Wei, Y., Zhao, Z., & Song, J. 2004. Urban building extraction from high-resolution satellite panchromatic image using clustering and edge detection. Paper presented at the Geoscience and Remote Sensing Symposium, 2004. IGARSS'04. Proceedings. 2004 IEEE International.

161. Weickert, J., 1999. Coherence-enhancing diffusion filtering. International Journal of Computer Vision, 31(2-3), 111-127.

162. Weidner U. and Forstner W., 1995. Towards automatic building extraction from high-resolution digital elevation models, ISPRS Journal of Photogrammetry and Remote Sensing, Elsevier Science, 50(4), 38-49.

163. Welch, R. M., Navar, M. S. and Sengupta, S. K., 1989. The effect of spatial resolution upon the texture-based cloud field classifications. Journal of Geophysical Research, 94, 14767–14781.

164. Wilkinson, G. G., 2005, Results and implications of a study of fifteen years of satellite image classification experiments. IEEE Transactions on Geoscience and Remote Sensing, 43, 433–440.

165. Woodcock, C.E. and Strahler, A.H., 1987. The factor of scale in remote sensing. Remote Sensing of Environment, 21, 311–332.

166. Xia, J. C., Arrowsmith, C., Mervyn, J., and William, C., 2008. The wayfinding process relationships between decision-making and landmark utility. Tourism Management, 29(3), 445-457.

167. Xiao, J., Gerke and M., Vosselman, G., 2012. Building extraction from oblique airborne imagery based on robust façade detection. ISPRS Journal of Photogrammetry and Remote Sensing 68, 56–68.

168. Yang, J. and Wang, R. S., 2007. Classified road detection from satellite images based on perceptual organization. International Journal of Remote Sensing, 28, 4653–4669.

169. Yooa H.-W., Janga D.-S., Junga S.-H., Parka J.-H., and Song K.-S., 2002. Visual information retrieval system via content-based approach, The Journal of The Pattern Recognition Society, Elsevier Science, 749–769.

170. Youwang K., Jianhui Z., Zhiyong Y., Chengzhang Q., Shizhong H., Zhong Z., Xuanmin J., Guozhong L., 2009. A Rapid Object Detection Method for Satellite Image with Large

Size", International Conference on Multimedia Information Networking and Security, IEEE.

171. Yun, Z., 2002. A new automatic approach for effectively fusing Landsat 7 as well as IKONOS images. IEEE/IGARSS'02, 24–28 June, Toronto, Canada (New York: IEEE), 2429-2431.
172. Zhang, Y., 1999. Optimisation of building detection in satellite images by combining multispectral classification and texture filtering. ISPRS Journal of Photogrammetry and Remote Sensing, 54(1), 50-60.
173. Zhang, K., Yan, J., and Chen, S.C., 2006. Automatic construction of building footprints from airborne LIDAR data. IEEE Transactions on Geoscience and Remote Sensing, 44(9), 2523-2533.
174. Zhang, Y. and Albertz, J., 1997. Comparison of four different methods to merge multisensory and multi-resolution satellite data for the purpose of mapping. In Proceedings of the ISPRS Joint Workshop 'Sensors and Mapping from Space' of Working Groups I/1, I/3 and IV/ 4, 29 September–2 October, Hannover, Germany, (Hannover: ISPRS Joint Workshop), 275–287.
175. Zhen, G.Q., Shi, T.Z., Chun, L.Z. and Jin, Y.F., 2004. Automatic building detection from high resolution images based on multiples features. In IEEE Commission II, ICWG II/IV (Piscataway, NJ: IEEE), 1–5.
176. Zhou, J., Civco, D.L. and VE Silander, J.A., 1998. A wavelet transform method to merge Landsat TM and SPOT panchromatic data. *International Journal of Remote Sensing*, 19, 743–757.

Appendix -1

LIST OF PUBLICATIONS

JOURNAL

1. Dahiya, S., & Garg, P. K., & Jat, M. K., "Content Based Object Extraction From High Resolution Satellite Images", International Journal of Engineering and Science Research, special Issue, 2012, Aritcle No-28, pp 157-170.
2. Susheela Dahiya, P. K. Garg, Mahesh K Jat, "Building Extraction from High Resolution Satellite Images", TECHNIA – International Journal of Computing Science and Communication Technologies, VOL.5 NO. 2, pp 829-834, Jan. 2013 (ISSN 0974-3375).
3. Susheela Dahiya, Pradeep Kumar Garg, Mahesh K. Jat, "A comparative study of various pixel based image fusion techniques as applied to an urban environment", International Journal of Image and Data Fusion, Taylor & Francis, Vol. 4, Issue 3, pp 197-213, 2013.

CONFERENCE

1. Dahiya, S., Garg P. K. and Jat M. K. "Content Based Methods for Building Extraction from Satellite Images", in Proc. International Conference on System Modeling & Advancement in Research Trends (SMART), 20 – 21 October, 2012, Moradabad.
2. Susheela Dahiya, P. K. Garg, Mahesh K Jat, "Object Oriented Approach for Building Extraction from High Resolution Satellite Images", 3rd IEEE International Advance Computing Conference (IACC), pp. 1300-1305, Feb. 2013.
3. Susheela Dahiya, Kapil Pandey, P. K. Garg and Mahesh K. Jat "Image Processing Techniques for Information Extraction from Satellite Images", International Geographical Union (IGU) Conference on Geoinformatics for Biodiversity and Climate Change, 14-16 March 2013, Rohtak, Haryana.
4. Susheela Dahiya, P. K. Garg and Mahesh K. Jat, "Building Extraction from High Resolution Satellite Images Using Matlab Software", 14th SGEM GeoConference on Informatics, Geoinformatics and Remote Sensing, SGEM2014 Conference Proceedings, ISBN 978-619-7105-12-4 / ISSN 1314-2704, June 19-25, 2014, Vol. 3, 71-78 pp. DOI: 10.5593/SGEM2014/B23/S10.009